MAIT cells in sterile and non-sterile inflammation

Lauren Jane Howson

Radcliffe Department of Medicine
Lincoln College
University of Oxford

This thesis is submitted as part of the requirements for the degree of Doctor of Philosophy in Medical Sciences

Trinity Term 2017

Abstract

Mucosal-associated invariant T (MAIT) cells are an innate-like T cell subset that recognize bacteria-derived metabolites presented on MR1, but can also be stimulated in a T cell receptor (TCR)-independent manner by pro-inflammatory cytokines. Therefore, their role in both sterile and non-sterile diseases are of great interest and only just beginning to be explored. To understand the role of MAIT cells in non-sterile inflammation, we utilized a controlled human infection model of live *Salmonella enterica* serovar Paratyphi A. We observed that at the time of diagnosis MAIT cells had an activated phenotype, which was maintained even after antibiotic treatment. We analysed the TCR repertoire of MAIT cells in diagnosed individuals to determine if the MAIT cell response to infection was antigen-driven. We found that infection led to redistribution of the repertoire, with transient contraction of the over-represented clones at the peak of infection. To understand the role of MAIT cells in sterile inflammation we examined cancer sections and found that MAIT cells infiltrate tumours derived from various tissues and that the source of MAIT cells was from tissue-resident MAIT cell subsets. We also determined that MAIT cells may respond to BCG immunotherapy of bladder cancer, as they are both present and activated in the bladder following treatment. Finally, we wanted to determine the extent to which both the TCRα and TCRβ usage affected MAIT cell responses. We found that the TRAJ usage, which relatively defines circulating versus tissue-resident MAIT subsets, has a large impact on the MAIT TCR response to both bacterial and ligand stimulation. We also investigated selected TCRβ clonotypes identified in *Salmonella*-infected individuals and found that the MAIT cell clonotypes that expanded after infection had stronger TCR-dependent activation than did contracted clonotypes from the same individual. In conclusion, we have characterised the function and phenotype of MAIT cells in human infection, cancer and cancer immunotherapy as well as provide insight into the usage and importance of the specific MAIT cells TCRα and TCRβ chains.

Acknowledgements

Firstly, I would like to thank my supervisor Vincenzo Cerundolo for his support and guidance during my PhD. My time in the Cerundolo lab has had an immense impact on both my personal and professional development, for which I am grateful for.

I am very thankful for the wonderful support network that has been the Cerundolo lab. I want to thank Giorgio, Dawn, Margarida and Hemza for their time and expertise that they contributed to my PhD project and also the skills and critical-thinking that you have taught me. Thank you to my lab mates not only for helping me technically, but also for the friendship and support over the past four years - you have made my time in Oxford such a positive experience.

I am very grateful for the funding from the Medical Research Council UK and Cancer Research UK that has supported my research. I also wish to thank the funding from Lincoln College, the Clarendon Fund and the Radcliffe Department of Medicine that has supported my studies at Oxford for the past four years.

Finally, I would like to thank my wonderful family who have provided so much love and support during my PhD. Although you were far away I felt your support as if you were right here with me. You kept me grounded through this whole experience and I cannot thank you enough.

Table of Contents

List of Figures

List of Tables

Commonly Used Abbreviations

5-A-RU	5-amino-6-(D-ribitylamino)uracil
ANOVA	Analysis of variance
APC	Antigen presenting cell
BCG	Bacillus Calmette–Guérin
CD	Cluster of differentiation
FBS	Foetal bovine serum
FW	Forward (primer)
Gr	Granzyme
HLA	Human leukocyte antigen
IFN	Interferon
Ig	Immunoglobulin
IL	Interleukin
LB	Lysogeny broth
MAIT	Mucosal-associated invariant T (cell)
MG	Methylglyoxal
MHC	Major histocompatibility complex
MOI	Multiplicity of infection
MR1	major histocompatibility complex, class I-related
NKT	Natural killer T (cell)
PBMC	Peripheral blood mononuclear cell
PBS	Phosphate buffered saline
PCR	Polymerase chain reaction
PFA	Paraformaldehyde
PMA	Phorbol 12-myristate 13-acetate
PRR	Pattern recognition receptor
RL-6,7-DiMe	6,7-dimethyl-8-(1-D-ribityl)lumazine
RV	Reverse (primer)
SEM	Standard error of the mean
SFC	Spot forming cell
TCR	T cell receptor
Th	T-helper
TNF	Tissue necrosis factor
TRAJ	T cell receptor alpha joining region
TRAV	T cell receptor alpha variable region
TRBJ	T cell receptor beta joining region
TRBV	T cell receptor beta variable region
WT	Wild-type

Chapter 1 – Introduction and Project Aims

Sections 1.2–1.8 of Chapter 1 are based on our previously published literature review (Howson *et al.*, 2015).

1.1 Overview of the immune system

The immune system is composed of two arms, innate and adaptive. Innate immunity protects against invading pathogens in a non-specific manner. It is comprised of epithelial barriers, circulating proteins and phagocytes (primarily neutrophils and macrophages) that express pattern recognition receptors (PRR) that can recognise pathogen-associated molecular patterns (Iwasaki and Medzhitov, 2015). This process initiates an inflammatory response and the antigen presenting cells (APCs), when sensing bacteria through PRR, can then activate the adaptive immune response (Dzopalic *et al.*, 2012).

Adaptive immunity is a specific immune response that develops at the later stages of infection. The adaptive immune system consists of lymphocytes that can recognise specific antigens. They can be divided into distinct subsets: T cells that mediate cellular immunity both cluster of differentiation (CD)8^+ cytotoxic and $CD4^+$ helper subsets, and B cells that mediated humoral (antibody-mediated) immune responses (Cooper and Alder, 2006). T cells have been researched extensively as they have a key role in both protective and aberrant immunity. They are characterized as expressing a T cell receptor (TCR), composed of α and β subunits, that is highly diverse and can recognize an enormous range of peptides derived from pathogens or aberrant proteins expressed by cancers. These peptides are displayed on the polymorphic major histocompatibility complex (MHC), either MHC class I on all nucleated cells by the $CD8^+$ T cells or MHC class II on "professional" APCs by the $CD4^+$ T cells (Cooper and Alder, 2006). However, there is a group of T cells that do not fit this classical αβ T cell description and are therefore referred to as unconventional αβ T cells.

1.1.1 Unconventional αβ T cells

Unconventional αβ T cells have gained great interest since their discovery, as these cells lie at the interface between innate and adaptive immunity. An outline of unconventional αβ T cells is shown in **Figure 1-1**. Some of the most well characterized unconventional αβ T cells are the CD1-restricted T cells. These can be divided into group 1 that are CD1a, CD1b or CD1c-restricted, and group 2 natural killer T (NKT) cells that are CD1d-restricted. All the CD1-restricted T cells recognise lipid antigens presented on CD1, primarily expressed by subsets of dendritic cells (Calabi *et al.*, 1989).

There are also unconventional peptide-reactive αβ T cells such as the human leukocyte antigen (HLA)-E-restricted T cells. These cells bind the leader sequence of peptides which can modulate $CD8^+$ T cell responses (Godfrey *et al.*, 2015).

During the past decade, a new unconventional αβ T cell subset has been the focus of much interest and research: mucosal-associated invariant T (MAIT) cells. These cells recognize a unique family of bacteria-derived metabolites presented on the MHC class I-related (MR1) molecule.

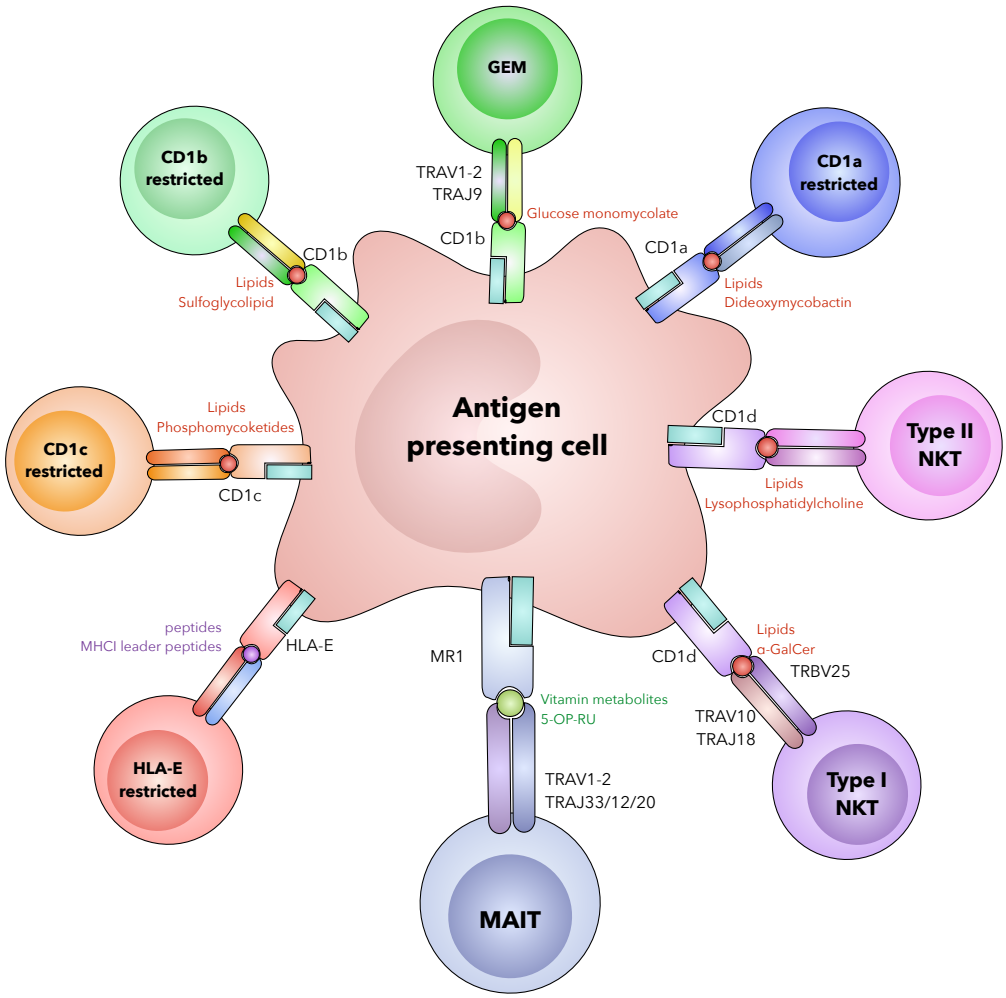

Figure 1-1 Overview of the unconventional αβ T cell family

Diagram shows unconventional αβ T cells interacting with their antigen presenting molecule. Also labelled are the antigen classification of lipids (red), vitamin metabolites (green) or peptides (purple). Specific example antigen and TCR receptor usage (if restricted) is labelled.

1.2 MR1

1.2.1 Structure and intracellular trafficking

The MR1 gene was first described in 1995 in a genome screen designed to identify novel MHC-related genes (Hashimoto *et al.*, 1995). The human MR1 gene was found on chromosome 1, the same location as the CD1 genes. Like MHC class I, MR1 associates with β_2-microglobulin but is non-polymorphic, despite a similar intron/exon organization to

classical MHC molecules. MR1 was also found to be highly conserved among mammalian species, with 90% sequence homology between human and mouse MR1 ligand binding domains. They also have a high level of functional cross-reactivity among mammalian species, a similar feature to CD1 (Riegert *et al.*, 1998, Huang *et al.*, 2009).

The MR1 intracellular trafficking pathway has only recently been discovered as having an "on-off-on" mechanism. A study of MR1 intracellular trafficking reported that MR1 is pre-synthesised and retained in the endoplasmic reticulum (ER) in the absence of exogenous ligand (McWilliam *et al.*, 2016). This suggests that, unlike other antigen presenting molecules, MR1 does not constitutively express self-ligands.(Lepore *et al.*, 2017) Only in the presence of its ligand can MR1 be stabilised and traffic to the cell surface. The MR1 complexes are then endocytosed and degraded intracellularly, with evidence that some MR1 molecules can be recycled in the endocytic compartment and traffic back to the cell surface. A separate study of MR1 trafficking of *Mycobacterium tuberculosis* ligands supported these findings and identified the trafficking molecules Stx18, VAMP4, and Rab6 as regulators of MR1 trafficking (Harriff *et al.*, 2016). This current model of MR1 trafficking is outlined in **Figure 1-2**.

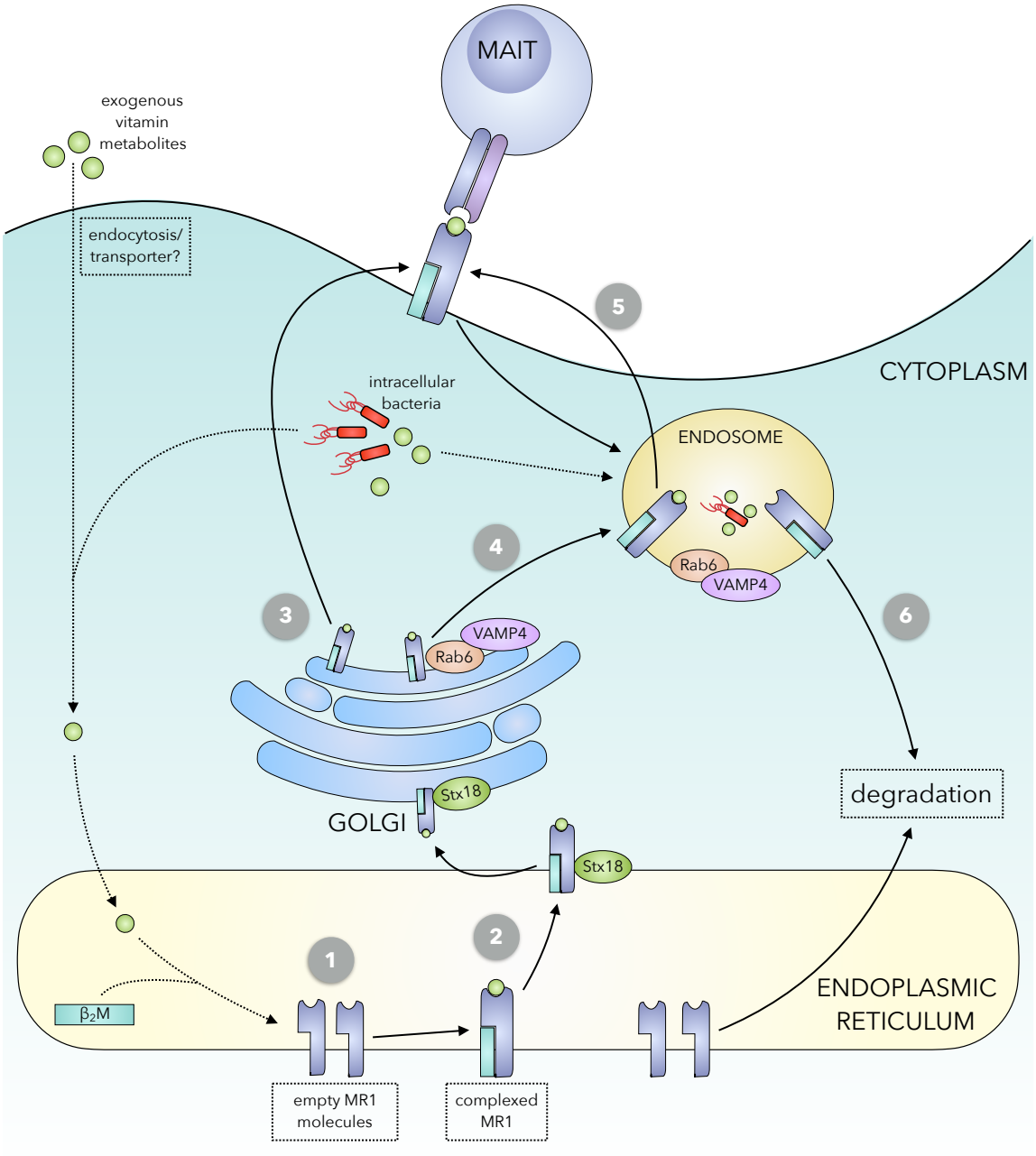

Figure 1-2 Current model for MR1 trafficking

(1) MR1 is pre-synthesised in the endoplasmic reticulum (ER). (2) Upon complex with β_2M and the vitamin metabolite ligand, MR1 can then traffic to the Golgi under the regulation of Stx18. MR1 then traffics through the Golgi apparatus and either (3) directly to the cell surface or (4) via endosomes under the regulation of Rab6 and VAMP4. (5) MR1 can then undergo recycling through the endosome and traffic back to the surface or (6) undergo degradation.

1.2.2 Function

The connection between MR1 and MAIT cells was made in 2003 when the central role of MR1, along with commensal flora and B cells, was implicated in MAIT cell development (Treiner *et al.*, 2003). Although MR1 is ubiquitously transcribed, its physiological expression at the cell surface has been difficult to demonstrate, except for B cell subsets in the intestinal mucosa (Gozalbo-Lopez *et al.*, 2009). A study of mouse MR1 reported that only the folded form of MR1 could activate MAIT cells and mutations in the putative binding groove disrupted MAIT cell activation, through disrupting the presentation of, what was at the time, unknown antigens (Huang *et al.*, 2005). These results led to an even greater interest in determining the identity of the MAIT cell antigens presented on MR1.

1.2.3 Ligand discovery

The observation that MAIT cells have antimicrobial activity provided important insights that helped identify the MAIT cell ligands. Kjer-Nielsen *et al.* (2012) showed that, similar to other MHC class I and MHC class I-like molecules, MR1 was unable to fold correctly in refolding buffer alone. This suggested that MR1 required the presence of its ligand to stabilize its structure. Refolding was attempted in various conditions using RPMI-1640 as a control. Surprisingly, it was found that MR1 could refold in RPMI-1640, which was known to contain vitamin metabolites normally produced by microbes, but not present in mammals. This observation-based approach led Kjer-Nielsen and colleagues to test the ability of vitamins to bind and stabilize MR1, and ultimately led to the discovery of a new class of antigen: vitamin B metabolites (Kjer-Nielsen *et al.*, 2012).

The first crystal structure of the MR1-ligand complex was with the folic acid (vitamin B9) metabolite 6-formylpterin (6-FP), which was unable to activate MAIT cells (Kjer-Nielsen *et al.*, 2012). To find the MAIT cell stimulatory ligands, MR1 molecules were refolded in

the presence of the supernatant from *Salmonella enterica* serovar Typhimurium bacterial cultures, as it was known that cells infected with *S.* Typhimurium strongly activate MAIT cells (Gold *et al.*, 2010, Le Bourhis *et al.*, 2010). The MR1 molecules from these refold experiments were then analysed by high-resolution mass spectroscopy (ESI–TOF-MS). The results of which showed that MR1 associated with a compound at *m/z* 329.1100, with an atomic composition matching that of several riboflavin (vitamin B2) derivatives: 6,7-dimethyl-8-D-ribityllumazine (RL-6,7-DiMe), 7-hydroxy-6-methyl-8-D-ribityllumazine (RL-6-Me-7-OH) and reduced 6-hydroxymethyl-8-D-ribityllumazine (rRL-6-CH_2OH). Functional assays revealed that these compounds were stimulatory and induced MAIT cells to express CD69, interferon (IFN)γ and tissue necrosis factor (TNF)α (Kjer-Nielsen *et al.*, 2012).

To understand the natural source of riboflavin-derived MAIT cell ligands, Corbett *et al*. (2014) utilized *Lactococcus lactis* mutants of the four-gene operon, that controls riboflavin biosynthesis. They confirmed that riboflavin biosynthesis is necessary to generate natural MAIT cell ligands and determined 5-amino-6-D-ribitylaminouracil (5-A-RU) as the key intermediate. 5-A-RU does not bind MR1, but forms MAIT cell-stimulating ligands through non-enzymatic condensation with glyoxal or methylglyoxal produced by bacteria or host cells (such as in the form of by-products of glycolysis). This condensation reaction yields unstable, potent intermediates 5-(2-oxoethylideneamino)-6-D-ribitylaminouracil (5-OE-RU) and 5-(2-oxopropylideneamino)-6-D-ribitylaminouracil (5-OP-RU). These molecules are captured and stabilized by MR1 as they form Schiff bases with Lys43 in the MR1 binding groove. Mass spectrometry analysis of MR1 refolded in the presence of bacterial culture supernatants from *S.* Typhimurium and *Escherichia coli* revealed molecules with matching properties to synthetic 5-OP-RU, raising the possibility that the compound initially identified as MR1 ligand was naturally occurring 5-OP-RU (Corbett *et al.*, 2014, Kjer-

Nielsen *et al.*, 2012). These results showed that MAIT cells can sense a wide range of bacteria, through recognising vitamin metabolites, including transitory intermediates, presented on MR1 molecules. An overview of the MAIT cell ligands and their chemical structures are shown in **Figure 1-3**.

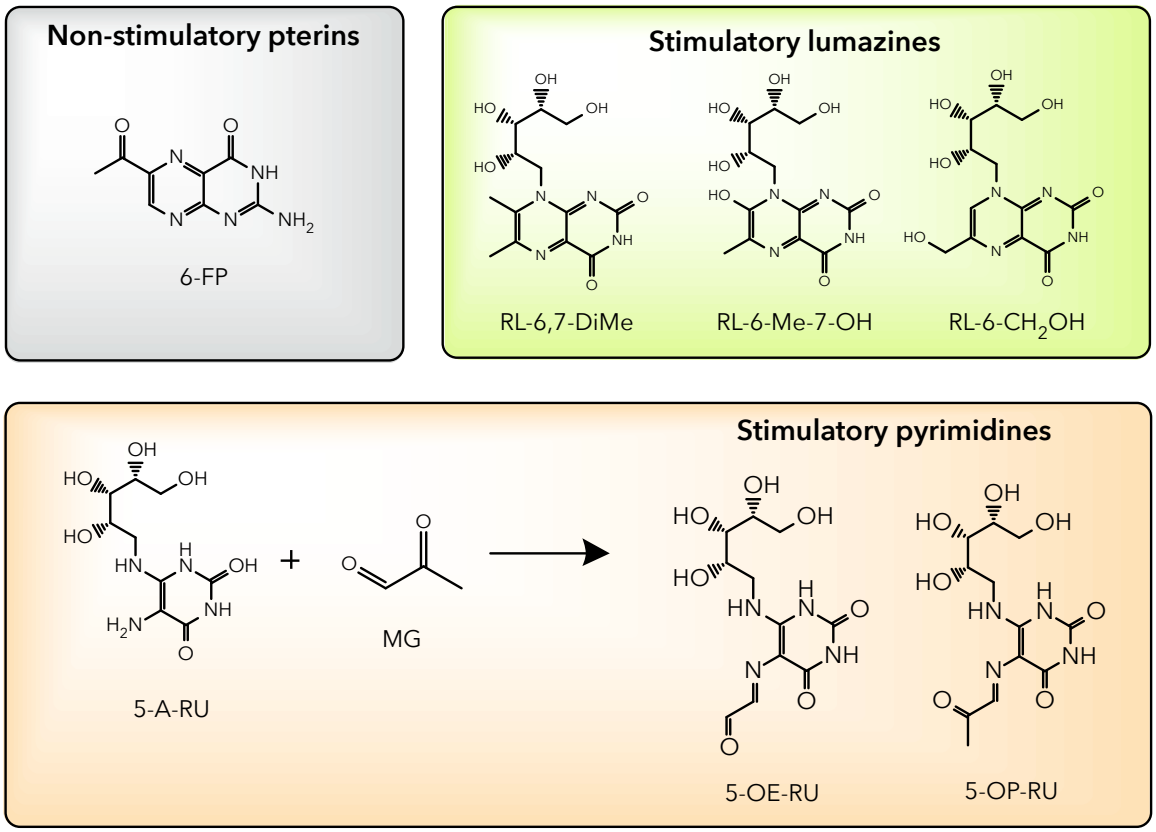

Figure 1-3 Overview of MAIT cell vitamin metabolite ligands

Non-stimulatory ligands include 6-formylpterin (6-FP). Stimulatory lumazines include: 6,7-dimethyl-8-D-ribityllumazine (RL-6,7-DiMe), 7-hydroxy-6-methyl-8-D-ribityllumazine (RL-6-Me-7-OH) and reduced 6-hydroxymethyl-8-D-ribityllumazine (rRL-6-CH_2OH). Stimulatory pyrimidines include 5-(2-oxoethylideneamino)-6-D-ribitylaminouracil (5-OE-RU), 5-(2-oxopropylideneamino)-6-D-ribitylaminouracil (5-OP-RU) as products of the condensation reaction between 5-amino-6-D-ribitylaminouracil (5-A-RU) and methylglyoxal (MG).

In addition to naturally-occurring bacteria-derived ligands, it has recently been discovered that drug and drug-like molecules can also bind MR1. A study that used an *in silico* discovery approach identified potential molecules that could bind MR1 (Keller *et al.*, 2017).

They then tested these molecules for their effect on MR1 upregulation and MAIT cell activation and found that some acted as inhibitors and others as stimulators (including diclofenac metabolites). Their results demonstrated that MR1 can capture a chemically diverse range of molecules and that certain drugs and drug-like molecules may influence MAIT cell function.

1.3 MR1-restricted T cells

1.3.1 Phenotype

1.3.1.1 MAIT cells

MAIT cells were first identified based on their surface phenotype and mucosal tissue localization. The MAIT cell invariant TCRα usage of TRAV1-2–TRAJ33 in humans was first described in 1993 as a preferentially used TCR in the double-negative T cell compartment (Porcelli *et al.*, 1993). This finding was the first evidence of a new subset of T cells potentially recognizing a limited set of antigens in the context of non-polymorphic antigen presenting molecules. It was not until 1999 that MAIT cells were defined as a conserved subpopulation, distinct from MHC class I- and CD1-restricted T cells, and characterized as having an activated/memory phenotype (Tilloy *et al.*, 1999). They also reported that the human MAIT cell TCR β chain usage was primarily TRBV6 or TRBV20.

Initially, research into MAIT cells was hampered by the lack of specific reagents, however the generation of a monoclonal antibody specific for the Vα7.2 TCR chain (Martin *et al.*, 2009) and MR1 tetramers (Reantragoon *et al.*, 2013) have recently enabled the functional and phenotypic analysis of MAIT cells and brought them to the forefront of innate-like lymphocyte research. MAIT cells are defined as $CD3^+$ TRAV1-2 $(Vα7.2)^+$ $CD161^{++}$ and majority being $CD8^+$ with small double negative and $CD4^+$ subsets (Martin *et al.*, 2009, Le

Bourhis *et al.*, 2010). It was also discovered through the use of tetramer staining, that along with TRAJ33 usage, a small proportion of MAIT cells also used TRAJ12 and TRAJ20 (Reantragoon *et al.*, 2013). Human MAIT cells express the transcription factor promyelocytic leukaemia zinc-finger protein (PLZF), which is also expressed by invariant NKT cells and is a known driver of the effector program in lineage development (Savage *et al.*, 2008). However, murine MAIT cells do not express PLZF (Martin *et al.*, 2009) and the functional relevance of this observation is unclear. MAIT cells can also be defined based on co-expression of interleukin (IL)-18R (Le Bourhis *et al.*, 2010) or CD26 (Sharma *et al.*, 2015). Other phenotypic characteristics of MAIT cells in adult peripheral blood are an effector memory phenotype defined as $CD45RO^{+}$, $CD62L^{lo}$, $CD95^{hi}$ $CD122^{int}$, $CD127^{int}$, and they express tissue-homing chemokine receptors: CCR5, CCR6, CXCR6 and intermediate levels of CCR9 (Dusseaux *et al.*, 2011). In contrast, MAIT cells do not express CCR7, a marker for trafficking to the lymph nodes.

1.3.1.2 Other MR1-restricted T cells

Production of the MR1 antigen-loaded tetramer identified a population of $tetramer^{+}$ cells that were TRAV1-2^{-}. These cells were found to have much more heterogeneous TCR usage compared to MAIT cells (Gherardin *et al.*, 2016). Structural analysis revealed that these atypical MR1-restricted cells TCR docking on MR1 was much more central with a different molecular footprint. This resulted in differing antigen affinity and specificity compared to MAIT cells.

These findings were supported by a functional study which isolated an MR1-restricted TRAV1-2^{-} clone that could respond to *Streptococcus pyogenes*, a species of bacteria known to lack the riboflavin synthesis pathway (Meermeier *et al.*, 2016). This suggested that MR1 could present non-riboflavin metabolite-derived ligands and stimulate non-classical MAIT

cells. Taken together, these studies revealed that there is greater diversity within the MR1-restricted T cell family than simply MAIT cells, as previously believed.

1.3.2 MAIT cell development

MAIT cells develop and undergo selection in the thymus and are selected by CD4/CD8 double-positive thymocytes, similar to invariant NKT cells (Seach *et al.*, 2013). It was only recently discovered that MAIT cells in mice and humans undergo a three-stage development pathway with each step being regulated by MR1 (Koay *et al.*, 2016). They develop from stage one ($CD161^{-}$ $CD27^{-}$) in the thymus where they egress at stage two ($CD161^{-}$ $CD27^{+}$) and continue to expand and mature into the cytokine-producing stage three ($CD161^{+}$ $CD27^{+}$) MAIT cells. Their maturation also requires expression of PLZF and miRNAs regulated by Drosha, similar to invariant NKT cells(Koay *et al*., 2016).

Thymic selection occurs independently of B cells and commensal flora (Martin *et al.*, 2009), however, B cells are essential for MAIT cell peripheral expansion and memory phenotype acquisition in mice (Martin *et al.*, 2009). This appears to be similar in humans as individuals with mutated Bruton's tyrosine kinase, where B cell development is disrupted, have lower MAIT cell TCR transcripts in the blood compared to healthy controls (Treiner *et al.*, 2003). These results are consistent with the observation that both primary B cells and B cell lines can efficiently present bacterial antigens to MAIT cells in an MR1-dependent manner (Salerno-Goncalves *et al.*, 2014). What continues to remain elusive is the identity and source of the antigen(s) capable of selecting MAIT cells in the thymus. Whether these selecting antigens are endogenous or sourced exogenously (such as maternal commensal flora-derived antigens crossing the placenta) is still unknown. An outline of MAIT cell development is shown in **Figure 1-4.**

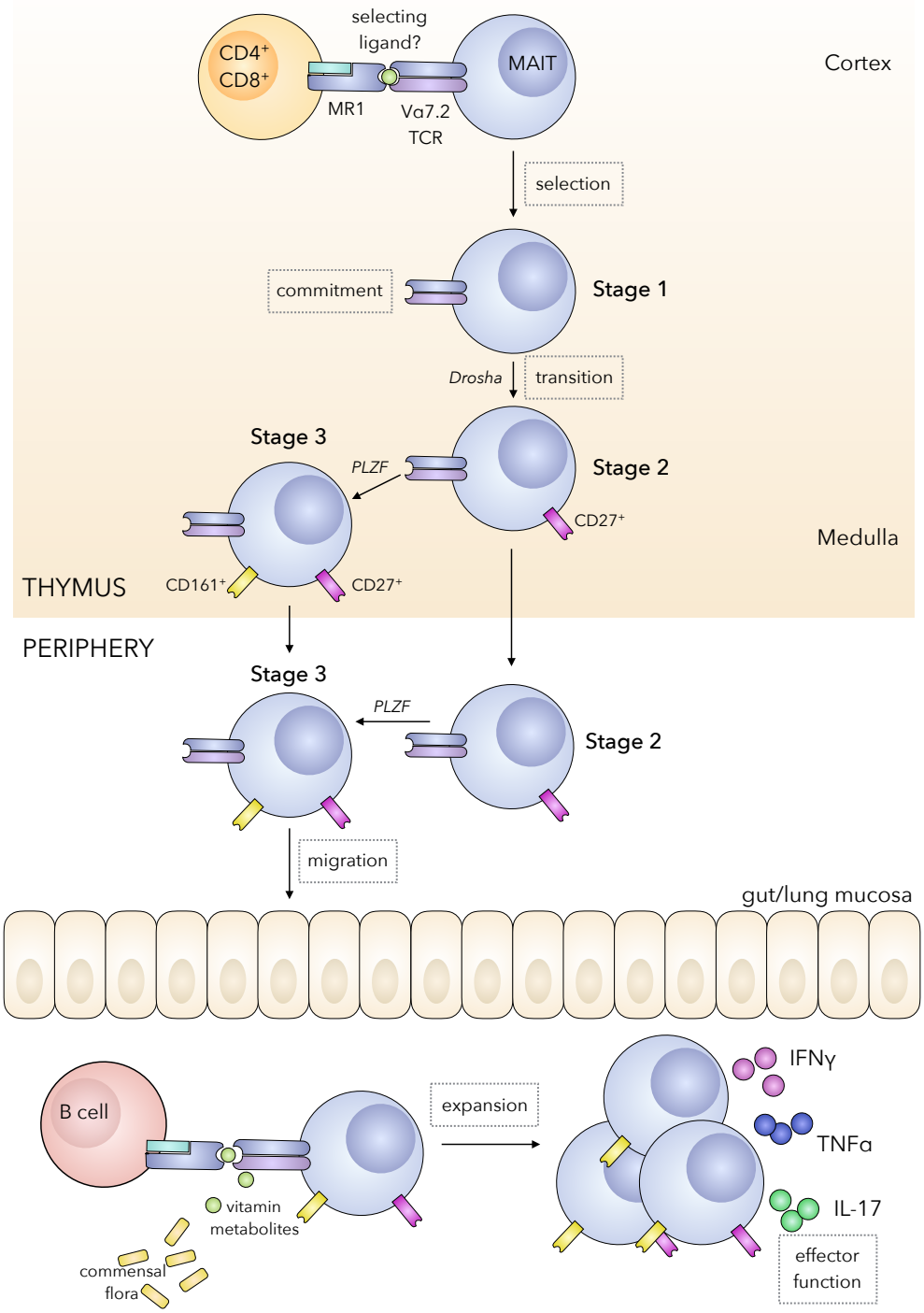

Figure 1-4 Overview of the development of MAIT cells

MAIT cells are selected in the thymus by double-positive (CD4/CD8) thymocytes expressing MR1. The selecting ligand presented by MR1 is yet to be identified. Selected MAIT cells then go through a three-stage development regulated by expression of MR1, Drosha and PLZF. They then leave and migrate to the periphery, where they interact with B cells, commensal flora (and their riboflavin vitamin metabolite by-products) and undergo expansion and acquisition of effector function with the ability to produce cytokines IFNγ, TNF and IL-17.

1.3.3 MAIT cell tissue distribution

MAIT cells are primarily located in mucosal tissues and blood. It was the expression of chemokine receptors CXCR6 and CCR9 by MAIT cells that suggested they traffic to the mucosal tissues. These tissues do have a high proportion of MAIT cells, composing 20–40% of liver T cells and 4–10% intestinal T cells (Dusseaux *et al.*, 2011, Tang *et al.*, 2013). There is also a high frequency of MAIT cells in human blood, composing 1–8% of T cells. A study analysing the TRAV1-2–TRAJ33 and TRAV1-2–TRAJ12 transcripts in different tissues revealed that MAIT cells are also present in the kidney and at a lower frequency in the tonsils and lymph nodes (Lepore *et al.*, 2014). They also reported variable expression of these transcripts in the prostate and ovary. Analysis of the TCRα chain usage revealed TRAV1-2/TRAJ33 is predominant in the blood and TRAV1-2/TRAJ12 is more predominant in the tissues indicating these might represent different MAIT cell subsets, which would explain the difference in their tissue-homing properties (Lepore *et al.*, 2014). What is not known is whether these two subtypes are functionally distinct in terms of their antigen/pathogen specificity or if they relate to infection history of the individual.

Circulating MAIT cells are more abundant than invariant NKT cells in humans, while MAIT cells in mice are less abundant than invariant NKT cells (Martin *et al.*, 2009, Tilloy *et al.*, 1999, Dusseaux *et al.*, 2011). Studies assessing the influence of age and gender of MAIT cells found that MAIT cells decrease with age, but are not significantly different between males and females (Lee *et al.*, 2014, Walker *et al.*, 2014, Novak *et al.*, 2014). The MAIT cell phenotype also changes depending on the tissue compartment they are found in. For example, liver MAIT cells have a more activated phenotype compared to blood MAIT cells, and they express higher levels of CD69, CD38 and HLA-DR, possibly reflecting continuous antigen exposure (Tang *et al.*, 2013).

1.4 MAIT cell activation

In 2010, two publications described a wide range of phylogenetically diverse bacteria and yeast that could activate MAIT cells. These microbes included: *E. coli*, *Pseudomonas aeruginosa*, *Klebsiella pneumoniae*, *Lactobacillus acidophilus*, *Staphylococcus aureus, Staphylococcus epidermidis, Saccharomyces cerevisiae, Candida glabrata* and *Candida albicans* (Le Bourhis *et al.*, 2010, Gold *et al.*, 2010). In contrast, viruses and some bacteria species such as *Enterococcus faecalis* and *Streptococcus* group A did not elicit MR1-dependent MAIT cell activation. This was later explained in 2012 when the MAIT cell ligand was discovered, as these bacteria lack the riboflavin synthesis pathway that produce the ligands that bind MR1 molecules and stimulate MAIT cells (Kjer-Nielsen *et al.*, 2012). An outline of modes of MAIT cell activation is outlined in **Figure 1-5**.

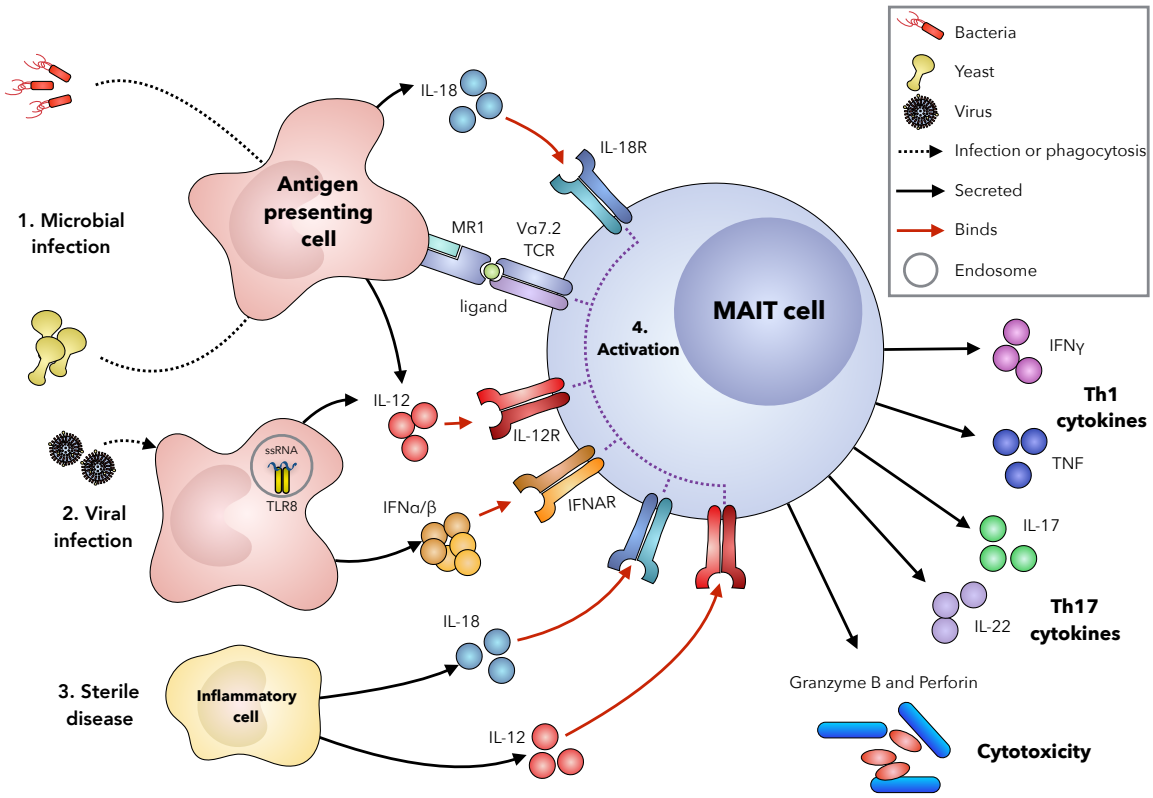

Figure 1-5 Overview of MAIT cell activation

(1) Bacteria or yeast stimulate MAIT cell activation by either infecting or being phagocytosed by an antigen presenting cell. These cells then present microbial-derived vitamin B metabolites via MR1 to the Vα7.2 TCR expressed by MAIT cells. The APCs can also produce IL-12 and IL-18 cytokines that can activate MAIT cells in a TCR-independent manner. (2) Viruses can stimulate MAIT cells through detection of pathogen-associated molecular patterns, such as single strand (ss)RNA by toll-like receptor (TLR)8, resulting in the production of IL-12 and IFNα/β. (3) In sterile disease, such as autoimmunity where cells pathologically express cytokines IL-12 and IL-18, can also activate MAIT cells. (4) The activation of MAIT cells results in the production of Th1 cytokines IFNγ and TNFα, Th17 cytokines IL-17 and IL-22 (particularly by small intestine resident MAIT cells) and perforin and granzyme B to directly kill infected cells.

1.4.1 Cytokine production

MAIT cells produce proinflammatory cytokines following activation. Stimulation with phorbol 12-myristate 13-acetate (PMA) and ionomycin or bacteria demonstrate that human MAIT cells are capable of producing IFNγ, TNFα, IL-2, and IL-17 (Dusseaux *et al.*, 2011, Tang *et al.*, 2013). *Ex vivo* mass cytometry in three donors reported that there are functionally distinct subsets of circulating MAIT cells that release different cytokine

combinations, most frequently macrophage inflammatory protein (MIP)1β, IFNγ, TNFα and IL-17, and to a lesser extent IL-4 and IL-10 (Lepore *et al.*, 2014). MAIT cells from the small intestine are also capable of producing IL-22 in response to *E. coli*, but this was not observed in MAIT cells from the liver or lung (Leeansyah *et al.*, 2014). Thus, MAIT cells have a mostly mixed T-helper(Th)1/Th17 cytokine profile with differences based on their peripheral location, possibly reflecting environmental imprinting.

1.4.2 Cytotoxicity

Another effector function of MAIT cells is cytotoxicity. In general, immune-mediated cytotoxicity occurs primarily through granule exocytosis and relies on the effector cell containing components that enable destruction of a target cell. These include perforin and granzymes that consist of five isoforms with different substrate specificities: granzyme (Gr)A, GrB, GrH, GrK and GrM (Pinkoski *et al.*, 1998).

MAIT cells have been shown to be able to lyse bacteria-infected epithelial cells (Le Bourhis *et al.*, 2013) and *E. coli*-infected THP1 cells (Kurioka *et al.*, 2014) in an MR1-dependent manner. At rest, human MAIT cells have a unique cytotoxic profile characterized by low perforin expression but high GrA and GrK that are contained in $CD107^{+}$ lytic granules (Kurioka *et al.*, 2014). Upon antigen stimulation, an MR1-dependent GrB upregulation and an MR1-independent perforin upregulation occurs, suggesting that antigen pre-exposure licenses MAIT cells to acquire a strong cytotoxic phenotype (Kurioka *et al.*, 2014). The ability to kill infected target cells suggests that MAIT cells could play an important role in clearing infections by intracellular bacteria. This has been addressed by infecting HeLa cells with *Shigella flexneri* and showing that the cells were readily killed by MAIT cells (Le Bourhis *et al.*, 2013).

1.4.3 MR1-independent activation

Like other unconventional αβ T cells, MAIT cells can also respond to infection in a TCR-independent manner. For example, the MAIT cell response to cells infected with *Mycobacterium bovis* Bacillus Calmette–Guérin (BCG) is largely MR1-independent *in vitro* (Chua *et al.*, 2012). The high expression of IL-18R on MAIT cells suggested that IL-18 could be one of the cytokines responsible for activating MAIT cells (Dusseaux *et al.*, 2011, Billerbeck *et al.*, 2010). This was confirmed by a study that showed that MAIT cells can produce IFNγ when their TCR is blocked if they are cultured in the presence of IL-18 and IL-12 (Ussher *et al.*, 2014).

Furthermore, it has been shown that cytokines can synergize with TCR stimulation to enhance MAIT cell activation. For example, liver-resident MAIT cells express high levels of IL-7R and IL-7 was shown to potentiate MAIT cells TCR-dependent secretion of Th1 cytokine and IL-17A (Tang *et al.*, 2013). Other cytokines that can act synergistically on MAIT cells to enhance their effector response include IL-15 and IFNα/β (van Wilgenburg *et al.*, 2016).

These results suggest that multiple factors could shape MAIT cells responsiveness during bacterial infection, and their ability to respond to cytokine stimulation, independent of the TCR. Therefore, MAIT cells could still have a role in controlling infections by microbes not containing MAIT cell ligands, such as viruses and certain bacterial species.

1.5 MAIT cells in bacterial infections

Mouse infection models and human infections have been studied to further our understanding of MAIT cells and their activation during pathological conditions. In a mouse model of lung infection with the live vaccine strain of *Francisella tularensis*, it was

demonstrated that MAIT cells colonise the lung in both early and intermediate phases of the infection, reach their peak expansion in the late clearance phase of infection and persist following clearance of the bacteria (Meierovics *et al.*, 2013). From day eight of infection onwards, MAIT cells in the lung produced IFNγ, TNFα and IL-17A. The evidence for the importance of MAIT cells in controlling infection came from MR1 knockout mice, which showed a delay in clearance of the bacteria in the lungs (but not in the spleen or liver) and delayed appearance of adaptive immune responses in the lung (Meierovics *et al.*, 2013). A similar increase in bacterial load in comparison with wild type mice was found when mice lacking MAIT cells were infected with *K. pneumonia* or *M. bovis* BCG (Chua *et al.*, 2012, Georgel *et al.*, 2011).

More recently, a study assessed the importance of MR1 and the riboflavin ligand in controlling *S.* Typhimurium infection in the mouse lung (Chen *et al.*, 2017). They found that both MR1 and the presence of the ligand are necessary for MAIT cell activation and migration into the lung. This suggests that MAIT cells role in controlling bacterial infections is MR1-dependent. Together, these studies indicate that the role of MAIT cells in controlling infection is not redundant, and is vital for timely mounting of effective adaptive immune responses.

1.5.1 Tuberculosis

The role of MAIT cells to anti-bacterial immunity in humans has been studied most extensively in *M. tuberculosis* infection. MAIT cells have been shown to respond *in vitro* to *M. tuberculosis* both in primary lung epithelium infected cells and dendritic cells (Gold *et al.*, 2010, Harriff *et al.*, 2014). In individuals with active *M. tuberculosis* infection, the frequency of circulating MAIT cells was lower compared to healthy individuals (Le Bourhis *et al.*, 2010, Gold *et al.*, 2010). This suggests that MAIT cells may migrate to inflamed

tissues, where they can have a localized response to infection. There is also evidence that there are tissue-resident MAIT cells that are enriched in the lung of healthy donors, and therefore, could be some of the early responders during infection (Gold *et al.*, 2010).

To assess whether reduced numbers of MAIT cells is accompanied by an altered functionality, a study has analysed the cytokine production by MAIT cells from individuals with tuberculosis in response to different stimuli. Despite low frequencies, a greater proportion of MAIT cells in individuals with active tuberculosis secreted IFNγ and TNFα in response to BCG stimulation as compared to healthy controls, although the overall response was still very low (Jiang *et al.*, 2014). More compelling evidence came from the observation that a lower proportion of MAIT cells responded to *E. coli* in the same cohort of infected individuals compared to healthy controls. These results suggest that there may be an overall enrichment of MAIT cells specific for BCG compared to *E. coli* upon *in vivo* antigen exposure.

This concept of pathogen-specific MAIT cell clonal expansion was suggested by a study reporting that the heterogeneity in the TCRα and TCRβ chain usage by MAIT cell clonotypes was directly related to their ligand specificity, and thus, to responses to different microbes (Gold *et al.*, 2014). While this is a very appealing hypothesis, it requires confirmation, as the MAIT cells assessed in this study were defined as $V\alpha7.2^{+}$ $CD8^{+}$ cells that produced TNFα in response to bacterial stimulation. Without using MAIT cell-specific markers, such as CD161, IL-18R, CD26 or the MR1 tetramer, this strategy could have included a proportion of conventional $V\alpha7.2^{+}$ T cells. Nevertheless, the TCRβ chain sequence has been shown to contribute to antigen binding specificity by a second study, where six MAIT cell TCRs with differing TCRβ chains were refolded and their biophysical parameters measured (Eckle *et al.*, 2014). This study showed that the CDR3β loop usage

has a direct impact on MAIT cell recognition of ligands through altering the TCR flexibility and contact with MR1 and the ligand (Eckle *et al.*, 2014). This structural evidence suggests a role of the TCR CDR3β loop in fine-tuning MAIT cell specificity.

Together, these studies suggest an exciting concept that this innate-like lymphocyte subset may be able to form memory-like responses upon selective expansion of specific MAIT cell clones following microbial exposure. If this is the case, the ability to form memory responses could have implications for the therapeutic use of MAIT cells.

1.5.2 Other bacterial infections

A decreased frequency in circulating MAIT cells have also been observed in individuals with cystic fibrosis that are also infected with the opportunistic pathogen *P. aeruginosa* (Smith *et al.*, 2014). In these individuals, the decreased MAIT cell frequency also correlated with cystic fibrosis pathogenesis, which included: lung disease severity, systemic inflammation and clinical status. However, whether the decreased frequency was a consequence of their migration to the airway mucosa, or alone had influenced colonisation and disease progression, was not addressed

The relevance of MAIT cells in invasive enteric infections was addressed in a human infection model of attenuated *Shigella dysenteriae* (Le Bourhis *et al.*, 2013). A decrease in frequency of circulating MAIT cells was observed on day 11 in subjects who received attenuated *S. dysenteriae* compared to controls. Individuals that responded to the vaccine by producing a specific IgA response, also had a higher baseline proportion of MAIT cells and an increased proportion of activated (HLA-DR^{+}) MAIT cells on day 11.

MAIT cells have also been studied in a clinical trial of the invasive enteric infection *S. enterica* serovar Typhi. In this study MAIT cells were observed to decrease in frequency,

become activated (HLA-DR$^+$ and CD38$^+$) as well as have a proliferative (Ki67$^+$) phenotype (Salerno-Goncalves *et al.*, 2017). Although *S.* Typhi is known to have a riboflavin biosynthetic pathway, and therefore the ability to induce MR1-driven responses, *in vitro* experiments to demonstrate the role of riboflavin metabolites and MR1 in the MAIT cell response to *S.* Typhi were not performed in this study.

MAIT cells have also been investigated in cases of severe infection with *Vibrio cholerae*. It was reported that MAIT cell activation (CD38$^+$), peaked seven days after the onset of infection (Leung *et al.*, 2014). In adults, the frequency of MAIT cells did not change upon infection, but interestingly, in children a significant and persistent decrease in MAIT cell frequency was observed. The reason for this age-related discrepancy is not clear and warrants further investigation. Similar to the *S.* Typhi study, *in vitro* experiments to assess the role of riboflavin metabolites and MR1 were not performed.

A decrease in MAIT cell frequency (but not in other subsets such as NKT or γδ T cells) was observed in severe infections requiring hospitalisation. Critically-ill patients admitted to the intensive care unit with sepsis had lower circulating levels of MAIT cells compared to healthy controls and non-septic critically-ill individuals (Grimaldi *et al.*, 2014). Patients with lower MAIT cell numbers were also more susceptible to hospital-acquired infections. Of interest, it was reported that streptococcal infections (for which certain bacteria strains do not stimulate MAIT cells *in vitro*) induced a less pronounced decrease in MAIT cell numbers compared with non-streptococcal infections, although there was a large overlap between groups and was not statistically significant.

Together, these studies provide evidence that MAIT cells could play an important role in the host immune response to bacterial infection as indicated by their activation and migration from circulation to locally-infected tissues.

1.6 MAIT cells in viral infections

1.6.1 Human immunodeficiency virus

Although it has been established that viral-infected cells do not directly activate MAIT cells *in vitro* (Le Bourhis *et al.*, 2010), several publications have investigated the frequency and activation of MAIT cells in human immunodeficiency virus (HIV). The rationale behind investigating MAIT cells in the context of HIV is because this virus increases the permeability of intestinal epithelia. This alteration can cause translocation of microbial products from the gastrointestinal tract, resulting in systemic immune activation (Brenchley *et al.*, 2006, Estes *et al.*, 2010).

Two groups reported that circulating MAIT cell frequency was low early in HIV infection when compared with healthy controls (Cosgrove *et al.*, 2013, Leeansyah *et al.*, 2013). This trend was also observed in individuals with chronic HIV, and the frequency was not restored following anti-retroviral therapy (Leeansyah *et al.*, 2013). As there was some speculation that the loss of MAIT cells could be a false result due to a downregulation of the MAIT cell marker CD161, MR1 tetramers loaded with 5-OP-RU confirmed the loss of MAIT cells as they showed that the tetramer-positive population is lower in frequency during HIV infection (Fernandez *et al.*, 2014).

The activation and effector function of circulating MAIT cells in HIV was also assessed and found to express less CD69 and produce less IFNγ and TNFα in response to *ex vivo* bacterial stimulation compared to healthy controls (Leeansyah *et al.*, 2013). Interestingly, after anti-retroviral therapy there was a partial restoration of cytokine production. However, it should be noted that this impaired activation and function of MAIT cells was not confirmed in a separate study (Fernandez *et al.*, 2014).

The MAIT cells in the rectal and colon mucosa of HIV infected individuals was also examined, and found to be lower in frequency, similar to circulating MAIT cells. However, the mucosal frequency could be restored after anti-retroviral therapy (Greathead *et al.*, 2014, Leeansyah *et al.*, 2013). The decline and possible impaired activation of MAIT cells in individuals with HIV are likely to affect the MAIT cells' ability to control bacteria and yeast infections, leaving the host extremely vulnerable and contributing to acquired immune deficiency syndrome (AIDS) pathogenesis.

1.6.2 Other viral infections

MAIT cells have also been studied in those infected with dengue virus, hepatitis C virus (HCV) and influenza virus. It was found that MAIT cells were activated in all three viral infections through the TCR independent mechanism of IL-18 in synergy with IL-12, IL-15 and/or IFNα/β (van Wilgenburg *et al.*, 2016). This activation of MAIT cells correlated with disease severity in dengue fever. IFNα treatment in HCV led to enhanced MAIT cell activation that was in parallel to an enhanced therapeutic response. These results suggest MAIT cells could be implicated in a wide range of viral infections, and their pathogenesis, due to their strong cytokine-driven responses.

1.7 MAIT cells in sterile diseases

The ability of MAIT cells to respond to cytokine stimulation suggests that these cells may play a role in sterile inflammation such as autoimmune disorders and cancer.

1.7.1 Autoimmune disorders

1.7.1.1 Multiple sclerosis

The role of MAIT cells in multiple sclerosis (MS) has been extensively researched. The MAIT cell TRAV1-2 TCR was identified in central nervous system MS lesions using single-

strand conformation polymorphism analysis (Illes *et al.*, 2004). Normal MAIT cell frequencies were observed in the blood of MS patients and MAIT cells were also detected in the cerebrospinal fluid of relapsing patients. This suggested a role for MAIT cells in the progression of this disease, which was functionally explored by a study using a mouse model for MS: experimental autoimmune encephalitis (EAE). In transgenic mice overexpressing the MAIT cell TCR MAIT cells protected against EAE through suppression of Th1 cytokine production and increased production of IL-10, primarily by B cells (Croxford *et al.*, 2006). It was also observed that in MR1 knockout mice, EAE was exacerbated, suggesting a new concept, where MAIT cells can have a regulatory role in inflammatory disorders.

However, conflicting results have emerged from human studies assessing the distribution of circulating MAIT cells in MS patients. A study of an Italian cohort assessing MAIT cells of monozygotic twins with discordant disease states showed a greater number of circulating $CD8^+$ $CD161^{++}$ cells in MS patients, compared with their healthy twin (Annibali *et al.*, 2011). In contrast, a study of a Japanese cohort showed decreased circulating MAIT cells in MS patients compared with healthy controls (Miyazaki *et al.*, 2011). This discrepancy between the two studies emphasises the difficulties of studies with human subjects and could be the result of confounding factors such as variation in the commensal flora or lifetime infection burden influencing the MAIT cell frequency differently in the two cohorts.

1.7.1.2 Other autoimmune disorders

IL-17A has been shown to be a vital component in the aetiology of psoriasis (Nograles *et al.*, 2008). As MAIT cells can produce this cytokine it was hypothesised that they might be the $CD8^+$ cells previously observed in psoriatic lesions. A study assessing this found that MAIT cells are present in the psoriatic lesions along with Th17 cells (Teunissen *et al.*, 2014). A more comprehensive study, which compared several skin conditions along with healthy

skin, found that MAIT cells are normally found in the skin, expressing the skin homing marker CD103. Although MAIT cells were found in all skin condition lesions, their frequency was elevated in dermatitis herpetiformis (Li *et al.*, 2016). These studies provided evidence that MAIT cells may contribute to skin inflammation, however, their activation in this setting is yet to be explored.

MAIT cells have also been studied in rheumatic diseases. It was found that individuals with systemic lupus erythromatosis (SLE) and rheumatoid arthritis had a lower frequency of circulating MAIT cells (Cho *et al.*, 2014, Chiba *et al.*, 2017). Furthermore, higher frequencies of MAIT cells have been detected in the synovial fluid of rheumatoid arthritis patients. MAIT cells from individuals with SLE had impaired activation, as they produced less IFNγ when infected with bacteria or stimulated with PMA and ionomycin. This impaired MAIT cell function was more prominent in individuals with a lower frequency of circulating MAIT cells, suggesting a correlation may exist between frequency and function. Conversely, in rheumatoid arthritis patients IFNγ secretion by MAIT cells was preserved. To assess whether the programmed cell death molecule 1 (PD-1) correlated with MAIT cell dysfunction, its expression on MAIT cells was assessed and found to be higher on MAIT cells from individuals with SLE compared to individuals with rheumatoid arthritis or healthy controls. However, after PD-1 blockade, MAIT cell activation was only partially restored. This suggested that other negative regulation mechanisms may be contributing to MAIT cell dysfunction in SLE.

Due to the abundance of MAIT cells in the small intestine mucosa they were hypothesised to be implicated in the pathogenesis of inflammatory bowel diseases (IBD) including Crohn's disease and ulcerative colitis. A study into this found a decrease in the frequency of circulating MAIT cells in Crohn's disease and ulcerative colitis compared with healthy

controls (Serriari *et al.*, 2014). A similar decrease in circulating MAIT cell frequency was reported in individuals with coeliac disease (Dunne *et al.*, 2013). It was also reported that there was a higher frequency of MAIT cells in inflamed compared to healthy intestinal tissues (Serriari *et al.*, 2014). Functional assessment of MAIT cells from individuals with IBD stimulated with PMA and ionomycin showed increased IL-17 production with increased IL-22 in ulcerative colitis but decreased IFNγ secretion in individuals with Crohn's disease. To further our understanding of the role of MAIT cells in IBD requires investigation into the MAIT cells from the inflamed gut tissues, to determine the extent of their pathogenic role.

1.7.2 Cancers

A less explored area of research is in to the potential role of MAIT cells in cancer. An early publication suggested MAIT cells may be present in renal and brain cancers through detection of their TCR transcripts in these tissues (Peterfalvi *et al.*, 2008). This presence correlated with the presence of pro-inflammatory cytokines in the tumour tissue, suggesting they could have anti-cancer functions.

Two more recent publications have assessed MAIT cells in colorectal cancer. They reported that the circulating MAIT cell frequency was decreased compared with healthy controls, and MAIT cells were detected infiltrating the tumour tissue (Ling *et al.*, 2016, Won *et al.*, 2016). They also made suggestions, based on preliminary data, that MAIT cells had cytotoxic (Won *et al.*, 2016) or cell cycle arresting (Ling *et al.*, 2016) MR1-restricted effector functions against cancer cells *in vitro*, although the exact mechanism for this needs further investigation. These studies provide preliminary evidence that MAIT cells could be implicated in cancer pathogenesis but further research needs to be done to determine the

mechanism, and whether MAIT cells are present and implicated in the pathogenesis of other types of cancer.

1.8 MAIT cells as a potential therapeutic target

MAIT cells may be an ideal cell to target and manipulate to enhance immune responses. This is due to their strong pro-inflammatory cytokine responses, ability to directly kill infected cells, capability of enhancing adaptive immune responses and now the ability to specifically target MAIT cells through the knowledge of their activating ligands and cytokines. Advances in understanding how to target and harness MAIT cell activity could assist in the designing of more effective vaccines and immunotherapies.

The use of bacteria as adjuvants to enhance immune responses was first explored in 1891, when William Coley injected of *S. pyogenes* and *Serratia marcescens* into tumours producing generalised inflammation and subsequent destruction of the tumour cells (Mellman *et al.*, 2011). This form of immunotherapy, using bacteria to stimulate anti-tumour immune responses, has not been highly successful with the notable exception of the intra-vesical instillation of BCG, the current gold standard treatment for non-invasive bladder cancer. Although successful, it is still not well understood what immune principles are underlying its success. It has previously been discussed that MAIT cells can respond to BCG-infected cells *in vitro* (Jiang *et al.*, 2014, Chua *et al.*, 2012). Understanding whether MAIT cells are key players in mediating the success of BCG immunotherapy may help in designing more targeted therapies and reveal the potential for MAIT cell-targeted immunotherapies for other cancers.

1.9 Project aims

With the recent discovery of MAIT cells and their vitamin metabolite antigens, there is great interest in understanding the role these cells may play in the pathogenesis of diseases of both sterile and non-sterile inflammation. Although observational studies have implicated MAIT cells in various diseases, the functional role these cells play is still largely unknown.

We hypothesise that MAIT cells use a combination of their innate and adaptive immune properties, particularly their TCR and its specificity to the vitamin metabolite ligand, in responding to various host inflammations.

To address this hypothesis, we set the following aims for this project:

1) Characterise the phenotype and function of MAIT cells during the non-sterile inflammatory setting of human *Salmonella* infection
2) Examine the TCR repertoire of MAIT cells during *Salmonella* infection
3) Determine whether MAIT cells are implicated in the sterile-inframammary setting of cancer
4) Examine the TCR repertoire of MAIT cells in cancer
5) Determine whether MAIT cells are playing a role in BCG immunotherapy for bladder cancer
6) Investigate how the MAIT cells TCR usage, identified in both infection and cancer, influences the MAIT cell response to antigen

Chapter 2 – Materials and Methods

2.1 Cell culture and media

2.1.1 Cell lines

THP1, C1R, K562 and J.RT3-T3.5 (JRT3) cell lines were cultured in R10 media composed of Roswell Park Memorial Institute (RPMI)-1640 (Sigma) supplemented with 10% foetal bovine serum (FBS) (Sigma), 1% penicillin/streptomycin (Sigma) and 2mM L-glutamine (Sigma). 293T cells were cultured in Dulbecco's Modified Eagle's Medium (DMEM) (Sigma) supplemented with 10% FBS, 1% penicillin/streptomycin and 2mM L-glutamine.

2.1.2 Primary MAIT cells

Sorted MAIT cells were cultured in Iscove's Modified Dulbecco's Medium (IMDM) (Gibco) supplemented with recombinant IL-2 (1000 U/mL) 5% human serum (Sigma), 1% penicillin/streptomycin, 2 mM L-glutamine, 1 mM sodium pyruvate (Gibco), 1X MEM non-essential amino acids (Gibco), 10 mM HEPES buffer solution (Gibco), 50 μM 2-mercaptoethanol (Gibco).

2.2 Human trials and samples

Healthy adult donors were laboratory volunteers or healthy leukocyte cones that were purchased from National Health Service (NHS) blood and transplant service.

2.2.1 BCG bladder cancer immunotherapy

Individuals undergoing treatment for high-risk non-invasive bladder carcinoma (aged 55–83) were recruited to the study. Treatment regime was weekly intravesical BCG (TICE® strain) therapy for six weeks, followed by maintenance doses every three months. Blood

samples were collected at various stages of treatment. Bladder tissue biopsies were taken after the treatment regime was completed.

2.2.2 Human *Salmonella* infection model

The human *S. enterica* serovar Paratyphi A infection model involved adult participants (aged 18–60) ingesting a single dose ($1–5\times10^3$ CFU) of *S.* Paratyphi A strain NVGH308 suspended in 20 mL $NaHCO_3$ solution. The following 14 days involved daily monitoring of blood and diagnosis was made if there was a positive blood culture for *S*. Paratyphi A or symptoms such as a persistently high (>38°C) temperature for more than 12 h. Participants took Ciprofloxacin (500 mg, twice daily) for 14 days once they were diagnosed, or after 14 days if remained asymptomatic and were not diagnosed.

2.2.3 Cancer samples

Renal cell carcinoma and ovarian cancer samples were obtained from individuals undergoing surgical resection of the tumour. For renal cell carcinoma, in addition to tumour core, adjacent non-cancerous tissue and blood was also collected. For ovarian cancers, ascites and blood were also collected.

2.2.4 Sample processing

Blood samples were collected in heparinised tubes and processed the same day. Blood samples were diluted in RPMI-1640 medium at a 1:1 ratio (or 1:12 for leukocyte cone). Up to 30 mL of diluted blood was overlaid onto 15 mL of Lymphoprep™ (AxisShield) and centrifuged for 30 min at 300 × *g* with no acceleration or brake. The peripheral blood mononuclear cell (PBMC) layer was collected and washed in RPMI-1640 medium.

Tissue samples were collected in MACS tissue storage solution (Miltenyi Biotec) and stored at 4°C (for up to 16 h) until processing. The tissue samples were processed using Human

Tumour Dissociation Kit (Miltenyi Biotec) following the manufacturer's instructions with mechanical digestion either performed by GentleMACS™ Dissociator or, if small biopsies, by pushing through 40 μm cell strainer. For some samples containing large amounts of red blood cells, Red Cell Lysis Buffer (Qiagen) was then added for 5 min and then cells were washed in RPMI-1640 medium.

2.2.5 Ethics

Written informed consent was obtained for all study volunteers in accordance with the Declaration of Helsinki and ethical approval was received from Oxford Research Ethics Committee. Samples obtained from the human *S.* Paratyphi A infection model were part of registered clinical trials (no. NCT02100397 and NCT02192008) and conformed to the Good Clinical Practice (GCP) guidelines.

Ethical approval for the BCG bladder cancer samples were collected under the Oxford Radcliffe Biobank (Medical Oncology Group) Research Tissue Bank, Urology Protocol ethical approval number 09/H0606/5. Renal cell carcinoma samples were collected under the OCHRe ethical approval number 13/A093. Ovarian cancer samples were collected under the ethical approval number 11/SC/0014. Cancer cryosections were cut by the Oxford Centre for Histopathology Research Centre and obtained under the ethical approval number 15/A147.

2.3 Flow cytometry and cell sorting

2.3.1 Antibodies

Table 2-1 Antibodies used for flow cytometry and cell sorting

TARGET (HUMAN)	CONJUGATED FLUOROPHORE	CLONE	SUPPLIER	CATALOGUE NUMBER
CD161	APC	HP-3G10	Biolegend	339912
CD25	PE-Cy™7	M-A251	BD Biosciences	557741
CD3	PE/Cy7	UCHT1	Biolegend	300420
CD3	APC/Cy7	HIT3a	Biolegend	300317
CD38	CF594	HIT2	BD Biosciences	562288
CD4	Alexa Fluor® 700	RPA-T4	Biolegend	300526
CD69	Pacific Blue™	FN50	Biolegend	310920
CD8	PerCP/Cy5.5	HIT8a	Biolegend	300923
GRANZYME B	PE	GB11	BD Biosciences	561142
IFN-γ	BV786	4S.B3	BD Biosciences	563731
IFN-γ	FITC	4S.B3	Biolegend	502506
IL-17A	PE	SCPL1362	BD Biosciences	560438
MOUSE IgG	Alexa Fluor 647®	-	Thermo-Fisher	A-21235
MR1	-	26.5	Biolegend	361103
TCR Vα7.2	BV605™	3C10	Biolegend	351720
TCR Vα7.2	PerCP/Cy5.5	3C10	Biolegend	351709
TCR γ/δ	BV421™	B1	Biolegend	331218
TNF	BV650	MAb11	BD Biosciences	563418
TNF	PE	MAb11	eBioscience	12-7347-81

2.3.2 Flow cytometry

2.3.2.1 Cell viability and surface staining

Cells were washed in phosphate buffered saline (PBS) and stained with LIVE/DEAD® Fixable Aqua Dead Cell Stain Kit (Life Technologies) for 10 min at room temperature, followed by addition of cocktail of antibodies (**Table 2-1**) for 20 min at 4°C. Cells were then washed in FACS buffer (PBS with 10% FBS).

For MR1 staining of cell lines, following Aqua dead cell staining, the cells were blocked in blocking buffer (PBS with 5% human serum and 1:20 dilution of Fc Receptor Binding Inhibitor Monoclonal Antibody (eBioscience)) for 20 min. Primary antibody diluted in

blocking buffer was then added for 30 min at 4°C. Cells were washed in FACS buffer then secondary antibody diluted in blocking buffer was added for 20 min at 4°C.

For fixing cells for flow cytometry, cells were washed in PBS and fixed in 100 µL IC Fixation Buffer (eBioscience) for 30 min at 4°C. Fixed cells were then resuspended in FACS buffer. Cells were stored at 4°C until analysed.

2.3.2.2 Intracellular staining

Cells were viability stained and fixed as described in Section 2.3.2.1. Cells were then permeabilised using Permeabilisation Buffer (eBioscience) diluted 1:10 in distilled water. The antibody cocktail was diluted in permeabilisation buffer and added to the cells for 45 min at room temperature. Cells were then washed in permeabilisation buffer then resuspended in FACS buffer. Cells were stored at 4°C until analysed.

2.3.2.3 Analysers and cell sorters

Flow cytometry data was collected on BD LSRFortessa™ X20 or Attune NxT (Thermo-Fisher Scientific). Cell sorting was performed on BD FACSAria™ Fusion Cell Sorter or BD FACSAria™ III. Data was analysed using FlowJo™ cell analysis software (FlowJo, LLC).

2.4 Mass cytometry

2.4.1 Antibody staining

Frozen cells were thawed, washed in R10 and pre-stained with the indicated antibodies listed in **Table 2-2** for 30 min at 37°C. Cells were left untreated at 37°C for 4 h in the presence of monensin and Brefeldin A.

Cells were washed twice in cold PBS, and incubated on ice with 200 µM cisplatin for 5 min. Cells were then washed with CyFACS buffer (PBS with 4% FBS and 0.05% sodium azide)

and stained with streptavidin α-Galactosylceramide (α-GalCer) with 10 μM free biotin for 30 min at room temperature. This was followed by incubation in primary antibody mix on ice for 30 min. Cells were then washed twice in CyFACS and stained with metal-tagged surface antibodies for 30 min. The cells were then washed twice with CyFACS and incubated in Foxp3 Fixation/Permeabilisation buffer (eBioscience) on ice for 30 min. Cells were then washed twice in 1 x Permeabilisation Buffer (Biolegend) and stained with biotin anti-human Foxp3 and metal-tagged intracellular antibodies for 30 min on ice. After washing twice in permeabilisation buffer, cells were incubated on ice with metal-tagged streptavidin for 10 min. Cells were then washed twice in permeabilisation buffer, once in PBS, and fixed in 2% paraformaldehyde (PFA) at 4°C. The following day, cells were washed twice in permeabilisation buffer and once with PBS. Cells were then incubated with cellular barcodes for 30 min as previously described (Wong *et al.*, 2015). Cells were then washed with permeabilisation buffer and incubated in CyFACS for 10 min on ice. Cellular DNA was labelled with 250 nM iridium interchelator (Fluidigm) diluted in PBS with 2% PFA for 20 min at room temperature. Cells were then washed twice with CyFACS and twice in distilled water prior to acquisition.

To accommodate the required numbers of samples, two barcoded batches were prepared, with each having comparable number of samples for each of the time-points. Mass-tag barcoding was used so all samples could be acquired simultaneously. A barcoded sample of PBMCs from a healthy donor was also included in batch as an internal control. EQ Four Element Calibration Beads (Fluidigm) were added at a final concentration of 1% prior to sample acquisition. Cells acquisition was performed on a CyTOF2 (Fluidigm).

2.4.2 Data analysis

After mass cytometry acquisition, the data was exported in flow cytometry file format, normalized (Finck *et al.*, 2013) and events with parameters having zero values were randomized using a uniform distribution of values between -1 and 0. Each sample containing a unique combination of two metal barcodes was de-convoluted using manual gating in FlowJo to select cells stained with two and only two barcoding channels.

Table 2-2 Antibodies used for mass cytometry

TARGET (HUMAN)	METAL	CLONE	SUPPLIER
anti-FITC (2°)	161	FIT-22	Biolegend
anti-PE (2°)	139	PE001	Biolegend
BCL-2	172	100	Biolegend
CCR2*	168	K036C2	Biolegend
CCR4	151	205410	R&D Systems
CCR5*	175	HEK/1/85a	Abcam
CCR6	170	G034E3	Biolegend
CCR7*	156	150503	R&D Systems
CCR9*	164	L053E8	Biolegend
CD103	150	B-Ly7	eBioscience
CD127	176	A019D5	Biolegend
CD16	209	3G8	Fluidigm
CD161*	162	HP-3G10	Biolegend
CD19	173	HIB19	Biolegend
CD25	169	M-A251	Biolegend
CD27*	157	LG.7F9	eBioscience
CD3	140	UCHT1	Biolegend
CD38	165	HIT2	Biolegend
CD4	149	SK3	Biolegend
CD45	89	HI30	Fluidigm
CD45RA	145	HI100	Biolegend
CD45RO	147	UCHL1	Biolegend
CD49a	154	TS2/7	Biolegend
CD49d	167	9F10	Biolegend
CD56	158	NCAM16.2	BD Biosciences
CD57	115	HCD57	Biolegend
CD8α	146	SK1	Biolegend
CLA	142	HECA-452	Biolegend
CX3CR1	174	K0124E1	Biolegend
CXCR3	163	49801	R&D Systems
CXCR5	166	RF8B2	BD Biosciences
Foxp3 biotin (1°)	-	PCH101	eBioscience
Granzyme B	144	CLB-GB11	Abcam
HLA-DR	141	L243	Biolegend
ICOS	159	C398.4A	Biolegend
Integrin β7*	171	FIB504	Biolegend
Ki-67	152	B56	BD Biosciences
PD-1	160	eBioJ105	eBioscience
Qdot800-CD14	112/114	TüK4	Invitrogen
Streptavidin (2°)	155	-	-
TCRγδ PE (1°)	-	5A6.E9	Invitrogen
Vα7.2*	143	3C10	Biolegend
Vδ1 FITC (1°)	-	REA173	Miltenyi Biotec
Vδ2	148	B6	Biolegend
α-GalCer	153	-	-

* indicates pre-stain antibody. 1°, primary antibody; 2°, secondary antibody.

2.5 Gene expression using lentiviral vectors

2.5.1 Generation of MR1 overexpressing cell lines

2.5.1.1 MR1 expression vector

The cloning strategy is outlined in **Figure 2-1**. A pHR vector containing the MR1 gene was used as a template to amplify the MR1 gene by conventional polymerase chain reaction (PCR) using Phusion® High-Fidelity DNA Polymerase master mix with HF buffer (NEB) and MR1 primers MR1_FW and MR1_RV (**Table 2-3**). The MR1 gene was then cut with *Bgl*II and *Xho*1 restriction enzymes (New England Biolabs) at 37°C for 90 min and products purified using QIAquick® PCR Purification Kit (Qiagen). A pHR-SIN-RAE-IRES-GFP vector (vector map shown in Appendix 1) was cut with *BamH*1 and *Xho*1 restriction enzymes (New England Biolabs) at 37℃ for 90 min to remove RAE. The vector was then dephosphorylated using Antarctic Phosphatase (New England Biolabs) at 37°C for 30 min before heat inactivation at 80°C for 2 min. The vector was gel purified using QIAquick® Gel Extraction Kit (Qiagen). The vector and MR1 insert were then ligated using T4 DNA ligase (New England Biolabs) for 3 h at room temperature.

2.5.1.2 Bacterial transformation

A 5 µL aliquot of the expression vector containing MR1 was transformed into 50 µL α-select competent cells (Bioline), by incubating for 10 min on ice, 45 sec at 42°C then 2 min on ice. After transformation, bacteria were incubated in 500 µL Lysogeny Broth (LB) at 37°C with shaking for 45 min. Transformed bacteria were plated on LB agar plates containing 100 µg/mL ampicillin (LB-AMP) and incubated overnight at 37°C. Single colonies were picked and grown in 5 mL LB-AMP broth at 37°C with shaking overnight. Cultures were then PCR screened for correct insert using MangoTaq™ DNA Polymerase PCR Kit (Bioline) following the manufacturer's instructions with MR1_FW and IRES_RV primers.

Positive cultures were purified using a QIAprep® Spin Miniprep Kit (Qiagen) and sequenced with SSFV_FW and IRES_RV primers and aligned using IGBLAST (NCBI) to the published MR1 sequence to confirm correct insertion.

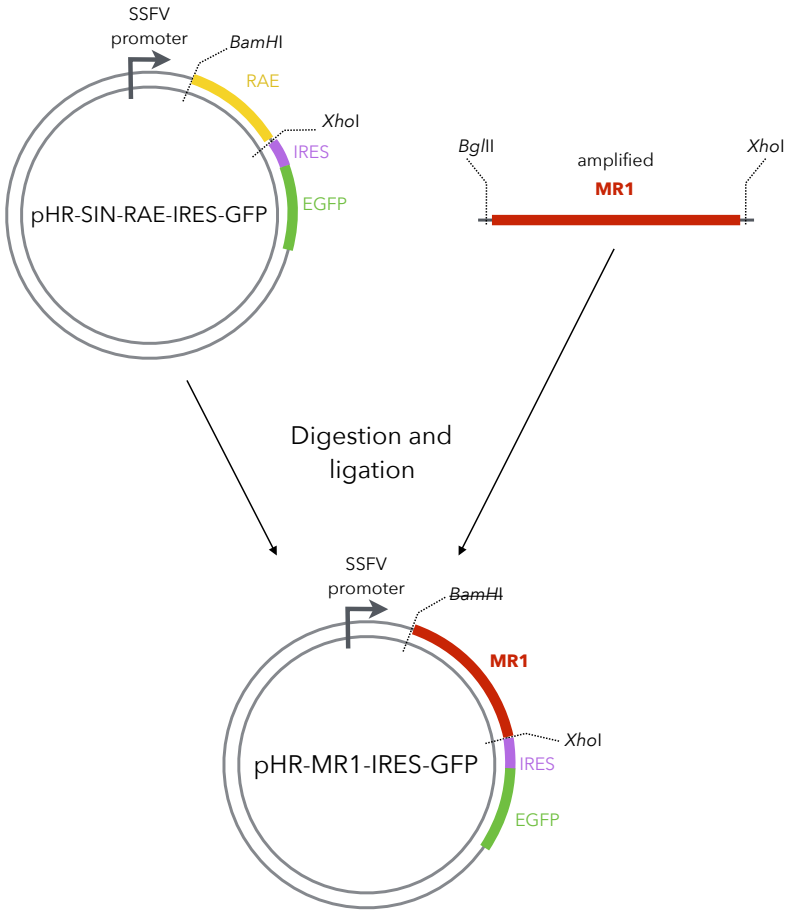

Figure 2-1 Cloning of MR1 into the pHR-SIN-IRES-RAE-GFP expression vector

The cloning strategy used to produce the MR1 overexpressing cell lines. Strikethrough indicates destruction of restriction site.

2.5.1.3 Lentiviral transduction

The MR1 vector (2 µg) was co-transfected into 293T cells with 1.4 µg HIV gag-pol expression plasmid and 1.4 µg VSV-G expression plasmid using 20.5 µL FuGENE 6 transfection reagent (Roche) following the manufacturer's instructions. After 72 h, the

culture supernatant containing the lentiviral particles was collected, centrifuged and used to transduce THP1, C1R and K562 cell lines. The GFP-positive cells from each cell line were cell sorted.

2.5.2 Generation of Jurkat.MAIT cell lines

The cloning strategy is outlined in **Figure 2-2**.

2.5.2.1 TCRα insertion into expression vector

To produce the MAIT cell TCRα chains of interest, primers were designed for the TCRα variable region TRAV1-2 leader sequence containing *Nco*I restriction site (LDRA/*Nco*I_FW) and the TCRα constant TRAC region containing *Not*I restriction site (TRAC/*Not*I_RV). Sorted MAIT cell complementary DNA (cDNA) (RNA extraction and cDNA synthesis protocol outlined in Section 2.7) was used as the template and Phusion® master mix was used to build the TCRα chain fragments by PCR products. The TCRα genes were then cut with *Not*I and *Nco*I restriction enzymes (New England Biolabs) as described in Section 2.5.1.1. A pHR-IRES-SIN-GFP expression vector was digested with *Not*I restriction enzyme as previously described in Section 2.5.1.1 followed by a partial digestion with *Nco*I restriction enzyme for 15, 30 and 45 min (due to a second restriction site contained within the vector backbone). The partially digested vector reactions were run on a gel, size selected for a single cut in the correct restriction site, then purified and dephosphorylated as previously described in Section 2.5.1.1. The TCRα chains were then ligated into the vector as described in Section 2.5.1.1, transformed and sequenced checked (using IRES_FW primer and TRAC/NotI_RV) as described in Section 2.5.1.2.

2.5.2.2 TCRβ insertion into expression vector

The TCRβ chain of interest with *BamH*I and *Xho*I restriction sites was either synthetically synthesized in forward and reverse fragments (TRBV6-1 fragment) (Integrated DNA Technologies) or constructed using overlapping primer design to produce forward and reverse fragments using Phusion® master mix with PBMC cDNA used as a template (list of TRBV6-4 and TRBV20-1 primers outlined in **Table 2-3**). The TCRβ chain genes were then cut with *BamH*I and *Xho*I restriction enzymes, ligated into the expression vectors (already containing the TCRα chain) and transformed into bacteria and sequenced as described previously in Sections 2.5.1.1 and 2.5.1.2, respectively.

2.5.2.3 Lentiviral transduction

The expression vector containing both TCRα and TCRβ chains (700 ng) was then co-transfected into 293T cells with 0.5 μg HIV gag-pol expression plasmid and 0.5 μg VSV-G expression plasmid using 5 μL X-tremeGENE™ 9 DNA Transfection Reagent (Sigma) following the manufacturer's instructions. After 48 h, the supernatant from the culture containing the lentiviral particles was harvested, centrifuged and used to transduce JRT3 cells. The TCR expression was confirmed by CD3 and Vα7.2 expression and positive cells were sorted.

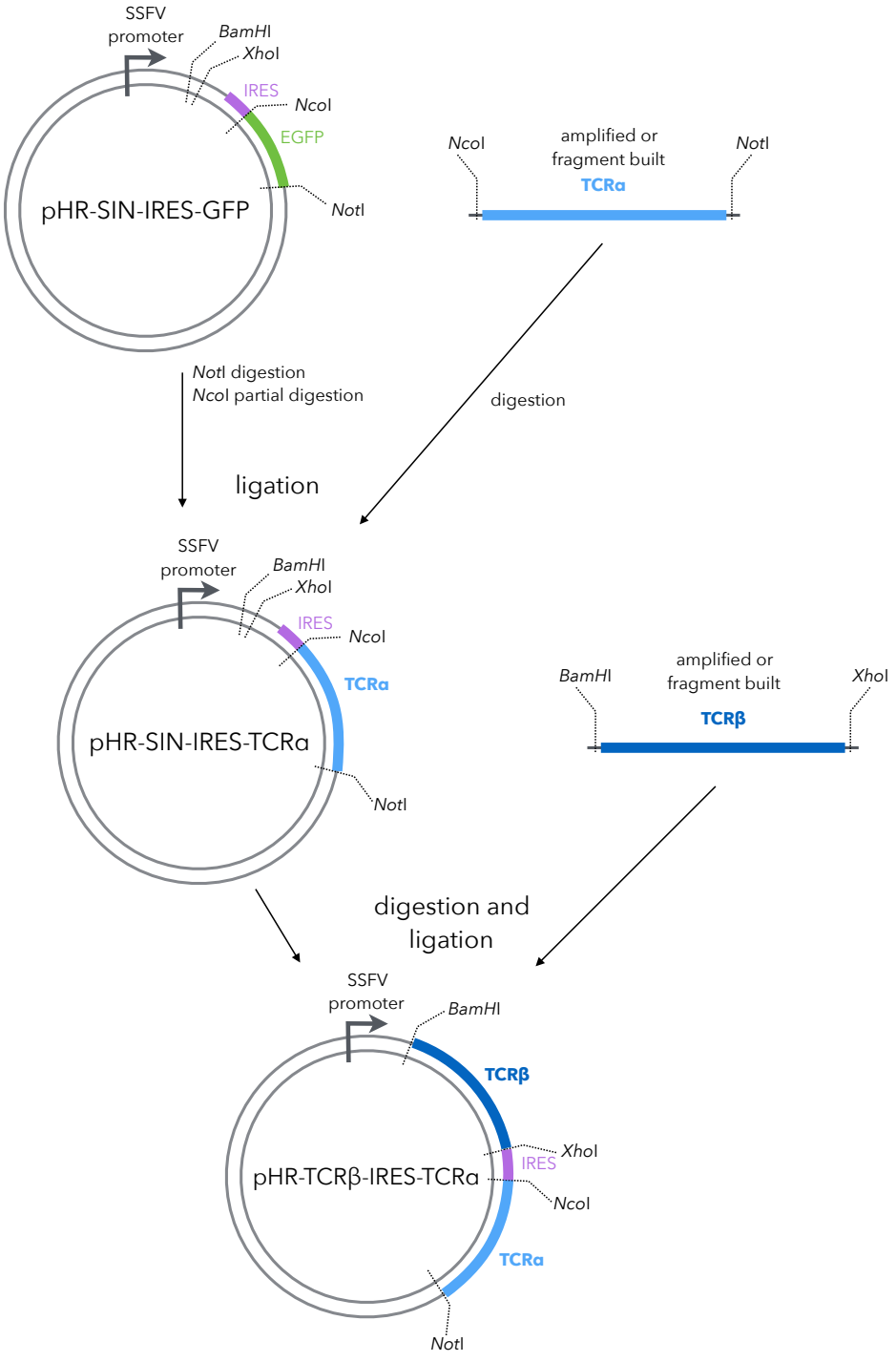

Figure 2-2 Cloning of TCRα/β into the pHR-SIN-IRES-GFP expression vector

The two-step cloning strategy used to produce the Jurkat.MAIT cells expressing TCRα and TCRβ chains of interest.

2.5.3 Primers

All primers for cloning and sequencing were ordered from Integrated DNA Technologies and resuspended to 100 µM stock in nuclease-free water (Ambion). Primer working concentration for all PCR reactions was 10 µM.

Table 2-3 Primers used for cloning and sequencing

PRIMER NAME	PRIMER SEQUENCE (5'-3')	USE
IRES_FW	CGAACCACGGGGACGTGG	Sequencing
IRES_RV	ACATATAGACAAACGCACACCG	Sequencing
LDRA/*Nco*I_FW	GGC**CCATGG**TGTGGGGAGTTTTCCTTC	Cloning
LDRB/20-1_FW	CTGGGGCCAGGCTCCGGGCTTGGTGCTGTCGTCTCTCA ACATC	Cloning
LDRB/6-4_FW	CTGGGGCCAGGCTCCGGGCTTATTGCTGGGATCACCCA GGCAC	Cloning
LDRB/*BamH*1_FW	AAT**GGATCC**ACCATGCTGCTGCTTCTGCTGCTTCTGGG GCCAGGCTCCGGGC	Cloning
MR1_FW	CCG**AGATCT**CCACCATGGGGGAACTGATGGCGTTCC	Cloning
MR1_RV	CCG**CTCGAG**TCATCGATCTGGTGTTGGAAG	Cloning
SSFV_FW	TGCTTCTCGCTTCTGTTCG	Sequencing
TRAC/*Not*I_RV	AAT**GCGGCCGC**TCAGCTGGACCACAGCCGCAG	Cloning/ sequencing
TRBC2/*Xho*I_RV	AAT**CTCGAG**TTAGCCTCTGGAATCCTTTCTCTTG	Cloning
TRBJ2-1/C_FW	GATGAGCAGTTCTTCGGGCCAGGGACACGGCTCACCGT GCTAGAGGACCTGAAAAACGTG	Cloning
TRBJ2-7/C_FW	CTACGAGCAGTACTTCGGGCCGGGCACCAGGCTCACGG TCACAGAGGACCTGAAAAACG	Cloning
TRBV20-1/J2-7_RV	CGGCCCGAAGTACTGCTCGTAGTCCCGCTGCCTAGCAC TGCAGATGTAGAAGCTGCTGTC	Cloning
TRBV6-4/J2-1_RV	CCCGAAGAACTGCTCATCGCTAGTCCCGTCACTGCTGG CACAGAAGTACACAGATGTCTG	Cloning

Enzyme restriction sites are show in **bold** (*Bgl*II, *Xho*1, *BamH*I, NcoI, *Not*I). LDRA, leader sequence alpha chain; LDRB, leader sequence beta chain; FW, forward primer; RV, reverse primer.

2.6 *In vitro* infection

2.6.1 Preparation of bacterial stocks

All work involving *S.* Paratyphi A was carried out in a CAT3 facility. *S.* Paratyphi A strain NVGH308 and *E. coli* strain DH5*α* were plated on LB agar plates overnight at 37°C. A single colony was picked and the bacteria plated and incubated overnight at 37°C. A single

colony was chosen and grown in LB supplemented with 10% sucrose (LB-S) at 37°C with shaking overnight. A 100 mL LB-S was inoculated with the overnight culture 1:100 and grown at 37°C with shaking for 3 h (known log-phase growth point). Frozen aliquots were stored at -80°C. The colony forming units (CFU) for each bacterial stock was calculated by plating diluted 10 uL droplets of the bacterial stock onto LB agar plates, incubating overnight at 37°C and colonies counted the following day.

2.6.2 PBMC infection

PBMCs were infected with live *S.* Paratyphi A strain NVGH308 or *E. coli* strain DH5*α* at a multiplicity of infection (MOI) ranging from 1–10 and incubated at 37°C for 1 h. Extracellular bacteria was then killed by adding 100 μg/mL gentamicin (Sigma) and samples incubated at 37°C overnight. For BCG infection, frozen stocks of BCG (TICE strain) vaccine diluted in PBS was added at an MOI of 0.1 to PBMCs and left overnight. For fixed *E. coli* infection, bacteria were fixed in 4% PFA for 30 min, washed in PBS and stored in frozen aliquots. For intracellular cytokine staining, 5 μg/mL Brefeldin A solution (Biolegend) was added and samples incubated for 6 h at 37°C. Samples were then stained and analysed by flow cytometry as described in Section 2.3.

2.6.3 Antigen presenting cell line co-culture

For live infection, C1R.MR1 cells were incubated at 37°C with live bacteria for 1 h prior to addition of 100 μg/mL gentamicin (Sigma) and Jurkat.MAIT cells (at an effector:target ratio of 2:1). Samples were incubated at 37°C for 16–18 h. For bacterial supernatant infections, LB was inoculated with bacteria and incubated at 37°C with shaking overnight. The following day LB was re-inoculated at 1:100 with bacteria and incubated at 37°C with shaking for 6 h. C1R.MR1 and Jurkat.MAIT cells (at an effector:target ratio of 2:1) were plated and the supernatant added and incubated at 37°C for 16–18 h. For ligand experiments,

RL-6,7-DiMe (Toronto Research Chemicals) or methylglyoxal (MG) with 5-amino-6-(D-ribitylamino)uracil (5-A-RU) (synthesized by Gurdyal Besra, University of Birmingham) was added directly to C1R.MR1 cells. Cells were then incubated at 37°C for 18–20 h. For MR1 blocking experiments, 10 μg/mL anti-MR1 antibody (clone 26.5, Biolegend) or mouse immunoglobulin (Ig)G2a isotype control (Biolegend) were pre-incubated for 1 h with C1R.MR1 cells prior to addition of bacteria/ligand. Samples were then stained and analysed by flow cytometry as described in Section 2.3.

2.7 Quantitative PCR

RNA was extracted from cells using the RNeasy Mini Kit (Qiagen) following the manufacturer's instructions. A column DNase treatment was performed using RNase-free DNase Set (Qiagen). cDNA was synthesised by High-Capacity cDNA Reverse Transcription Kit (Applied Biosystems) following the manufacturer's instructions. qPCR was performed using commercially available TaqMan® probes (Life Technologies) for MR1 (Hs01042278_m1) and glyceraldehyde 3-phosphate dehydrogenase (GAPDH) (Hs02786624_g1). Each reaction contained 10 ng cDNA, TaqMan® master mix, TaqMan® probe and nuclease-free water (Ambion). Samples were run in duplicate on 7500 Fast Real-Time PCR System (Applied Biosystems).

2.8 TCR repertoire analysis

2.8.1 RNA extraction

Samples for TCR repertoire analysis were either sorted directly into lysis buffer (if ≤10 000 cells) or sorted into FACS buffer, followed by centrifuging at 1000 × *g* and resuspended in the lysis buffer from the appropriate RNA extraction kit. For fresh samples, RNA was

extracted from cells using RNAqueous® Total RNA Isolation Kit (Ambion) following the manufacturer's instructions.

2.8.1.1 RNA extraction from fixed cells

For samples that were fixed and permeabilised prior to sorting, RNA was extracted following a published protocol (Hrvatin *et al.*, 2014). Briefly, cells were sorted into FACS buffer, then centrifuged at 3000 × g for 5 min at 4°C. RNA was isolated using RecoverAll™ Total Nucleic Acid Isolation Kit for FFPE (Ambion), starting from the protease digestion step and following the manufacturer's instructions.

2.8.2 TRAV1-2 TCRα repertoire analysis

cDNA was synthesised using the oligo-dT primer method of the RETROscript® Kit (Ambion) following the manufacturer's instructions. The TCRα chain was amplified by PCR using Phusion® master mix and primers specific for TRAV1-2 (TRAV1-2_FW) and the TRAC region (AC1R_RV) primer details outlined in **Table 2-4**. The PCR products were purified using PCR purification kit. A 1 µL aliquot of the purified product was used as a template for a second nested PCR using primers Smart_TRAV1-2_FW and AC2R_RV. PCR product was purified and 1 µL of this reaction was used as a template for a third nested PCR using primers Step_1_FW and Hum_bcj_RV containing a barcoded sequence. Samples were then purified, concentration measured by Qubit fluorometric quantitation using the Qubit® dsDNA HS Assay kit (Thermo Fisher). Up to 20 samples were then pooled for MiSeq analysis.

2.8.3 TCRβ repertoire analysis

Template switch cDNA synthesis was performed using a Switch_oligo primer, SMARTScribe™ Reverse Transcriptase (Clontech) and a TRBC region primer BC1R_RV

following a previously published protocol (Mamedov *et al.*, 2013). A 1 μL aliquot of cDNA was then used in a nested PCR using Phusion® master mix with Smart20_FW primer and BC2R_RV primer. Products were purified using PCR purification kit. A 1 μL aliquot of PCR product was then used in a second nested PCR using primers Hum_step1_FW and Hum_bcj_RV containing a barcoded sequence. Samples were then purified, concentration measured and pooled as described in Section 2.8.2.

2.8.4 Primers

Table 2-4 Primers used for TCR repertoire analysis

PRIMER NAME	PRIMER SEQUENCE (5′-3′)	USE
AC1R_RV	ACACATCAGAATCCTTACTTTG	TCRα
AC2R_RV	TACACGGCAGGGTCAGGGT	TCRα
BC1R_RV	CAGTATCTGGAGTCATTGA	TCRβ
BC2R_RV	TGCTTCTGATGGCTCAAACAC	TCRβ
HUM_ACJ_RV	NNNN(XXXXX)GGGTCAGGGTTCTGGATAT	TCRα
HUM_BCJ_RV	NNNN(XXXXX)ACACSTTKTTCAGGTCCTC	TCRβ
HUM_STEP1_FW	NNNN(XXXXX)CACTCTATCCGACAAGCAGT	TCRα/β
SMART20_FW	CACTCTATCCGACAAGCAGTGGTATCAACGCAG	TCRβ
SMARTTRAV1-2_FW	CACTCTATCCGACAAGCAGTCAGCAACATGCTGGCGAAGC	TCRα
SWITCH_OLIGO	AAGCAGTGGTATCAACGCAGAGTACTCTT(rG)$_3$	TCRβ
TRAV1-2_FW	CAGCAACATGCTGGCGAAGC	TCRα

Primer sequences based on those already published (Mamedov *et al.*, 2013). (XXXXX) indicates barcoded sequences, N indicates randomly assigned nucleotide.

2.8.5 Next generation sequencing

Samples were prepared for next generation sequencing using NEBNext® Ultra™ DNA Library Prep Kit for Illumina® and NEBNext® Singleplex Oligos for Illumina® following the manufacturer's instructions. Samples were sequenced on Illumina MiSeq platform using MiSeq reagent kit V2 300 cycle (Illumina). Samples were analysed using MiLaboratory MiTCR software (Bolotin *et al.*, 2013) and post-analysis performed using MiLaboratory VDJTools software (Shugay *et al.*, 2015) and tcR software (Nazarov *et al.*, 2015).

2.9 Immunohistochemistry

Frozen sections were thawed at room temperature for 15 min. Sections were fixed by adding 4% Formaldehyde Pierce™, Methanol-free (Thermo Scientific) for 10 min. Sections were washed in tris-buffered saline (TBS) containing tween (0.01%) (TBS-T) twice before blocking endogenous peroxidase activity with Peroxidase Block (Dako) for 15 min. Sections were washed with TBS-T and Protein Block, Serum-free (Dako) was added and incubated for 15 min. Slides were drained and primary antibody added, diluted in Antibody Diluent (Dako). Slides were incubated for 1 h prior to washing in TBS-T and addition of EnVision+ System-HRP Labelled Polymer Anti-mouse (Dako) for 30 min. Sections were washed prior to adding Liquid DAB+ Substrate Chromogen System (Dako) for 10 minutes. Sections were washed in water and counterstained in Haematoxylin Solution, Mayer's (Sigma) for 3 min. After washing in water, sections were blued in ammoniated water for 2 min. Slides were then mounted in Limonene Mounting Medium (Abcam) and cover-slipped. All images were captured on a light microscope (Leica) with ×20 objective.

Table 2-5 Antibodies used for immunohistochemistry

TARGET (HUMAN)	CLONE	SPECIES	SUPPLIER	CATALOGUE NUMBER
CD3	-	Rabbit	Dako	A0452
TCR Vα7.2	3C10	Mouse	Biolegend	351702
IgG1	MOPC-173	Mouse	Biolegend	400124

2.10 IFNγ ELISpot

For IFNγ ELISpot experiments, APC lines were infected with either *E. coli* and or BCG (TICE strain) as described in Section 2.6.2. After overnight incubation at 37°C, APCs were plated 20 000 cells/well of a Polyvinylidene fluoride membrane plate that had been coated with capture monoclonal antibody (1-D1K) from the Human IFN-γ ELISpot BASIC (ALP)

kit (Mabtech). MAIT cells were added 5 000/well and the coculture was incubated at 37°C for 48 h. The ELISpot plate was developed following the manufacturer's instructions using SIGMAFAST™ BCIP®/NBT (Sigma). Spots were counted on an ELISpot Reader.

2.11 Confocal microscopy

Cell suspensions were fixed in 4% PFA for 30 min at 4°C. Cells were attached to frosted microscope slides by cytospinning for 5 min at 500 RPM. The slides were then blocked for 1 h in PBS containing 5% human serum (Sigma), 5% goat serum (Sigma), 5% FBS and 0.1% triton. Primary MR1 antibody (26.5, Biolegend) diluted in blocking buffer was added and incubated overnight at 4°C. Cells were then washed and anti-mouse IgG Alexa Fluor 647® (Thermo Fisher) secondary antibody diluted in blocking buffer was added and incubated for 1 h at room temperature. Cells were washed before mounting with Fluoromount-G™ , with DAPI (Invitrogen). Images were acquired on a Zeiss LSM 780 inverted confocal microscope.

2.12 Statistical analysis

Statistical analysis was performed using Prism software (Graphpad). Student's paired T test or Student's unpaired T test was used to determine statistical significance between two groups. One-way analysis of variance (ANOVA) with Dunnett's test to control for multiple comparisons was used when determining statistical significance across three or more groups. For assessing correlation between two (nonparametric) measures, Spearman's rank was used. A result was considered significant where $P < 0.05$.

Chapter 3 – Characterisation of MAIT cells in a human infection model of *S.* Paratyphi A

The response of MAIT cells to bacteria has been extensively studied *in vitro,* with limited *in vivo* studies due to their low proportion and altered phenotype in mice. We utilized a controlled human infection model of live *S.* Paratyphi A to further our understanding of the dynamic response of MAIT cells during a bacterial infection.

3.1 Healthy MAIT cell response to *in vitro S.* Paratyphi A infection

3.1.1 Healthy donor MAIT cells are activated in a partially MR1-dependent manner to *in vitro S.* Paratyphi A infection

To determine whether MAIT cells from healthy adult donors would be activated by *S.* Paratyphi A, a bacterial species known to have the riboflavin synthesis pathway that produce MAIT cell ligands, PBMCs were infected with either live *S.* Paratyphi A or *E. coli in vitro* and analysed by flow cytometry. The flow cytometry and cell sorting gating strategy used to identify Vα7.2^{+} CD161^{+} MAIT cells is outlined in **Figure 3-1A**.

In response to *S.* Paratyphi A *in vitro* infection, we observed 17.2±3.4% of MAIT expressing CD38, a marker of activation (**Figure 3-1B**). The activation was similar but overall lower than the response induced by the known MAIT cell activating bacteria *E. coli,* in which 34.6±8.4% MAIT cells were activated at the same multiplicity of infection (MOI). Activation in response to *S.* Paratyphi A was reduced to 11.9±3.1% CD38^{+} MAIT cells by the addition of an anti-MR1 blocking antibody and significantly reduced to 14.7±4.6% CD38^{+} MAIT cells in response to *E. coli*. These findings demonstrate that MAIT cell activation in response to *S.* Paratyphi A is partially MR1-dependent.

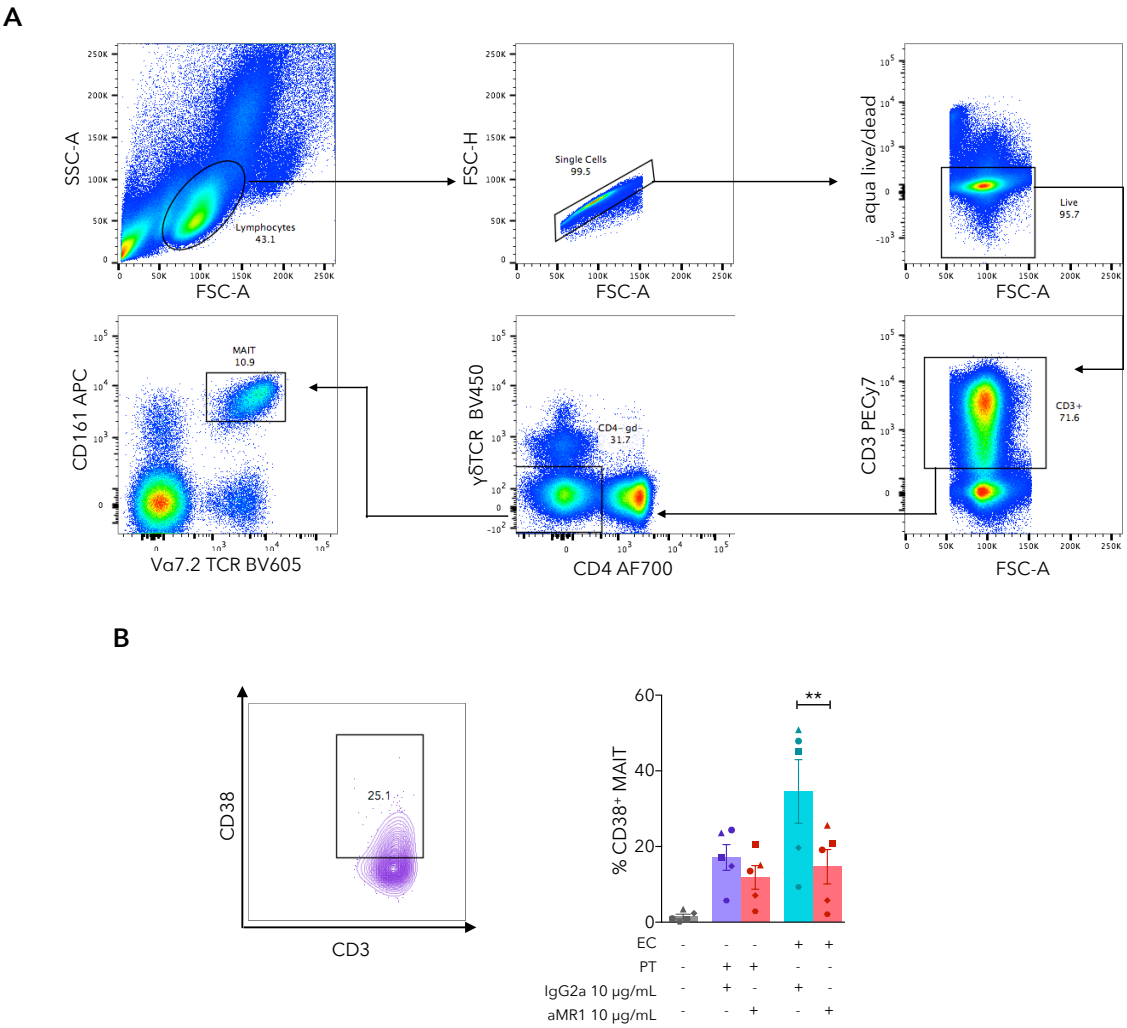

Figure 3-1 Healthy MAIT cell activation in response to *S.* Paratyphi A *in vitro* infection

PBMCs were isolated from five healthy donors and exposed to live *S.* Paratyphi A (PT) multiplicity of infection (MOI) 5 or *E. coli* (EC) MOI 5 *in vitro* with anti-MR1 blocking antibody (aMR1) or IgG2a isotype control. (A) Cells were analysed by flow cytometry and the gating strategy used to identify MAIT cells is shown. (B) MAIT cells were assessed for expression of CD38. Example contour plot shows CD38 expression on MAIT cells in response to PT. On the bar graph each symbol represents a donor, error bars represent standard error of the mean (SEM). Statistical significance calculated using Student's two-tailed paired T test, where ** $P < 0.01$. FSC, forward scatter; SSC, side scatter.

3.1.2 Healthy donor MAIT cells produce pro-inflammatory cytokines and cytotoxic granules in a partially MR1-dependent manner to *in vitro S.* Paratyphi A infection

To determine whether the MAIT cell activation in response to *S.* Paratyphi A was coupled with enhanced effector function, we assessed the pro-inflammatory cytokine and cytotoxic granule production by MAIT cells after *in vitro* infection.

We observed 67.0±5.7% of MAIT cells producing the cytotoxic granule GrB in response to *S.* Paratyphi A, and 90.6±2.8% in response to *E. coli* (**Figure 3-2A**). Both *S.* Paratyphi A and *E. coli* induced GrB production significantly decreased after addition of an anti-MR1 blocking antibody to 50.8±8.7% and 58.3±6.5% respectively. We then analysed the cytokine production by MAIT cells and found 19.8±6.2% produced IFNγ and 4.6±1.2% produced TNF in response to infection *S.* Paratyphi A (**Figure 3-2B**). The MAIT cell cytokine production in response to *E. coli* was higher for IFNγ (37.0±8.7%) but similar for TNF (4.6±0.96%). The TNF production by MAIT cells in response to *S.* Paratyphi A was significantly dependent on MR1, with the addition of an anti-MR1 blocking antibody decreasing TNF close to baseline levels (0.56±0.2%).

As MAIT cell responses can also be cytokine driven, we used both MR1 and IL-12 blocking antibodies at different concentrations to establish their contributions to the MAIT cell effector function against *S.* Paratyphi A infection. We observed that, similar to MR1 blocking causing a partial reduction in effector function, IL-12 also caused a partial reduction (or in the case of IFNγ, a complete reduction) in the MAIT cell effector response to *S.* Paratyphi A (**Figure 3-2C**). By using a combination of IL-12 and MR1 blocking antibodies, we observed GrB, IFNγ and TNF decrease to their no stimulation baseline level.

These results demonstrate that the MAIT cell response to *S.* Paratyphi A is both MR1- and IL-12-dependent, with TNF production being the most MR1-restricted effector response.

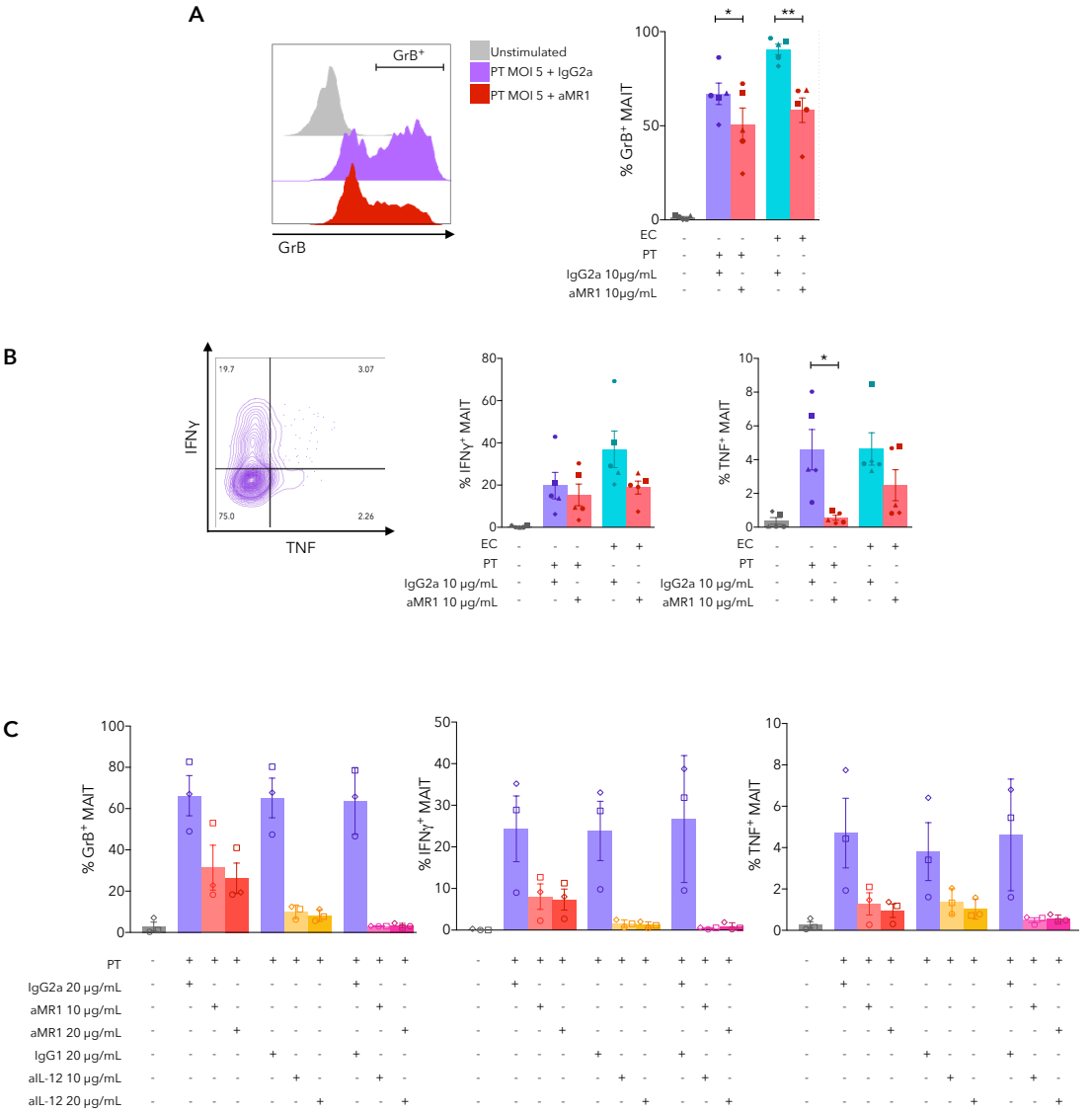

Figure 3-2 Healthy MAIT cell cytokine and cytotoxic granule production in response to *S.* Paratyphi A *in vitro* infection

PBMCs were isolated from healthy donors and exposed to live *S.* Paratyphi A (PT) multiplicity of infection (MOI) 5 or *E. coli* (EC) MOI 5 *in vitro* with anti-MR1 blocking antibody (aMR1) or IgG2a isotype control (n = 5). Cells were analysed by flow cytometry and MAIT cells were assessed for intracellular expression of (A) Granzyme B (GrB), and cytokines (B) IFNγ and TNF. Statistical significance calculated using Student's two-tailed paired T test, where * $P < 0.05$ and ** $P < 0.01$. (C) Comprehensive blocking experiments of the effector function of MAIT cells from healthy donors (n = 3) in response to live *in vitro* infection with *S.* Paratyphi A MOI 5 using varying concentrations of aMR1 and IL-12p40 blocking antibody with corresponding isotype controls IgG2a and IgG1, respectively. For all graphs, each symbol represents a donor and error bars represent SEM.

3.2 Characterisation of MAIT cell responses in a human *S.* Paratyphi A infection model

3.2.1 MAIT cells decrease in frequency and become activated in individuals challenged with *S.* Paratyphi A and diagnosed with enteric fever

Using a human model of *S.* Paratyphi A, we assessed the phenotype and function of circulating MAIT cells in individuals during infection compared to a baseline (pre-infection) sample. An outline of the infection model and blood sampling is shown in **Figure 3-3.**

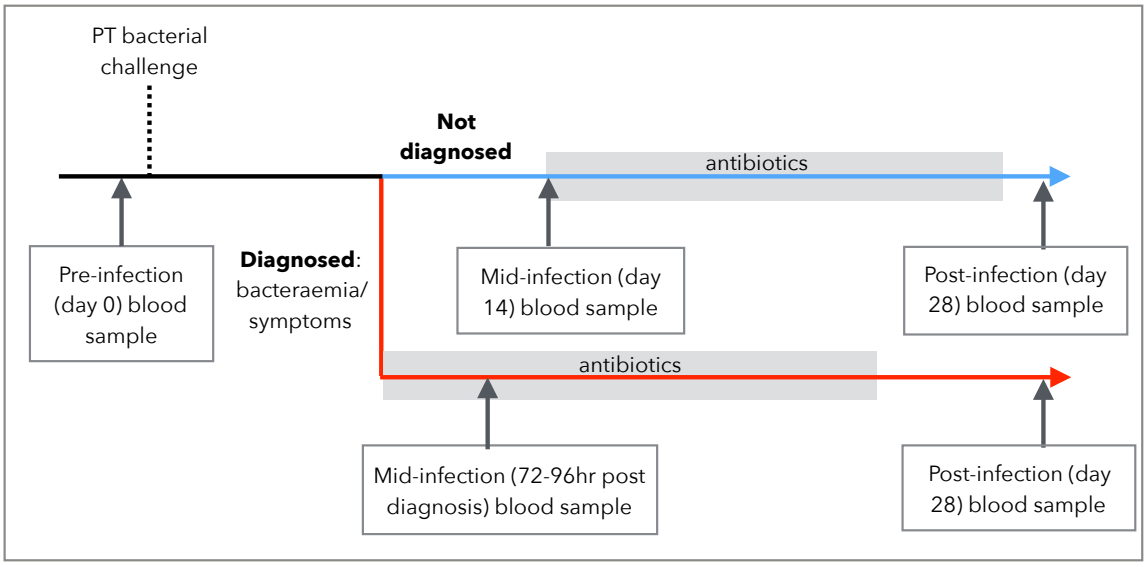

Figure 3-3 Outline of *S.* Paratyphi A human infection model

Outline of blood sampling in human *S.* Paratyphi A (PT) infection model. Individuals were challenged with *S.* Paratyphi A and monitored daily. Individuals were either diagnosed with enteric fever, if they had a positive bacteria blood culture (bacteraemia) or persistent high fever (symptoms), or not diagnosed if they remained asymptomatic. All individuals underwent a two-week course of antibiotics.

To determine whether MAIT cell frequency changed during *S.* Paratyphi A infection, we assessed the frequency of circulating MAIT cells in individuals not diagnosed and diagnosed with enteric fever following ingestion of *S.* Paratyphi A. The frequency of MAIT cells was relatively stable in individuals not diagnosed with infection (**Figure 3-4A**), with a small

decrease in proportion to 0.76±0.06 occurring on day 10, but this was not statistically significant. In contrast, there was an early decrease in the frequency of MAIT cells prior to diagnosis of enteric fever to 0.88±0.04 on day four and decreasing significantly to 0.63±0.06 7–8 days after challenge (**Figure 3-4B**). The frequency of MAIT cells in the diagnosed individuals then recovered after antibiotic treatment (day 28) and, in the majority (59%) of challenged individuals an increase in frequency from baseline was observed.

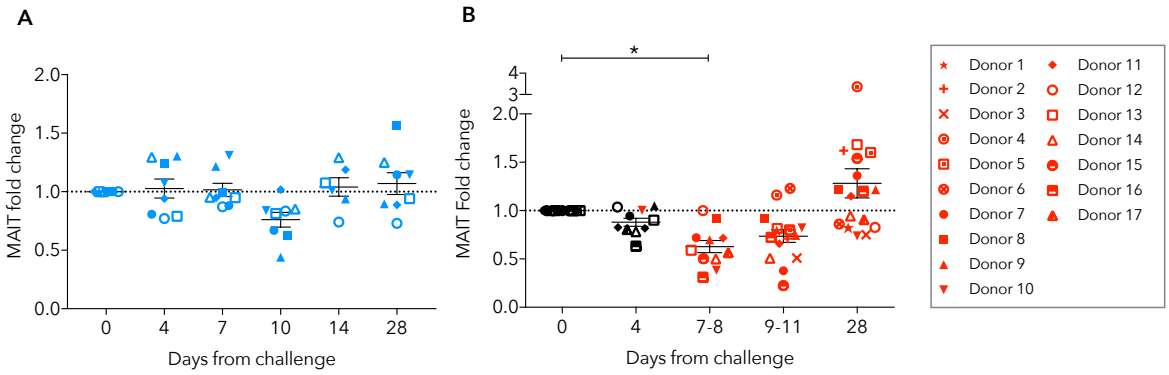

Figure 3-4 Frequency of MAIT cells in individuals challenged with *S.* Paratyphi A

PBMCs were isolated at various time points from 25 individuals challenged with live *S.* Paratyphi A and analysed by flow cytometry. Graphs showing the frequency of MAIT cells in the $CD3^+$ T cell compartment represented as fold change from baseline in individuals (A) not diagnosed (n = 8) or (B) diagnosed with enteric fever (n = 17). Each symbol represents an individual and a key for diagnosed individual identification is provided. Black symbols represent samples collected prior to diagnosis, red symbols represent samples taken on/after diagnosis. Line indicates mean and error bars represent SEM. Statistical significance was calculated using one-way analysis of variance (ANOVA) with Dunnett's test, where * $P <$ 0.05.

We then examined the activation of circulating MAIT cells in challenged individuals by expression of CD38. There was no increase in the expression of CD38 on MAIT cells over time from individuals who were not diagnosed with enteric fever (**Figure 3-5A**). In contrast, the expression of CD38 was significantly increased on 16.8±4.2% of MAIT cells 9–11 days after challenge in individuals that developed enteric fever (**Figure 3-5B**). This significant

upregulation of CD38 was maintained, even following antibiotic treatment where 16.3±2.5% of MAIT cells were still expressing CD38.

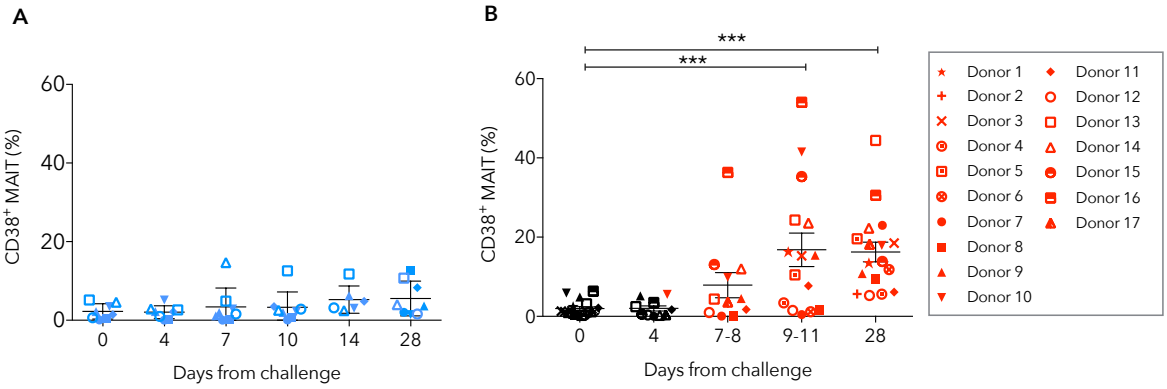

Figure 3-5 Activation of MAIT cells in individuals challenged with *S.* Paratyphi A

PBMCs were isolated at various time points from 25 individuals challenged with live *S.* Paratyphi A and analysed by flow cytometry. Graphs showing the percentage of activated MAIT cells in challenged individuals (A) not diagnosed (n = 8) and (B) diagnosed (n = 17) with enteric fever analysed by expression of CD38. Each symbol represents an individual and a key for diagnosed individual identification is provided. Black symbols represent samples collected prior to diagnosis, red symbols represent samples taken on/after diagnosis. Line indicates mean and error bars represent SEM. Statistical significance was calculated using one-way ANOVA with Dunnett's test, where *** $P < 0.001$.

To further characterize the MAIT cell phenotype during infection, mass cytometry analysis was performed on blood samples from four diagnosed individuals. We found that 56.8±8.6% of MAIT cells expressed the intracellular proliferation marker Ki67 following diagnosis and this correlated with the increased expression of CD38 (**Figure 3-6A**). Interestingly, no $Ki67^+$ cells were observed following antibiotic treatment, although 16.5±4.0% of MAIT cells had still retained CD38 expression. Additional analysis of surface markers revealed higher expression of the activation marker CD56 and decreased expression of the IL-7 receptor CD127 and cell survival marker BCL2 on $CD38^+Ki67^+$ compared to $CD38^-Ki67^-$ cells at the peak of infection (**Figure 3-6B**). However, there were no substantial differences in the

expression of tissue-homing markers between $CD38^{+}Ki67^{+}$ and $CD38^{-}Ki67^{-}$ cells at the peak of infection.

Together, the decreased frequency and acquisition of an activated and proliferating phenotype suggests that circulating MAIT cells in individuals diagnosed with enteric fever are responding to the *in vivo S.* Paratyphi A infection.

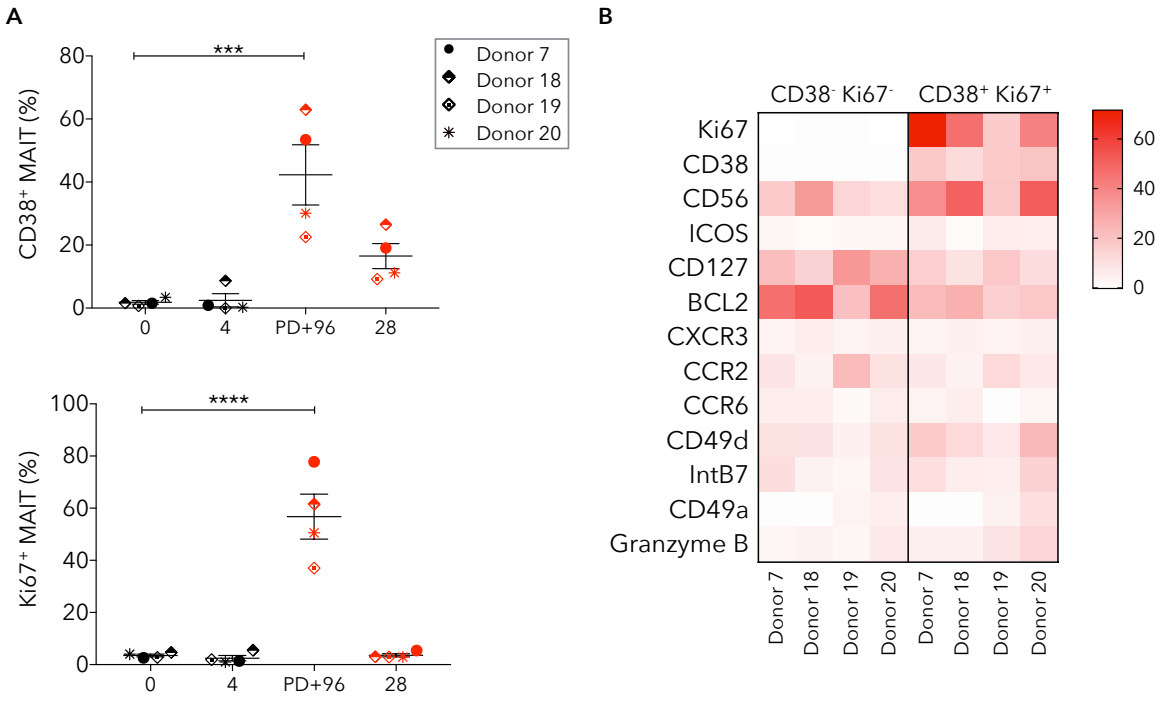

Figure 3-6 Expression of proliferation, activation and migration markers by MAIT cells at the peak of *S.* Paratyphi A infection

Frozen PBMCs from four diagnosed individuals at various time points were thawed and analysed by mass cytometry. (A) Graphs shows the expression of Ki67 and CD38 on MAIT cells over time. Numbers on x-axis represent days from bacterial challenge. Each symbol represents a diagnosed individual and a key is provided for identification. Black symbols represent samples taken before diagnosis and red symbols represent samples taken on/after diagnosis with enteric fever. Line is at the mean and error bars represent SEM. (B) Heatmap shows the signal intensity for various activation and cell migration markers of proliferating and activated MAIT cells ($Ki67^{+}$ $CD38^{+}$) compared to the non-activated and non-proliferating ($Ki67^{-}$ $CD38^{-}$). One-way ANOVA with Dunnett's test was used to assess statistical significance, where *** $P < 0.001$, **** $P < 0.0001$. PD+96; 96 h post-diagnosis.

3.2.2 MAIT cells have an enhanced response to *S.* Paratyphi A *ex vivo* challenge in individuals diagnosed with enteric fever

To determine whether the effector function of MAIT cells alters after a human bacterial infection, we examined the pro-inflammatory cytokine production by MAIT cells after *ex vivo* challenge with a low dose (MOI 1) of *S.* Paratyphi A from challenged individuals.

We observed that, when you compare circulating MAIT cells response to *S.* Paratyphi A pre- and post-infection in individuals not diagnosed with enteric fever, there was a significant increase from 2.9±1.2% to 8.1±2.0% in IFNγ producing MAIT cells, and a small increase from 2.1±0.6% to 4.7±1.0% TNF producing cells (**Figure 3-7A**). In contrast, in individuals diagnosed with enteric fever the circulating MAIT cells in response to *S.* Paratyphi A showed an increase in IFNγ and TNF production mid-infection from 2.5±0.9% to 11.6±4.1% $IFN\gamma^+$ and 2.7±1.0% to 11.7±2.4% TNF^+. However, post-infection $IFN\gamma^+$ MAIT cells reduced to 4.6±0.9% while TNF production remained high with 8.4±2.0% TNF^+ MAIT cells (**Figure 3-7B**). It should be noted that, due to the small sample size in diagnosed individuals, these differences were not statistically significant.

These results suggest that changes are occurring to the circulating MAIT cell population that is altering their *ex vivo* effector function, which in individuals diagnosed with enteric fever is predominantly occurring to the MR1-restricted TNF production response of MAIT cells to *S.* Paratyphi A.

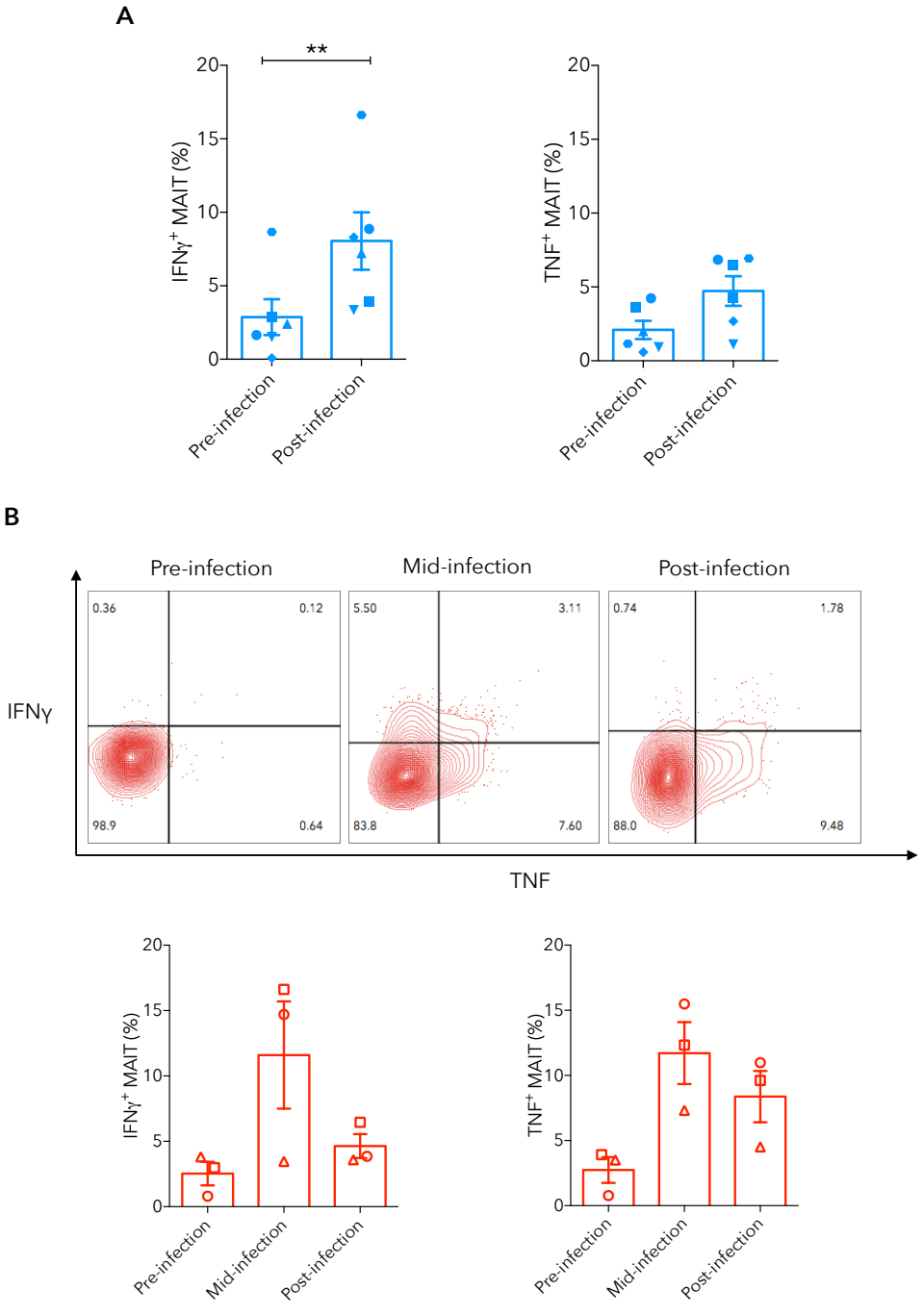

Figure 3-7 *Ex vivo S.* Paratyphi A infection of circulating MAIT cells from individuals challenged with *S.* Paratyphi A

PBMCs were isolated at various time points from 10 individuals challenged with live *S.* Paratyphi A and exposed to live *S.* Paratyphi A MOI 1 *ex vivo*. Cells were analysed by flow cytometry and MAIT cells were assessed for intracellular expression of IFNγ and TNF. Results shown for individuals (A) not diagnosed (n = 7) and (B) diagnosed (n = 3) with enteric fever. For graphs, each symbol represents a donor, error bars represent SEM. Statistical significance calculated using Student's two-tailed paired T test, where ** $P < 0.01$.

3.3 Next generation sequencing analysis of MAIT cell TCRβ repertoire in response to *S.* Paratyphi A infection

3.3.1 MAIT cell TCRβ chain usage undergoes changes during *S.* Paratyphi A infection

To investigate whether the increase in the MR1-restricted TNF production by MAIT cells we observed following infection was driven by changes in their TCR repertoire, we investigated the TCRβ chain usage of MAIT cells in challenged individuals diagnosed with enteric fever.

Consistent with previous findings by Lepore *et al.* (2014), we found the TRBV usage of MAIT cells was oligoclonal, characterized by the preferential use of TRBV20 and TRBV6 in all diagnosed individuals, with inter-donor variation ranging from 31–84% of the total chain usage (**Figure 3-8A–B**).

When comparing TRBV usage in individuals before, during and after infection, the oligoclonality is maintained, with only a small redistribution of the TRBV and TRBJ (**Figure 3-8C**) usage in some individuals when compared to the stable TCRβ chain usage observed in healthy (not challenged, control) individuals over time (**Figure 3-9A–B**).

These results suggest that MAIT cells maintain their oligoclonal TCR usage over time, even during an infection, so we next wanted to investigate whether TCR repertoire changes were occurring on the clonotypic level.

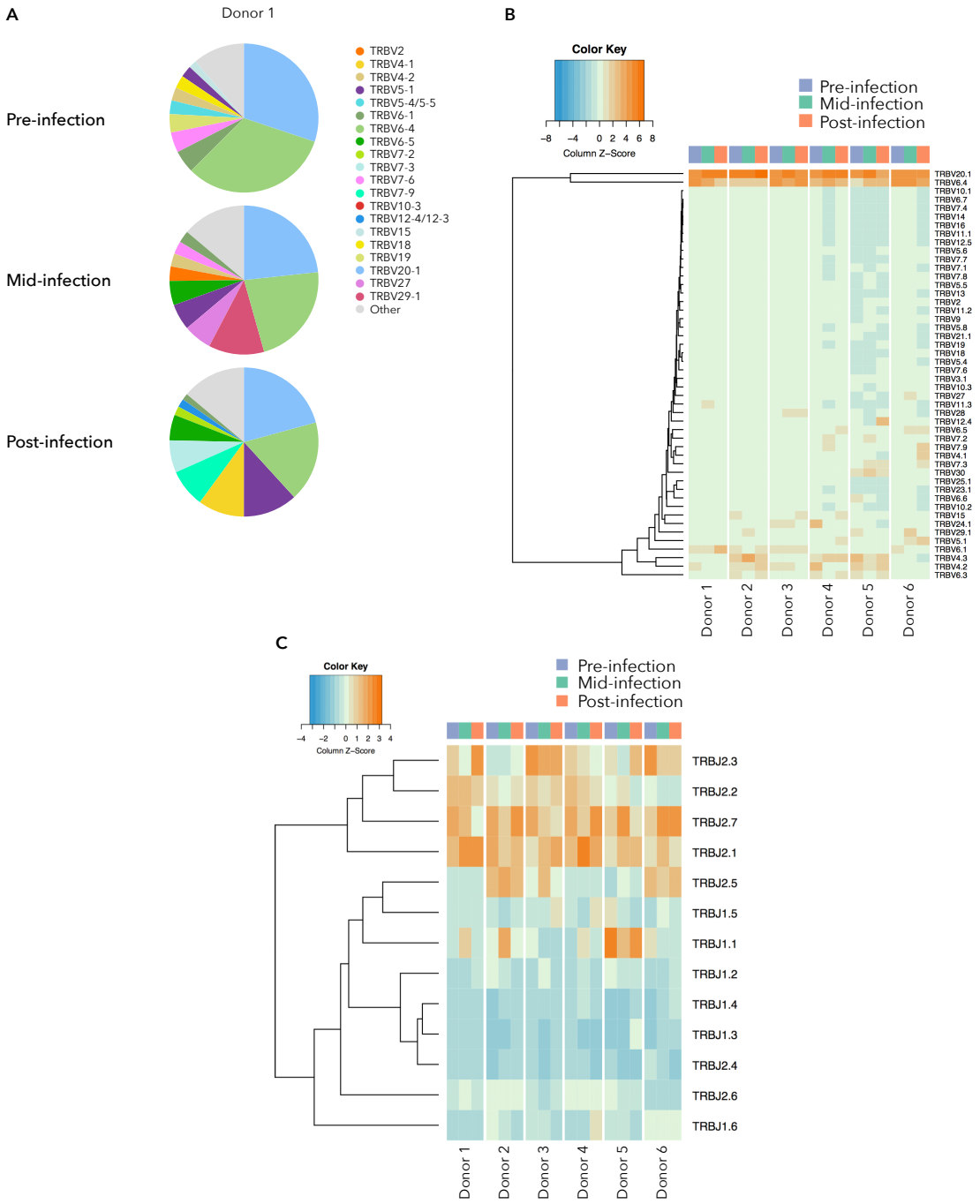

Figure 3-8 Circulating MAIT cells maintain TCRβ oligoclonality in individuals challenged with live *S.* Paratyphi A and diagnosed with enteric fever

MAIT cells were sorted from frozen PBMCs from six individuals challenged with *S.* Paratyphi A and diagnosed with enteric fever (pre-, mid- and post-infection) and the TCRβ usage analysed. (A) Pie charts of TRBV usage from a representative diagnosed individual D6. The weighted (B) TRBV and (C) TRBJ usage profile for diagnosed individuals shown as a heatmap with hierarchical clustering performed using euclidean distance. Lower x-axis labels diagnosed individual donors. Top x-axis colour bars indicate sample time point.

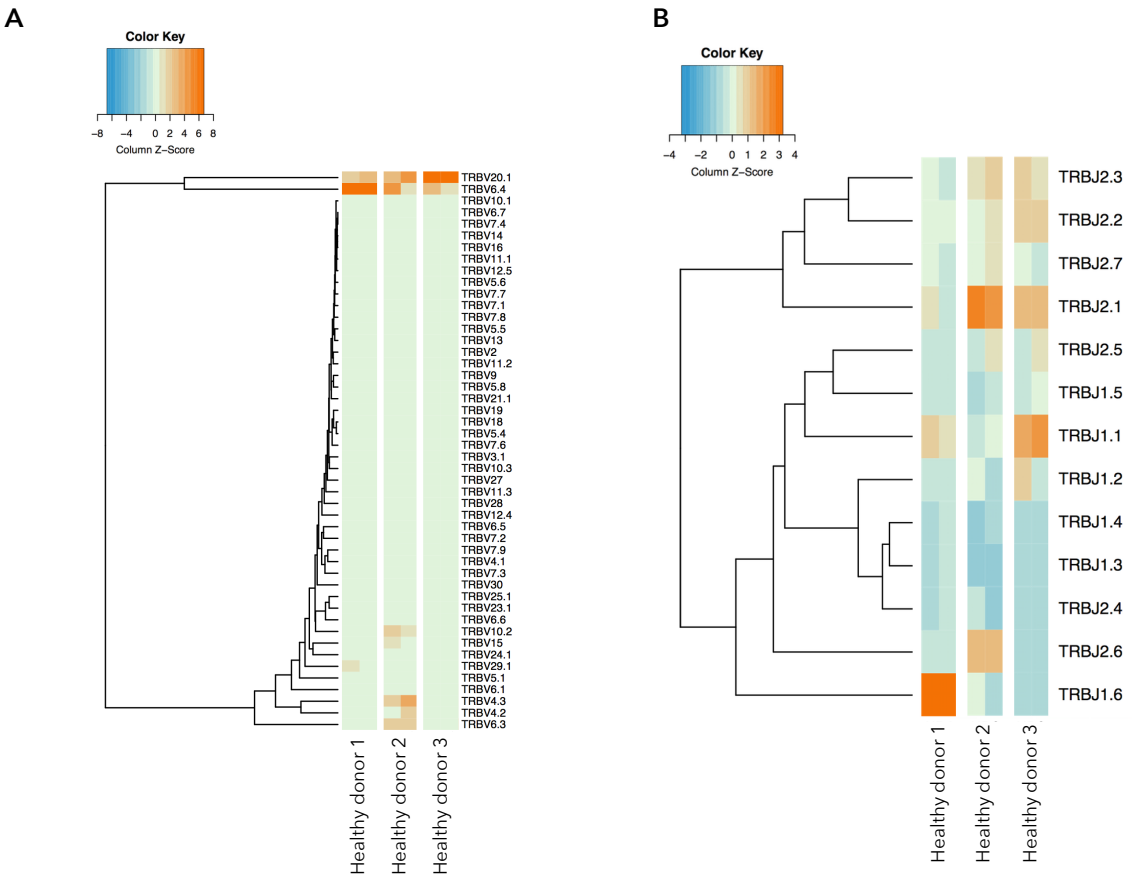

Figure 3-9 Circulating MAIT cell TCRβ chain usage in healthy individuals is oligoclonal and stable over time

Frozen PBMCs collected 21 days apart from three healthy control donors were sorted for MAIT cells and the TCRβ chain usage analysed. The weighted (A) TRBV and (B) TRBJ usage profile is shown as a heatmap with hierarchical clustering performed using euclidean distance. Bottom x-axis labels healthy (not challenged) donors.

3.3.2 Over-represented circulating MAIT cell clonotypes undergo transient contraction in individuals diagnosed with enteric fever

To determine whether changes were occurring in MAIT cells at the clonotypic level, we analysed circulating MAIT cell clonotypes based on the CDR3β sequences in six diagnosed individuals. Consistent with the findings of Lepore *et al*. (2014), we confirmed that the MAIT cell clonotypes were stable over time, shown by the example clonotype scatterplot of a healthy control individual (**Figure 3-10**). However, MAIT cells in the diagnosed individual pre- and post-infection scatterplot appear less stable over time.

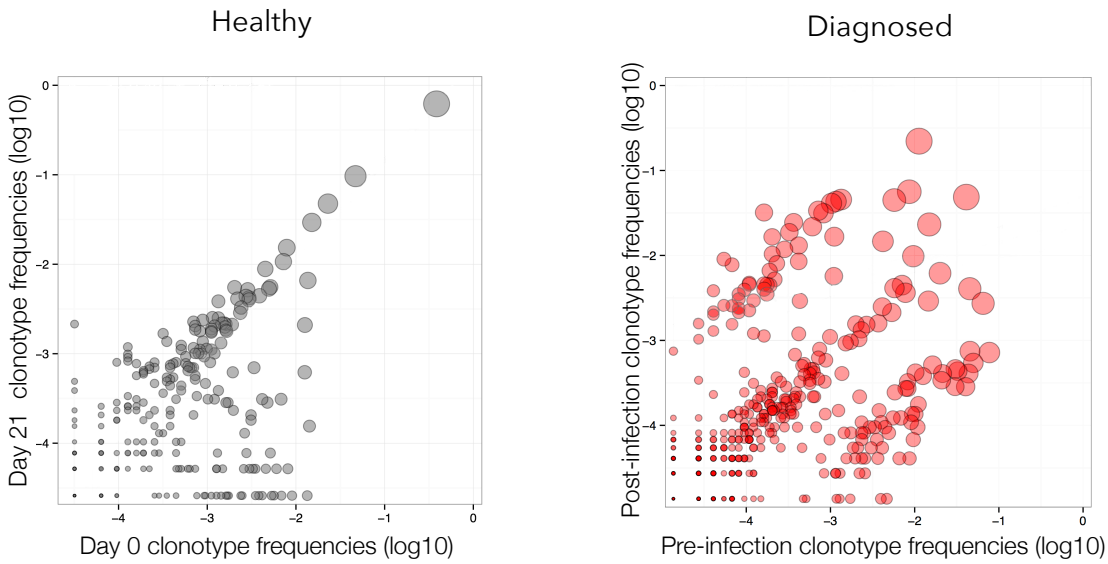

Figure 3-10 Circulating MAIT cell clonotypes are unstable in individuals challenged with *S.* Paratyphi A and diagnosed with enteric fever

MAIT cells were sorted from frozen PBMCs from individuals challenged with *S.* Paratyphi A and diagnosed with enteric fever (pre- and post-infection) and the TCRβ repertoire analysed. MAIT cells from healthy individuals sampled twice (21 days apart) were analysed as a control. Examples of clonotype abundance scatterplots for a healthy and a diagnosed individual (donor 1). Scatterplot axes represent log10 clonotype frequencies in each sample (only overlapping clonotypes shown) and point size is scaled to the geometric mean of the clonotype frequency in both sample time points.

To explore the changes to MAIT cell clonotypes further, we analysed the clonal space homeostasis of MAIT cell clonotypes over time to understand whether the distribution of the clonotype abundances underwent changes in response to infection. In a healthy control individual, the clonal distribution was relatively stable over time (**Figure 3-11A**). In contrast, when we analysed the clonal distribution in a diagnosed individual (donor 1), we observed marked changes, particularly in the proportion of space used by the over-represented MAIT cell clonotypes. When comparing the clonal distribution in all diagnosed individuals, there was a significant decrease in the proportion of over-represented clones from 0.17±0.05 at baseline to 0.10±0.04 mid-infection, but there was no significant difference between the baseline and post-infection (**Figure 3-11B**). There were also no

significant changes to the MAIT cell clonal distribution in the undiagnosed individuals (**Figure 3-12**). These results demonstrate that changes to MAIT cell clonotypes in response to infection occur most notably to those that are over-represented.

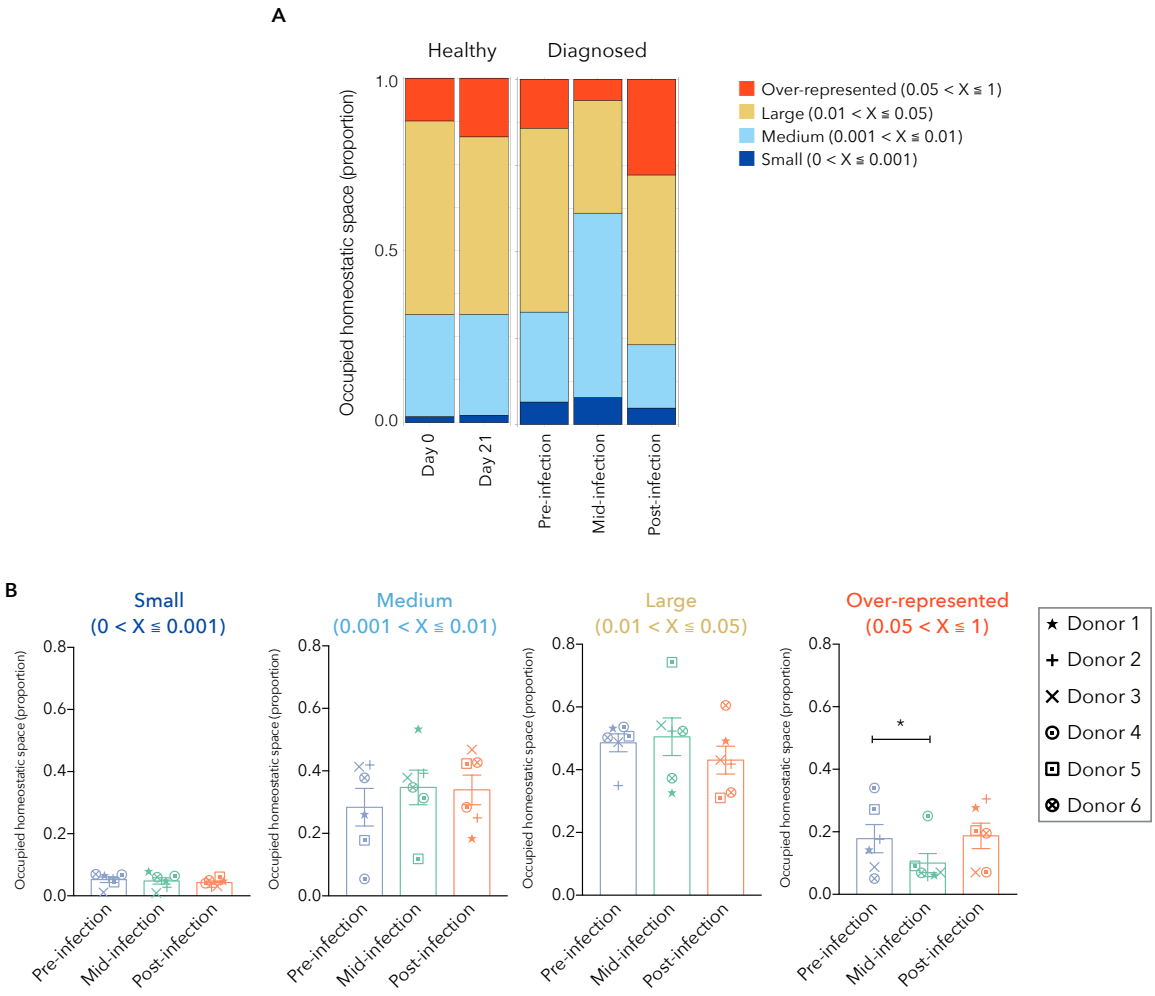

Figure 3-11 The over-represented circulating MAIT cell clonotypes undergo transient contraction in individuals challenged with *S.* Paratyphi A and diagnosed with enteric fever

MAIT cells were sorted from frozen PBMCs from six individuals challenged with *S.* Paratyphi A and diagnosed with enteric fever (pre-, mid- and post-infection) and the TCRβ repertoire analysed. (A) Example graphs of the occupied homeostatic space of MAIT cell clonotypes in a healthy and diagnosed (donor 1) individual. Measured as a proportion taken up by over-represented (0.05–1), large (0.01–0.05), medium (0.001–0.01), and small (0–0.001) clonotypes. (B) Summary graphs of occupied homeostatic space taken up by MAIT cell clonotypes in diagnosed individuals. Line is the mean with error bars representing SEM. Each symbol represents a diagnosed individual and a key is provided for identification. Statistical significance was calculated using Student's paired two-tailed T test, where * $P <$ 0.05.

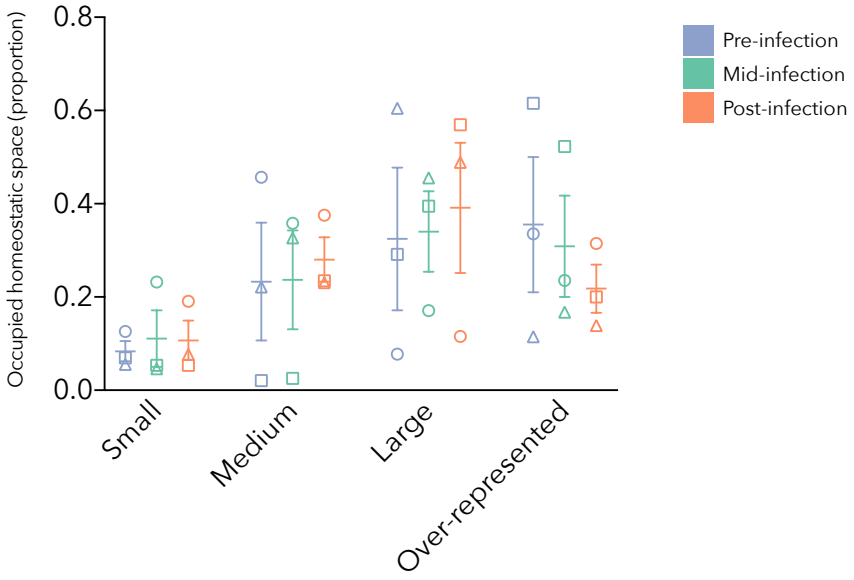

Figure 3-12 Circulating MAIT cell clonotypes occupied homeostatic space from individuals challenged with *S.* Paratyphi A and not diagnosed with enteric fever

MAIT cells were sorted from frozen PBMCs from three individuals challenged with *S.* Paratyphi A and not diagnosed with enteric fever (pre-, mid- and post-infection) and the TCRβ repertoire analysed. Graph shows summary of occupied homeostatic space taken up by MAIT cell clonotypes in not diagnosed individuals. Measured as a proportion taken up by over-represented (0.05–1), large (0.01–0.05), medium (0.001–0.01), and small clonotypes (0–0.001). Each symbol represents a volunteer.

3.3.3 Circulating MAIT cells clonotype composition changes in response to *S.* Paratyphi A infection

To determine whether the over-represented MAIT cell clonotypes following infection were different to those present before infection, we analysed the circulating MAIT cell clonotype composition based on the CDR3β sequence in six diagnosed individuals. An example clonotype tracking heatmap for a diagnosed individual (donor 1) shows that the clonotypes present at high frequency following infection were not the same clonotypes that were at high frequency before infection (**Figure 3-13**).

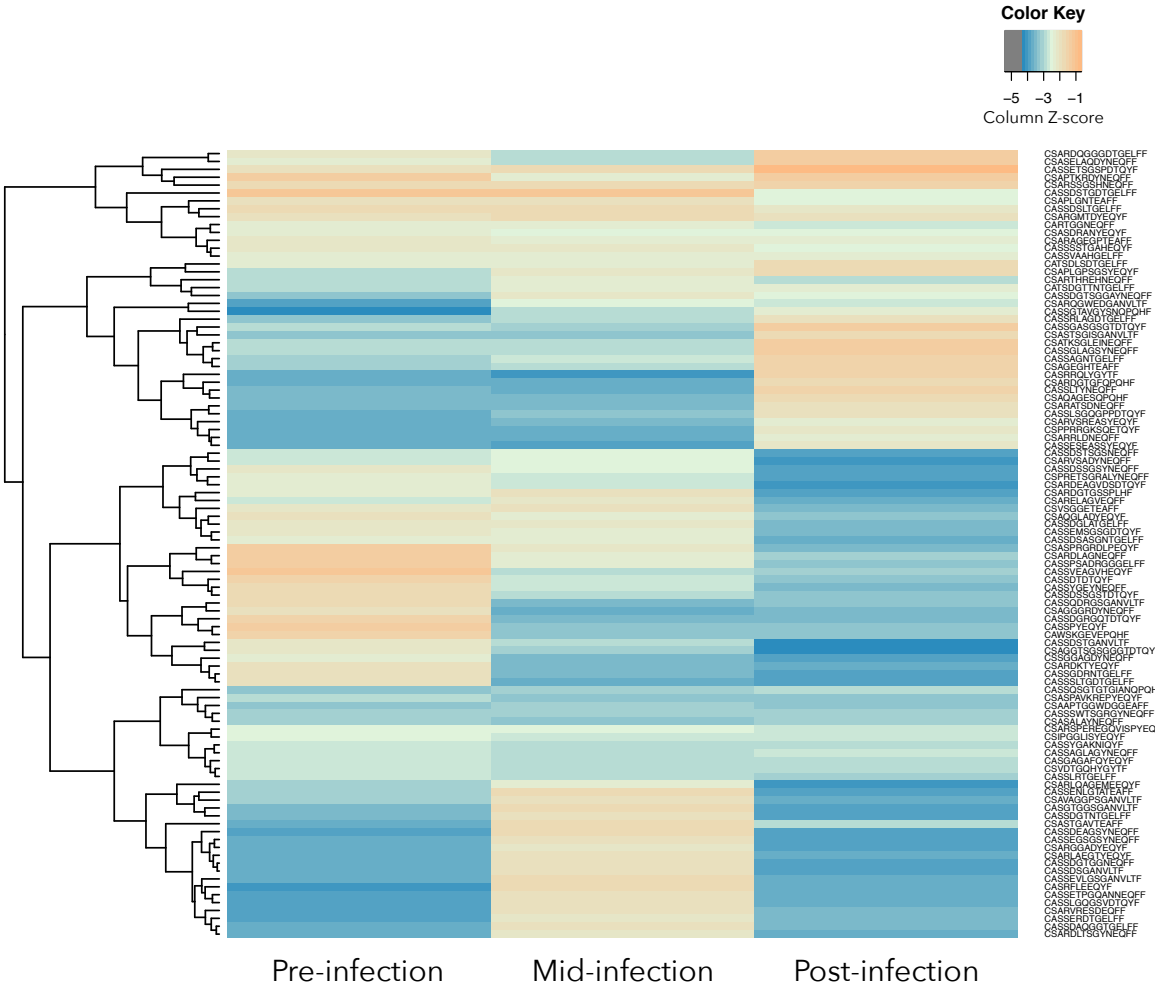

Figure 3-13 Circulating MAIT cell clonotype composition is altered after challenge with *S.* Paratyphi A and diagnosis with enteric fever

MAIT cells were sorted from frozen PBMCs from individuals challenged with *S.* Paratyphi A and diagnosed with enteric fever (pre-, mid- and post-infection) and the TCRβ repertoire analysed. A representative clonotype tracking heatmap is shown for a diagnosed individual (donor 1) showing top 200 clonotypes with hierarchical clustering on the left y-axis and the CDR3β sequences on the right y-axis.

Shared clonotype abundance plots with the top five clonotypes displayed for two diagnosed individuals shows clonal expansion and contraction occurring, with a predominating clonotype present post-infection in donor 1 (**Figure 3-14A**). When comparing the top five clones across all diagnosed individuals, we observed significantly greater proportion of top clonotypes undergoing clonal expansion/contraction (0.53±0.11) compared to healthy controls (0.13±0.07) (**Figure 3-14B**). These results demonstrate that the composition of

MAIT cell clonotypes in circulation undergoes changes in response to *S.* Paratyphi A infection.

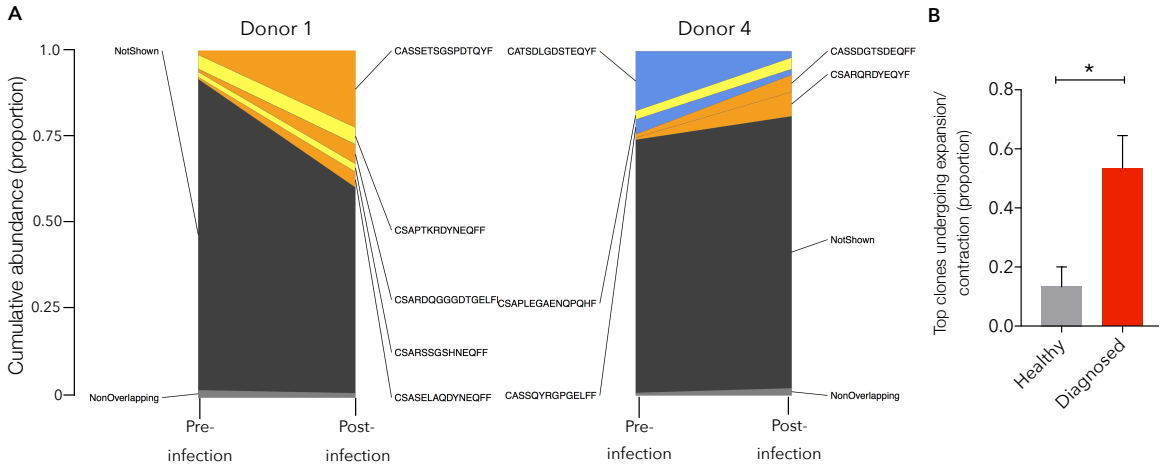

Figure 3-14 Top five circulating MAIT cell clonotypes undergo expansion/contraction in individuals challenged with *S.* Paratyphi A and diagnosed with enteric fever

MAIT cells were sorted from frozen PBMCs from individuals challenged with *S.* Paratyphi A and diagnosed with enteric fever (pre- and post-infection) and the TCRβ repertoire analysed. MAIT cells from healthy individuals sampled twice (21 days apart) were analysed as a control. (A) Example shared clonotype abundance plots for diagnosed donors 1 and 4. The top five clonotypes shared pre- and post-infection are displayed. Orange indicates expanded clone (≥ 2-fold increase), blue indicates contracted clone (≥ 2-fold decrease) and yellow indicates a stable clone. (B) Graph summarizing the clonotype abundance plots, showing the proportion of the top five clonotypes undergoing either contraction/expansion over time in healthy control (n = 3) and diagnosed individuals (n = 6). Bars plotted as mean with error bars representing SEM. Statistical significance calculated using Student's unpaired two-tailed T test where * $P < 0.05$.

3.3.4 The differing TCRβ repertoires of cytokine-producing subsets of circulating MAIT cells from healthy donors when challenged with *S.* Paratyphi A *ex vivo*

To confirm whether certain MAIT cell clonotypes preferentially produce cytokines in response to *S.* Paratyphi A, PBMCs from two healthy donors were challenged with *S.* Paratyphi A *ex vivo* and the cytokine-producing subsets of MAIT cells (TNF^+, $IFN\gamma^+$ and $TNF^+/IFN\gamma^+$) were sorted (**Figure 3-15A**) and the TCRβ chain usage analysed.

We observed that the TRBV (**Figure 3-15B**) and TRBJ (**Figure 3-15C**) usage was oligoclonal but differed between the cytokine-producing MAIT cell subsets within the same donor. When comparing between the two donors there was inter-donor variation as different TCRβ chains were preferentially being used by each subset.

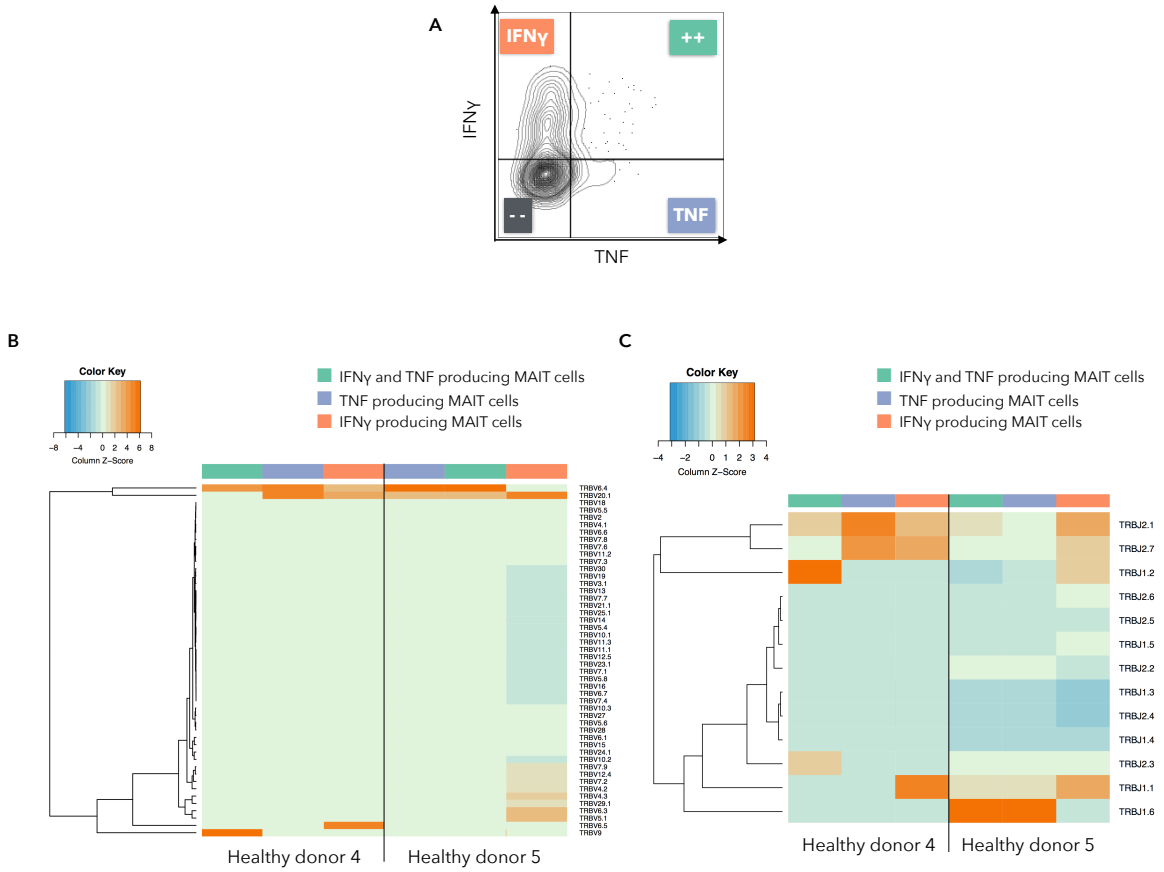

Figure 3-15 The TCRβ usage of cytokine-producing subsets of circulating MAIT cells from healthy donors when challenged with *S.* Paratyphi A *ex vivo*

PBMCs from two healthy donors were challenged with *S.* Paratyphi A *ex vivo* prior to intracellular staining and cell sorting for cytokine-producing subsets of MAIT cells (TNF^+, $IFN\gamma^+$ and $TNF^+/IFN\gamma^+$). The TCRβ repertoire was then analysed. (A) The gating strategy for defining the cytokine producing MAIT ($V\alpha7.2^+$ $CD161^+$) cells. The weighted (B) TRBV and (C) TRBJ usage profile is shown as a heatmap with hierarchical clustering performed using euclidean distance.

In healthy donor 4 we were able to compare the clonotypes present in the cytokine-producing subsets and to the non-cytokine producing MAIT cell subset. In this donor, it was evident that the TNF^+ and $TNF^+/IFN\gamma^+$ subsets had a similar clonotype composition to each

other but different composition compared to the IFNγ^+ and non-cytokine producing MAIT cell subsets (**Figure 3-16**).

These results support the observation that TNF production is a more MR1-restricted cytokine produced by MAIT cells and that certain MAIT cell clonotypes may preferentially produce TNF based on their TCR affinity to the MAIT cell antigen.

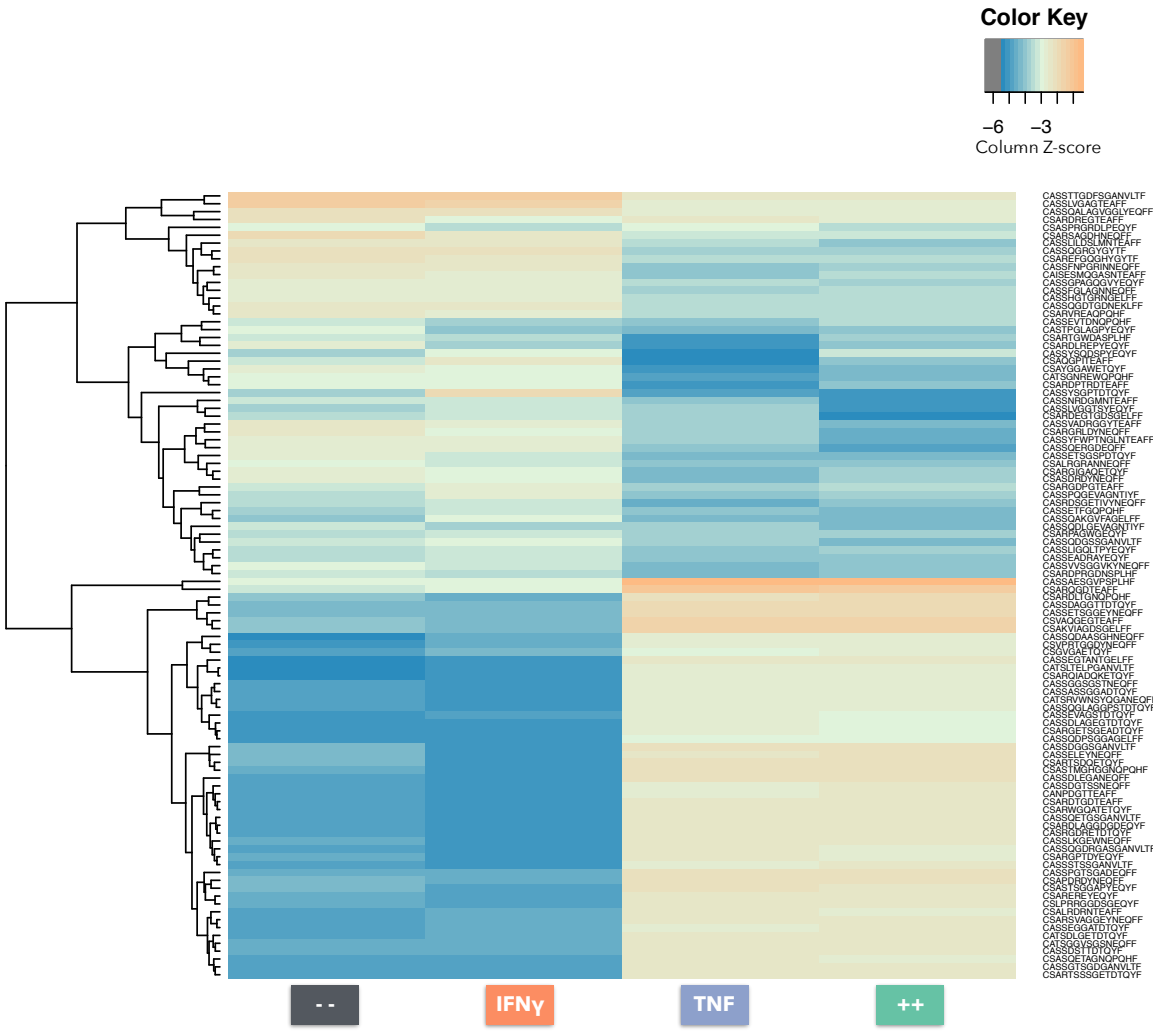

Figure 3-16 Circulating MAIT cells challenged with *S.* Paratyphi A *ex vivo* have different clonotype compositions depending on the cytokine-producing subset

PBMCs from healthy donor 4 were challenged with *S.* Paratyphi A *ex vivo* prior to intracellular staining and cell sorting for cytokine-producing subsets of MAIT cells ($TNF^-/IFN\gamma^-$, TNF^+, $IFN\gamma^+$ and $TNF^+/IFN\gamma^+$). The TCRβ repertoire was then analysed. A clonotype tracking heatmap is shown for donor 4 showing top 200 clonotypes with hierarchical clustering on the left y-axis and the CDR3β sequences on the right y-axis. Bottom x-axis shows the cytokine producing subsets of MAIT cells. - -, $TNF^-/IFN\gamma^-$; ++, $TNF^+/IFN\gamma^+$.

3.4 Discussion

MAIT cells and their bacterial reactivity are conserved across species, indicating their vital role in the host immune response to bacterial infections (Treiner *et al.*, 2005). We had a unique opportunity to further our understanding of MAIT cells and their response during bacterial infections by utilising samples from a controlled human infection model of the invasive bacterial pathogen *S.* Paratyphi A in healthy volunteers. This has provided a powerful tool to study how the MAIT cell response progresses during a systemic bacterial infection.

We first confirmed that MAIT cells responded to the intracellular pathogen *S.* Paratyphi A, and compared it their response to another extracellular bacteria that contains the riboflavin synthesis pathway, *E. coli*. We found that their MAIT cell activation and effector response to *S.* Paratyphi A is similar, but generally lower, to *S.* Paratyphi compared with *E. coli*. This response to *S.* Paratyphi A was important to demonstrate, as a previous study reported a lack of response of MAIT cells to *Salmonella,* and suggested that *Salmonella* interfered with MR1 loading of antigen (Le Bourhis *et al.*, 2013). This study claimed that a response from MAIT cells to *Salmonella* could be only be elicited when MR1 was overexpressed. However, this was not consistent with our results, suggesting the importance of an appropriate APC, as Le Bourhis and colleagues used epithelial cells as APCs in their experiments. Therefore, with the confirmation that MAIT cells do respond to *S.* Paratyphi A, and in a partially MR1-dependent manner, we next wanted to determine whether they played a role in the host response to systemic infection with *S.* Paratyphi A.

We observed that the relative frequency of circulating MAIT cells significantly decreased early in individuals challenged with *S.* Paratyphi A that developed enteric fever. This could indicate that, as early as day four, the MAIT cells in these individuals are responding to the

presence of *S*. Paratyphi A in the host. This migration of MAIT cells from circulation in response to infection has been suggested previously by studies reporting lower frequency of circulating MAIT cells in infected patients compared with healthy individuals (Grimaldi *et al.*, 2014, Le Bourhis *et al.*, 2010). In addition to this, a decrease in circulating MAIT cell frequencies was observed in trials that administered live *S*. Typhi (Salerno-Goncalves *et al.*, 2017) and live-attenuated *Shigella dysenteriae 1* vaccine (Le Bourhis *et al.*, 2013). The findings of these previous studies are in line with what we have observed, and suggest that circulating MAIT cells are responsive to *in vivo* bacterial infection and may decrease in frequency in the blood as they move to locally inflamed and infected tissues. This accumulation of MAIT cells in infected tissues has been demonstrated by studies using lung infection mouse models (Meierovics *et al.*, 2013, Chen *et al.*, 2017). We also observed a recovery in MAIT cell frequency following antibiotic treatment, suggesting that MAIT cell redistribution and reduction in circulating frequency is reversible in bacterial infection. This is unlike the non-reversible decrease of MAIT cell frequency that is observed in human immunodeficiency virus (HIV) infection (Cosgrove *et al.*, 2013, Fernandez *et al.*, 2014).

We show that a proportion of circulating MAIT cells in diagnosed individuals were activated, proliferating and had enhanced effector function at the peak of infection, again indicating that they were playing a role in the host response to *S*. Paratyphi A. Similar observations have been made by studies assessing MAIT cell responses in vaccination and live infection trials (Greene *et al.*, 2016, Le Bourhis *et al.*, 2013, Salerno-Goncalves *et al.*, 2017). However, the mode of activation of MAIT cells has not been addressed in these human *in vivo* studies. This is an important point, as our *in vitro* experiments along with other studies (Ussher *et al.*, 2014, van Wilgenburg *et al.*, 2016, Sattler *et al.*, 2015) have demonstrated that MAIT cells can become activated both through TCR stimulation or through TCR-independent cytokine stimulation.

To address whether the activation we observed was due to the MR1-TCR interaction, and thus due to the presence of bacteria-derived ligand, we assessed the MAIT cell TCR repertoire and found that it had undergone reshaping and clonal contraction/expansion during infection. This suggests that the TCR-MR1 interaction was influencing the circulating MAIT cell population. There are several studies which have indirectly provided evidence that the TCR-MR1 interaction is important for MAIT cell responses to bacterial infection *in vivo*. In a study of critically-ill patients, the circulating MAIT cell proportion in patients with streptococcal infections (a bacterial species for with some strains which lack the riboflavin synthesis pathway) was higher than those with infections by bacteria which do produce riboflavin metabolites (Grimaldi *et al.*, 2014). Also, a recent study using *Salmonella typhimurium* in a mouse lung infection model demonstrated that the MAIT cell response to infection required MR1 and the ability for bacteria to produce the riboflavin-derived ligand (Chen *et al.*, 2017). The results from these studies support our finding, that the riboflavin metabolite ligands are important for the MAIT cell response to bacterial infection and that the changes we observed in TCR repertoire could be driven by the riboflavin metabolite antigen.

When we assessed the TCRβ repertoire of MAIT cell cytokine-producing subsets in response to *S*. Paratyphi A, we observed differential TCRβ clonotypes present in the TNF-producing subsets compared with the IFNγ and non-cytokine producing MAIT cells. This provided further evidence that the MAIT cell TCRβ usage influenced the effector response of MAIT cells to bacteria, and that the TCR-MR1 interaction could drive clonal expansion of certain MAIT cell clonotypes.

In summary, we have determined the timing and dynamics of the MAIT cell response to *S*. Paratyphi A infection *in vivo*. We have clearly shown for the first time that MAIT cells

undergo an adaptive clonal response during infection, which is likely driven in part by their interaction with MR1 and the MAIT cell ligand. A summary of these results is shown in **Figure 3-17**.

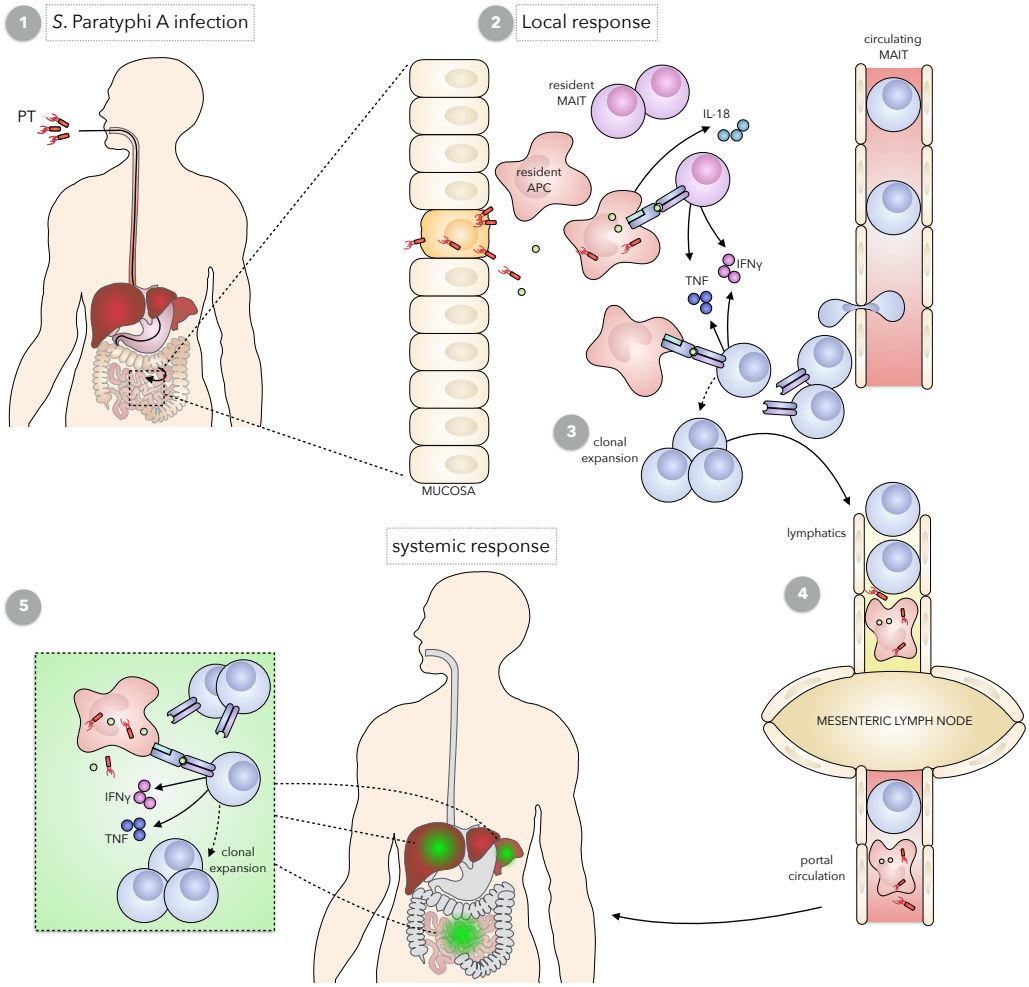

Figure 3-17 Proposed model of the MAIT cell response to *S.* Paratyphi A infection in diagnosed individuals

(1) Following oral challenge with *S.* Paratyphi A (PT) the bacteria invade the small intestine mucosa through the specialised M cells (shown in orange). (2) The bacteria then establish a localised infection as an intracellular pathogen within antigen presenting cells (APCs). These cells would be able to activate local MAIT cells both through cytokine production such as IL-18 as well as antigen-dependent activation. The local infection would attract circulating immune cells, including MAIT cells, to the site of infection. (3) These circulating MAIT cells would also be activated, with certain TCRs showing a higher functional avidity resulting in clonal expansion. (4) As the bacteria disseminates, it moves through the lymphatics to the mesenteric lymph nodes and eventually to the liver and spleen. (5) Systemic infection in areas with a high frequency of MAIT cells, especially the liver that has a T cell population of up to 40% MAIT cells (Le Bourhis *et al.*, 2010), there would be further antigen presentation, MAIT cell activation and clonal expansion occurring.

Chapter 4 – Evaluation of MAIT cells in cancer and during cancer immunotherapy

Due to their ability to be activated in a cytokine-dependent manner, MAIT cells have recently been the focus of studies of sterile inflammation, with the majority focussing on their potential role in autoimmune disorders. A form of non-sterile inflammation in which MAIT cells are yet to be studied in detail is cancer.

4.1 Immunohistochemical analysis of MAIT cell infiltration into human tumours

4.1.1 Immunohistochemical validation of Vα7.2 antibody on human spleen

The Vα7.2 (3C10) antibody specific for the MAIT cell TCR has been produced and validated for use in flow cytometry, but a number of studies have reported that it can be used to stain frozen tissue sections (cryosections) (Zabijak *et al.*, 2015, Le Bourhis *et al.*, 2010, Serriari *et al.*, 2014). To validate the specificity of the Vα7.2 (3C10) antibody in our immunohistochemistry experiments, we stained cryosections of spleen with Vα7.2, CD3 and an IgG1 isotype control. We observed that in areas of high $CD3^+$ cell staining in the spleen (white pulp) (**Figure 4-1A**) there were very specific $V\alpha7.2^+$ cells staining, with primarily cytoplasmic and surface localisation, as expected (**Figure 4-1B**). As the concentration of Vα7.2 antibody required for this staining is very high (50 μg/mL) an isotype control at the same concentration was stained to ensure antibody staining was specific. This control showed a low level of non-specific staining, but this did not correlate with the staining observed in the Vα7.2 stained section (**Figure 4-1C**). Thus, the Vα7.2 (3C10) antibody was considered specific and used to identify the $V\alpha7.2^+$ cell subset, for which we infer the presence of MAIT cells as these would comprise the majority of this subset.

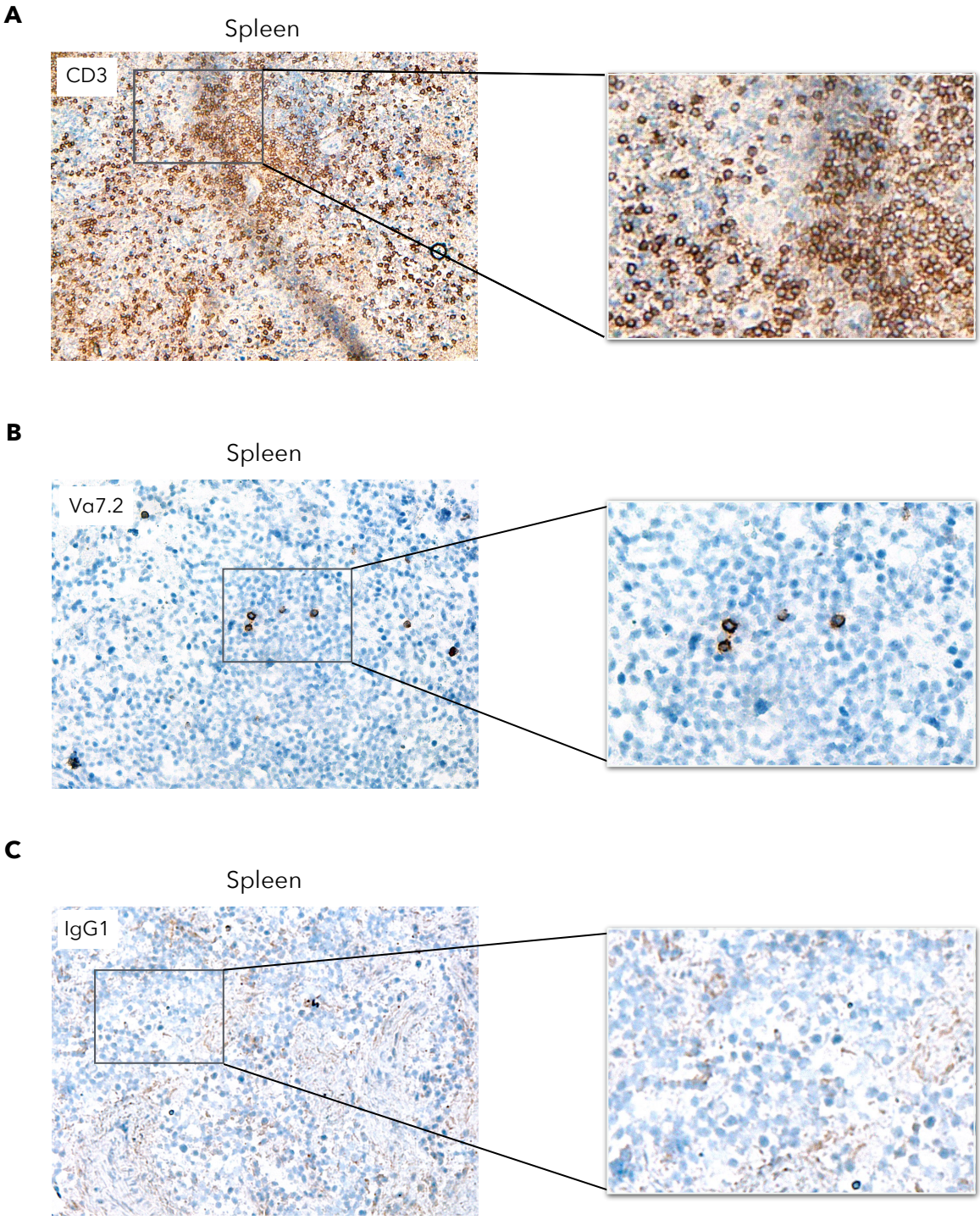

Figure 4-1 Vα7.2 (3C10) antibody can be used for immunohistochemical identification of MAIT cells in human tissue cryosections

Cryosections of spleen were stained with (A) CD3, (B) Vα7.2 and IgG1 (C) isotype control. Positive cells are brown (DAB^+) and slides were counterstained with haematoxylin (blue). Original images were taken at ×200 magnification. Representative images are shown. Left panel shows original magnification, right shows higher magnification of the area indicated.

4.1.2 Vα7.2$^+$ cells infiltrate tumours derived from mucosal tissue sites

Cryosections of colorectal cancer and lung cancer, both tumour types from tissue with mucosal tissue, were stained with the Vα7.2 antibody (**Figure 4-2A–B**) or IgG1 isotype control (data not shown). In all colorectal and lung cancers, the presence of Vα7.2$^+$ cells were observed infiltrating the stromal areas of the tumours, and in some cases, closely associated with tumour cells. These results confirm that Vα7.2$^+$ cells (which includes MAIT cells) infiltrate colorectal cancers as previously reported (Ling *et al.*, 2016, Zabijak *et al.*, 2015), and also that Vα7.2$^+$ cells infiltrate lung tumours.

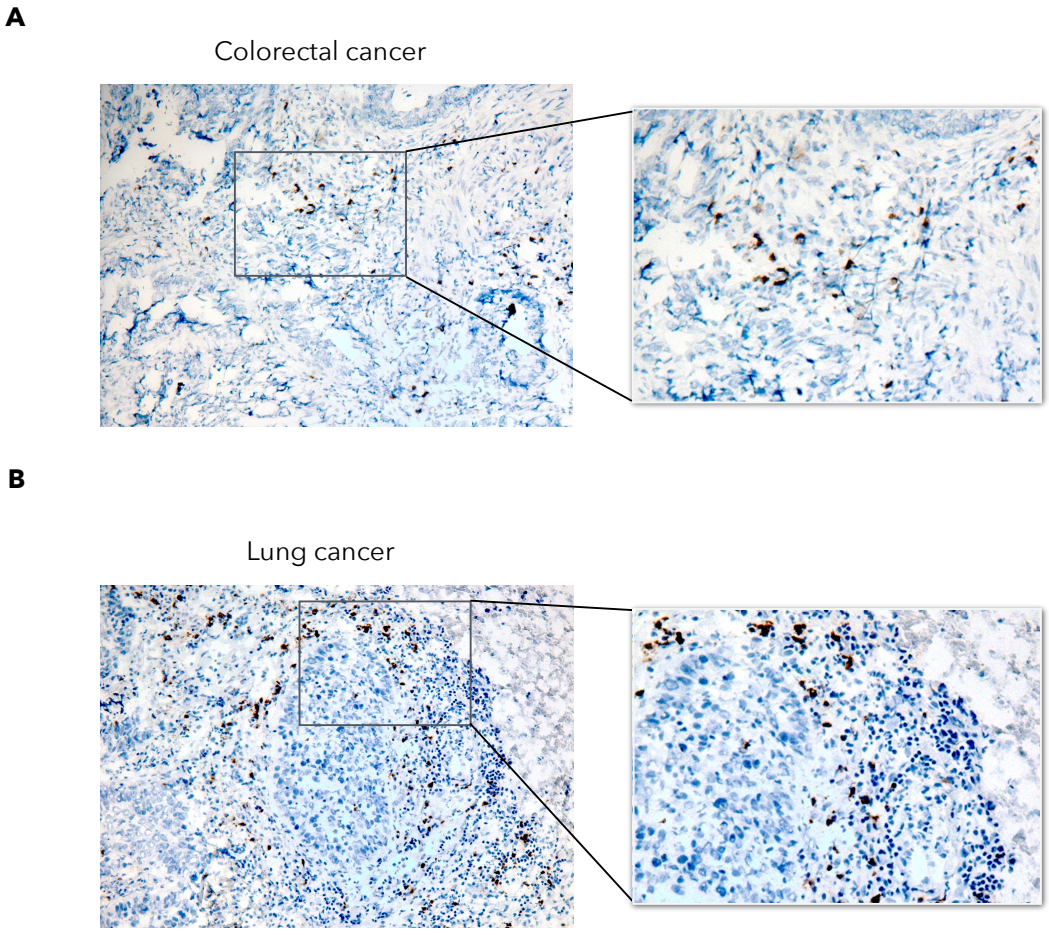

Figure 4-2 Vα7.2$^+$ cells infiltrate colorectal and lung tumours

Cryosections of (A) colorectal and (B) lung cancer were stained for Vα7.2. Positive cells are brown (DAB$^+$) and slides were counterstained with haematoxylin (blue). Original images were taken at ×200 magnification. Representative images are shown. Left panel shows original magnification, right shows higher magnification of the area indicated.

4.1.3 Vα7.2$^+$ cells infiltrate tumours derived from skin

A flow cytometry study of MAIT cells in healthy and inflamed skin suggested that cutaneous lymphocyte antigen (CLA)$^+$ CD103$^+$ (skin-associated) MAIT cells are present in the skin, both during inflammation and steady-state (Li *et al.*, 2016). Therefore, we wanted to determine whether MAIT cells would also be present in skin tumours. We assessed the most immunogenic tumour-type, melanoma, for the presence of Vα7.2$^+$ cells. Since melanomas can contain brown melanin pigment, isotype controls are shown to distinguish positive staining. We observed Vα7.2$^+$ cell infiltration into all melanomas, the extent to which varied between individual tumours (**Figure 4-3A–B**). These results provide the first evidence of Vα7.2$^+$ cells (including MAIT cells) infiltrating tumours derived from the skin.

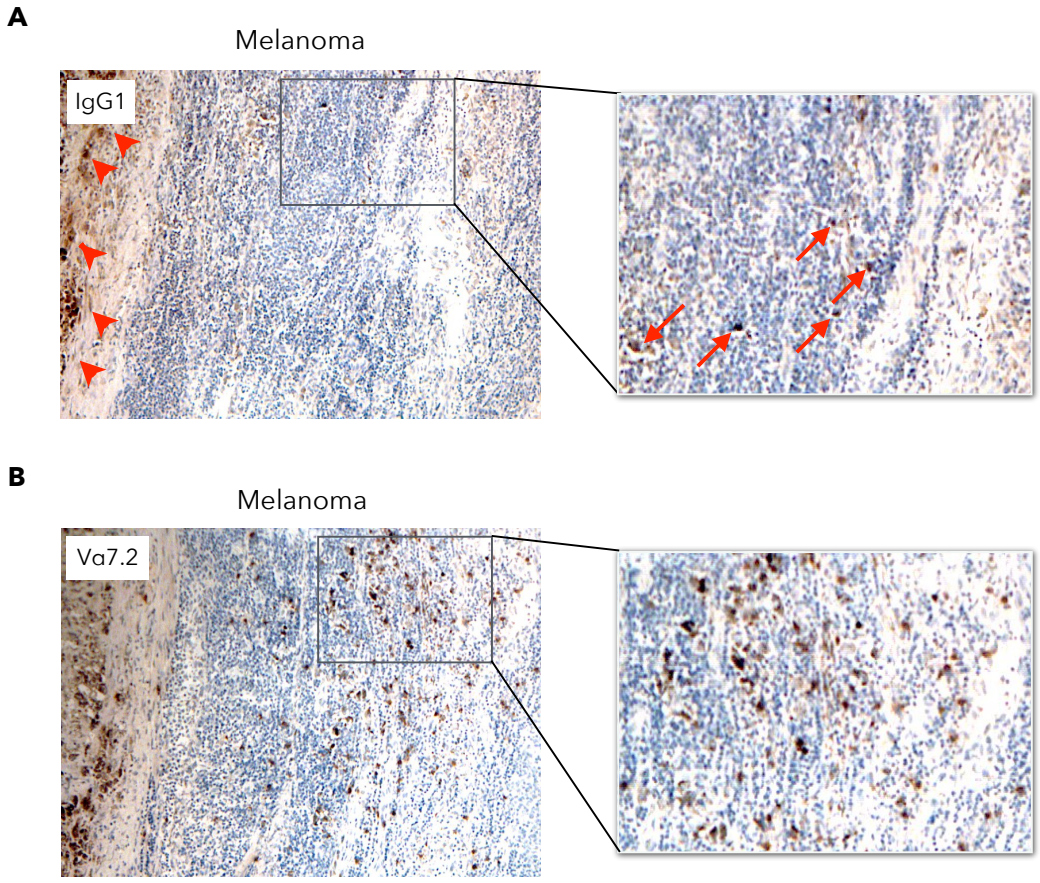

Figure 4-3 Vα7.2$^+$ cells infiltrate melanomas

Cryosections of melanoma were stained for (A) IgG1 isotype control or (B) Vα7.2. Positive cells are brown (DAB$^+$) and slides were counterstained with haematoxylin (blue). Red arrows indicate melanin. Original images were taken at ×200 magnification. Representative images are shown. Left panel shows original magnification, right shows higher magnification of the area indicated.

4.1.4 Vα7.2$^+$ cells infiltrate tumours derived from various organs

To determine whether MAIT cells infiltrated tumours from organs where the presence of MAIT cells is not known, we stained cryosections of breast cancer with Vα7.2 or IgG1 isotype control (data not shown). We observed Vα7.2$^+$ cells infiltrating the breast cancer sections analysed (**Figure 4-4A**). However, no Vα7.2$^+$ cells were observed infiltrating renal cancers (**Figure 4-4B**). When looking at the histology of the renal tumours, these sections were very acellular, with a large amount of necrosis occurring. Therefore, these are likely

sections of tumour core known to often be necrotic (Brinker *et al.*, 2000), which is a possible explanation as to why very little infiltration of cells, including MAIT cells, is observed.

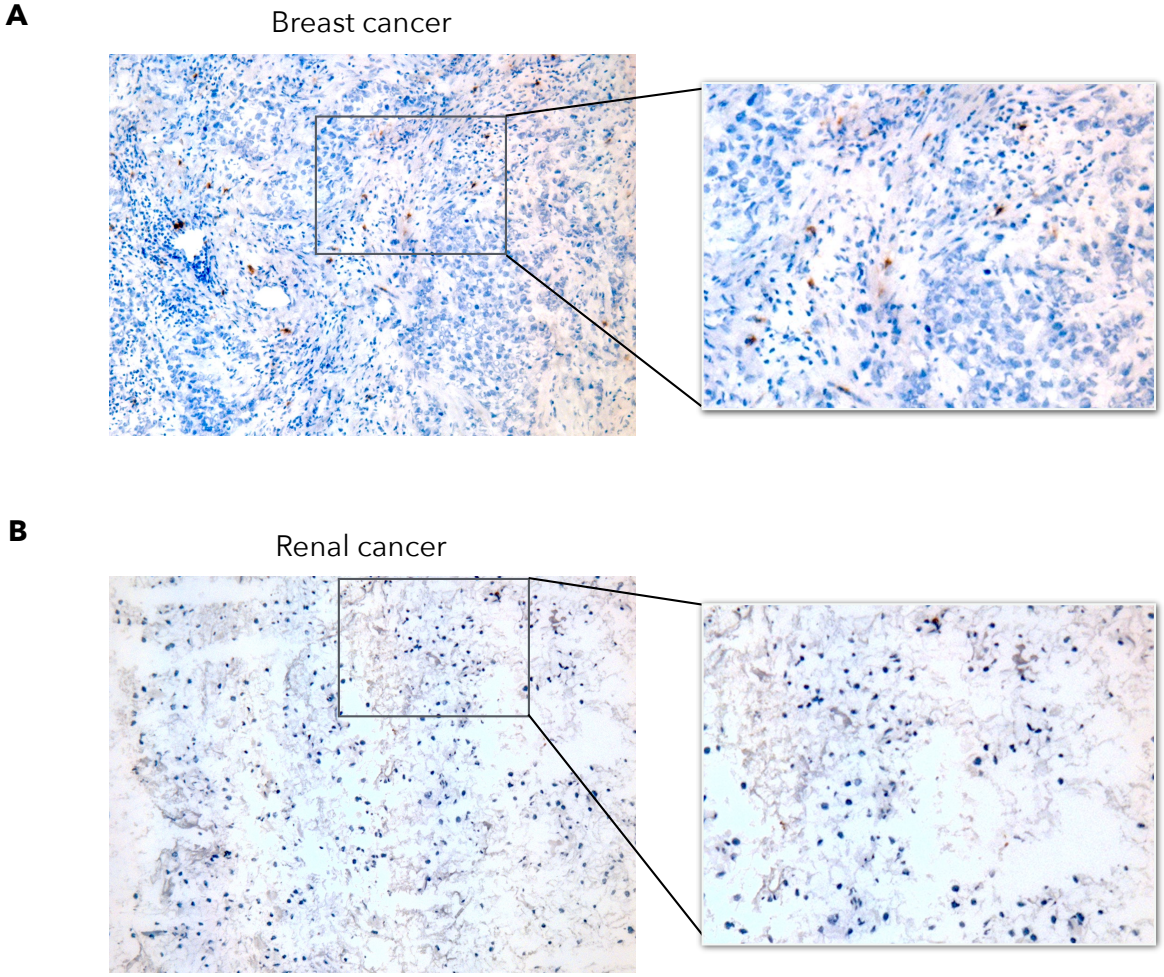

Figure 4-4 MAIT cells infiltrate breast tumours but not renal tumours

Cryosections of (A) breast and (B) renal cancers were stained for Vα7.2. Positive cells are brown (DAB^+) and slides were counterstained with haematoxylin (blue). Original images were taken at ×200 magnification. Representative images are shown. Left panel shows original magnification, right shows higher magnification of the area indicated.

A summary of the level of $V\alpha7.2^+$ cell infiltration into the various tumours is summarised in **Figure 4-5**. These summary results show that the mucosal tissue-derived tumours (colorectal and lung) generally have a higher infiltration of $V\alpha7.2^+$ cells compared to other tissue types. These results suggest that $V\alpha7.2^+$ cells can infiltrate various tumour types, but are more prevalent in mucosal tissues, in which they normally reside at high frequency in

healthy individuals. It should be noted that these observations are limited and only inferences as we were only able to use Vα7.2^{+} cells as a representation of the MAIT cell subset and could have also included a small subset of conventional T cells that also express Vα7.2.

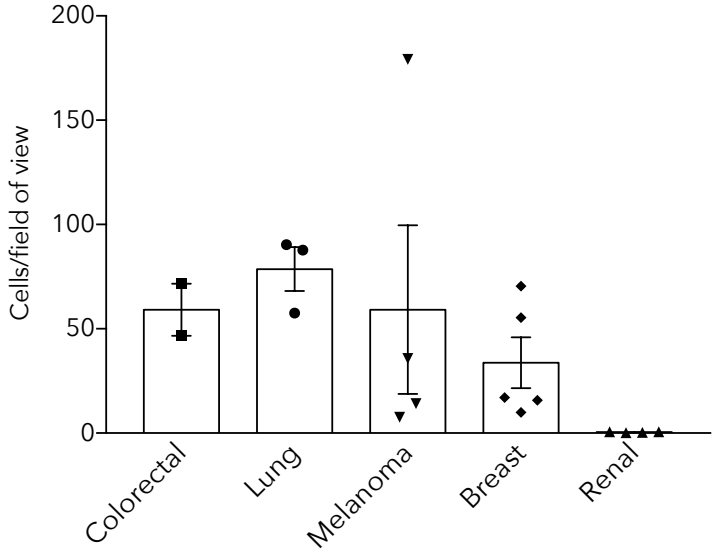

Figure 4-5 Summary of Vα7.2^{+}cell infiltration into various tumour types

Summary of immunohistochemistry of frozen tumour sections assessing MAIT (Vα7.2^{+}) cell infiltration into colorectal (n = 2), lung (n = 3), melanoma (n = 4), breast (n = 5) and renal (n = 4) cancers. The top five highest infiltrated fields of view (at ×200 magnification) were chosen and the positive cells counted in each. The mean of the five field for each sample were plotted with the bar indicating mean across samples and error bars showing SEM.

4.2 MAIT cell phenotype in cancer

4.2.1 MAIT cells are present in ovarian primary tumours, secondary tumours and ascites

With the knowledge that MAIT cells can infiltrate a wide variety of tumours, we investigated whether they could be detected by flow cytometry in primary and secondary ovarian tumours as well as peritoneal cavity fluid (ascites), which can often be rich in immune cell infiltrate (Giuntoli *et al.*, 2009). We observed that the frequency of MAIT cells in blood, tumour and

ascites was comparable, with some cases showing an enrichment of MAIT cells in tumours and ascites (**Figure 4-6A**). We also found when analysing the blood of an individual with ovarian cancer following chemotherapy, a very large frequency of MAIT cells (16.7% of total T cells) in the blood following treatment (**Figure 4-6B**). This result suggests that MAIT cells have an advantage for surviving chemotherapy and are a predominant cell type present following chemotherapy.

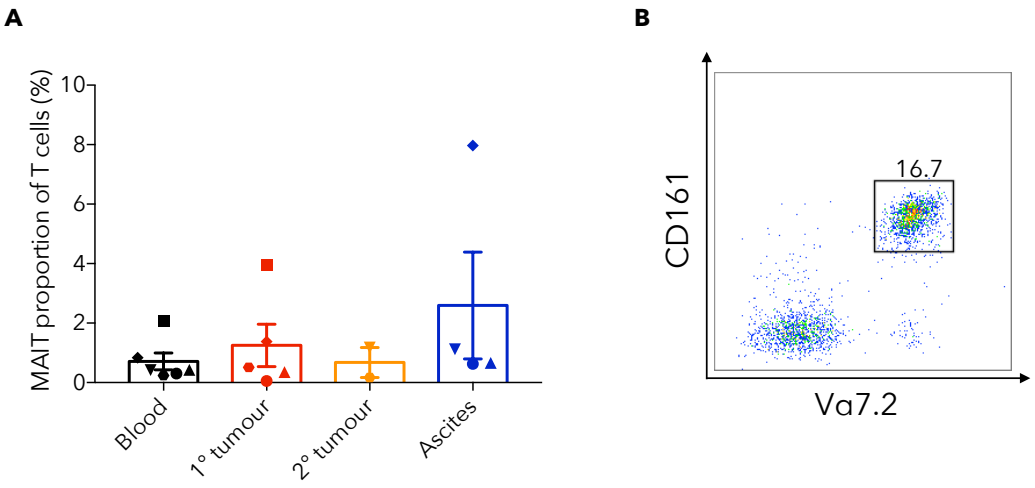

Figure 4-6 MAIT cells are present in blood, tumour tissue and ascites of individuals with ovarian cancer

PBMCs and processed tumour tissue samples from individuals with ovarian cancer were analysed by flow cytometry. (A) Graph showing the frequency of MAIT cells ($V\alpha7.2^+$ $CD161^+$) in the $CD3^+$ T cell compartment. Each symbol represents an individual. Bar indicates mean and error bars represent SEM. (B) Dot plot showing frequency of circulating MAIT cells in the $CD3^+$ T cell compartment from an individual following chemotherapy.

4.2.2 MAIT cells have an activated phenotype in ovarian primary tumours, secondary tumours and ascites

We next investigated the phenotype of MAIT cells in tumours compared to blood by flow cytometry. We observed only 9.8±3.8% of MAIT cells were expressed the activation marker CD38 in the blood of individuals with ovarian cancer (**Figure 4-7**). In contrast, the MAIT cells in tumours and ascites were up to 70% positive for CD38. None of the MAIT cells in

these individuals expressed the programmed cell death marker PD-1, although other conventional T cell subsets in these individuals were observed to express PD-1 (data not shown). These results suggest that MAIT cells in ovarian cancer tissues are phenotypically distinct from those in the blood and have an activated/tissue-resident phenotype.

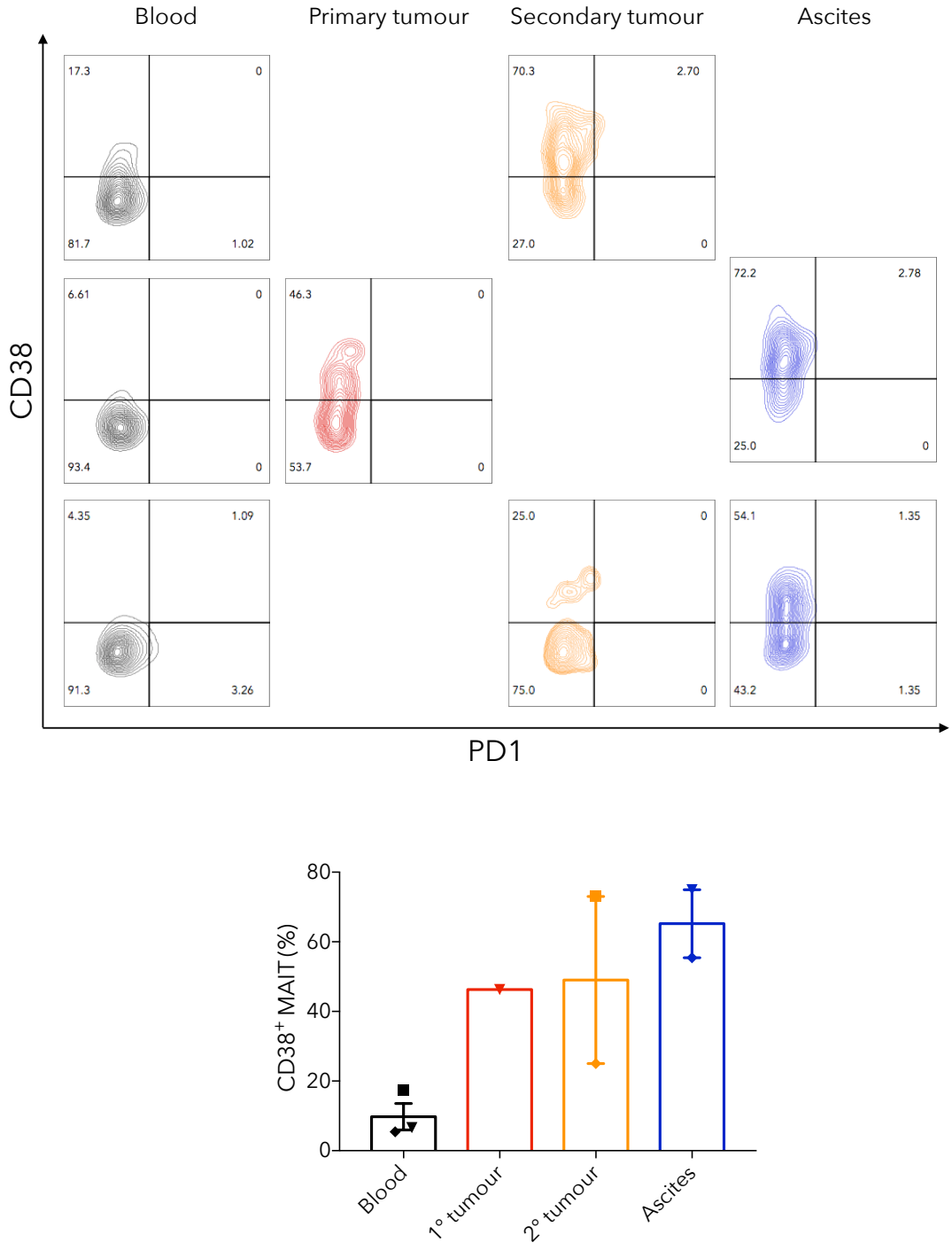

Figure 4-7 A higher proportion of MAIT cells express CD38 in tumour tissue and ascites compared to blood in individuals with ovarian cancer

PBMCs and processed tumour tissue samples from individuals with ovarian cancer were analysed by flow cytometry. Contour plots showing CD38 and PD1 expression on MAIT cells for all tumours that had MAIT cell infiltration. Each row of plots is from the same individual. Graph showing the summary of CD38 expression by MAIT cells. Each symbol represents an individual. Bar indicates mean and error bars represent SEM.

4.2.3 MAIT cells that infiltrate tumours have distinct TCRα TRAJ usage

As our results suggested that the MAIT cells present in the tumour are phenotypically distinct from those in the blood, we next wanted to definitively determine whether there was a difference between these two populations of MAIT cells. A previous study of MAIT cell tissue distribution and TCRα chain usage in healthy individuals revealed that the MAIT cells present in tissues predominantly use TRAJ12 instead of TRAJ33, which is the opposite of what is normally observed in the blood (Lepore *et al.*, 2014).

Therefore, we wanted to assess whether the MAIT cells present in tumours used the TRAJ region associated with tissue-residency. We analysed the TRAV1-2 repertoire by MAIT cells in the blood, ascites and tumour of two individuals with ovarian cancer. We observed that in both the tumour and ascites there was much greater usage of the more tissue resident TRAJ12 region (**Figure 4-8A**). We were also able to assess the usage of TRAJ20, an MR1-restricted MAIT cell TRAJ for which its tissue distribution is yet to be analysed. Similar to TRAJ12, we observed an over-representation of TRAJ20 in the tumour and ascites.

To determine whether this differential TRAJ usage would be observed in other tumour types, we analysed the TRAV1-2 repertoire of two renal cell carcinomas. We previously reported in Section 4.1.4 that renal cancers did not have MAIT cell infiltration due to necrosis of the tissue. For this TRAV1-2 repertoire analysis, we had access to fresh samples in which we could dissect out the necrotic tissue. We confirmed by flow cytometry that this dissected portion of the tumour tissue contained MAIT cells with an activated phenotype (**Figure 4-8B**). We observed that, similar to ovarian tumours, the renal tumours had a higher proportion of either TRAJ12 or TRAJ20 usage, compared to what is normally seen in the blood. We also had the opportunity to study a sample of "healthy" kidney tissue adjacent to the renal tumour and found in this case it used majority TRAJ33, similar to blood.

These results suggest that the MAIT cells observed infiltrating tumours overall have a distinct tissue-resident TCRα chain phenotype.

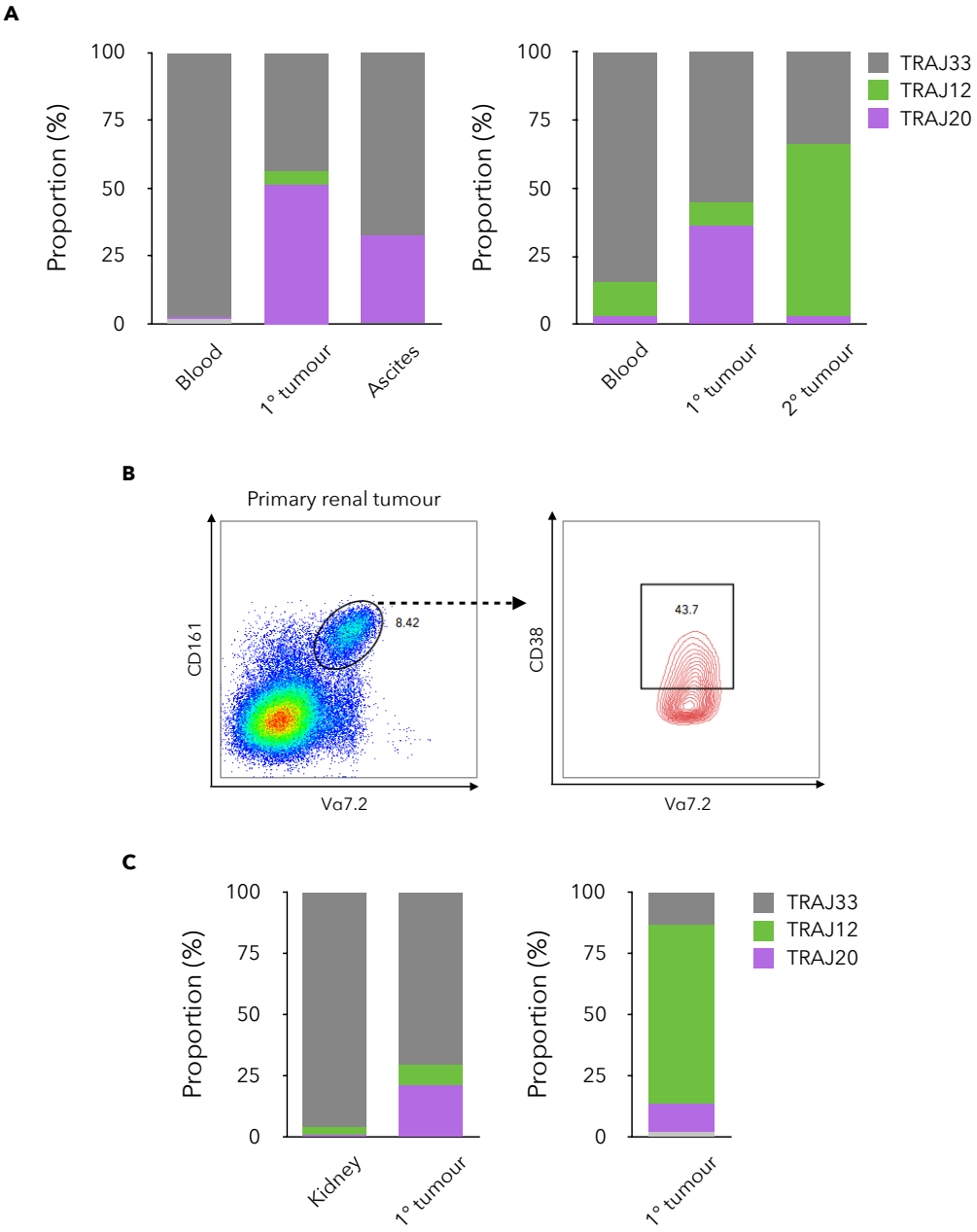

Figure 4-8 Distinct TRAJ usage by MAIT cells infiltrating tumours

PBMCs and processed tumour tissues from individuals with cancer were used for TRAV1-2 repertoire analysis. (A) Graphs show the proportion of the MAIT cell TRAV1-2 chains using either TRAJ33 (grey), TRAJ12 (green) or TRAJ20 (purple) for individuals with ovarian cancer (n = 2). (B) Example flow cytometry dot plot showing MAIT cells in renal tumours and contour plot showing expression of CD38 on MAIT cells. (C) Graphs show the proportion of the MR1-restricted TRAV1-2 chains using either TRAJ33, TRAJ12 or TRAJ20 in healthy kidney or primary tumours from individuals with renal cancer (n = 2).

4.2.4 MAIT cells that infiltrate primary ovarian tumour and ascites have a distinct clonotype composition

As the TCRα usage differs in blood compared to tumour tissues, we wanted to investigate whether there was also a difference in TCRβ usage. We therefore analysed the TCRβ repertoire of blood, ascites and tumour from an individual with ovarian cancer. We found similar oligoclonal usage of TRBV across blood, ascites and tumour, with the expected TRBV6 and TRBV20 predominating (**Figure 4-9A**). The TRBJ usage differed more, particularly in the ascites indicating that there may be a difference in the distribution of clonotypes across blood, ascites and tumour (**Figure 4-9B**).

We determined that the clonotype abundances differed depending on location, with blood, ascites and tumour all having distinctly different top clonotypes present, although all 200 top clones that were present were detectable across the three locations (**Figure 4-9C**). These results suggest that MAIT cells that infiltrate tumours, along with having a distinct tissue-resident TCRα chain usage, are also using different TCRβ clonotypes compared to blood.

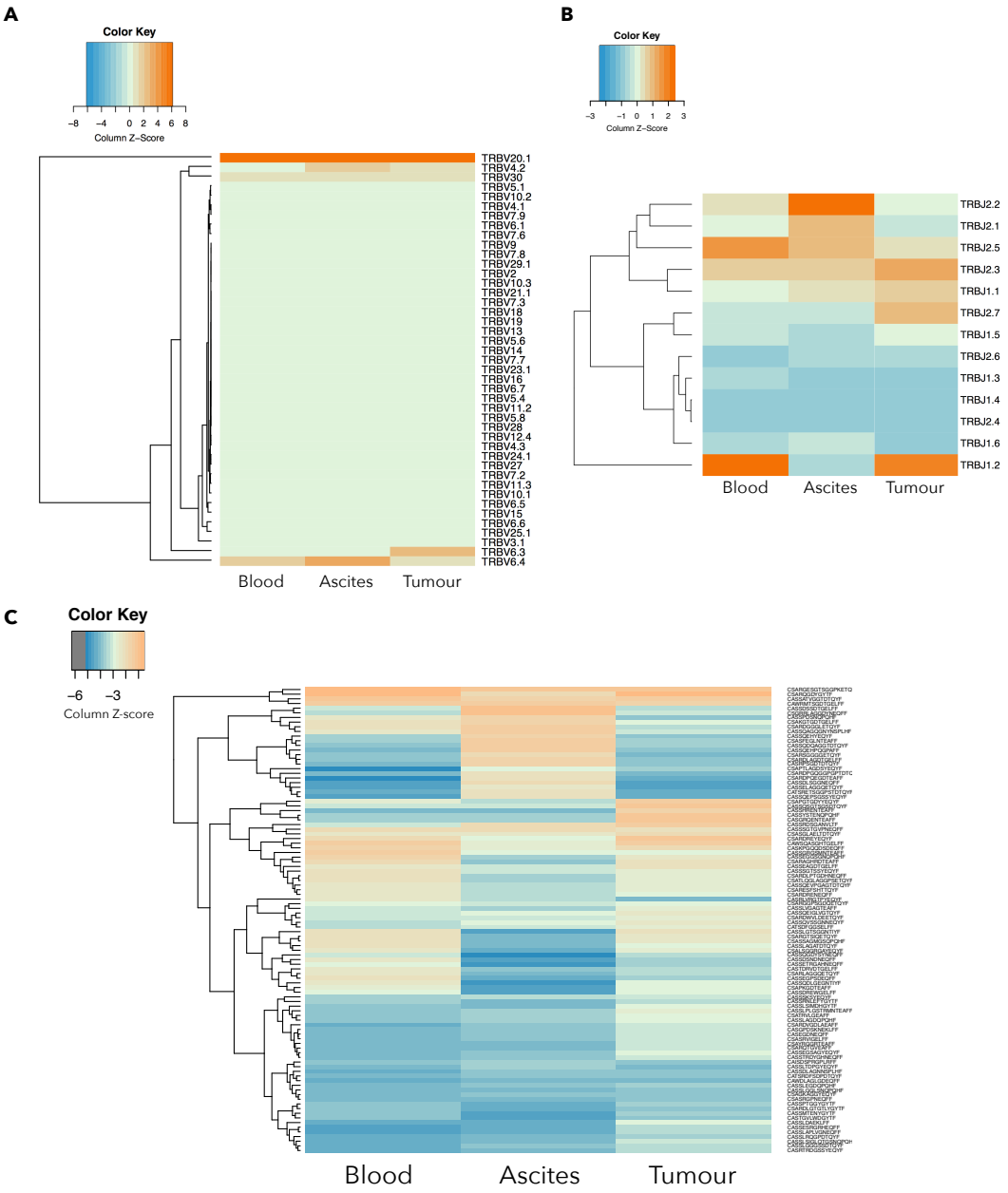

Figure 4-9 The MAIT cell TCRβ chain usage in ovarian cancer is oligoclonal but differ in clonotype abundances

PBMCs and processed tumour tissue and ascites from an individual with ovarian cancer were sorted for MAIT cells and their TCRβ repertoire analysed. The weighted (A) TRBV and (B) TRBJ usage profile is shown as a heatmap with hierarchical clustering performed using euclidean distance. A clonotype tracking heatmap is shown for donor 2 showing top 200 clonotypes with hierarchical clustering on the left y-axis and the CDR3β sequences on the right y-axis.

4.3 Analysis of MAIT cells during BCG treatment for bladder cancer

The most successful immunotherapy, which has become a gold-standard treatment, is intravesical BCG for high-risk non-invasive bladder carcinoma. Although highly successful, the immune mechanisms responsible for its success are largely unknown. We first wanted to determine whether MAIT cells could potentially play a role in the success of BCG bladder cancer by testing whether MAIT cells could respond to the strain of BCG used for this treatment *in vitro*.

4.3.1 Healthy donor MAIT cells are activated and produce cytokines in response to *in vitro* BCG infection

We observed that when we infected healthy PBMCs with low-dose BCG (TICE) they became activated and produced IFNγ and TNF (**Figure 4-10**). The addition of an anti-MR1 blocking antibody revealed that the production of TNF was the more MR1-restricted effector response of MAIT cells, similar to what we observed for the MAIT cell response to *S.* Paratyphi A *in vitro* infection in Section 3.1.2. This *in vitro* response to BCG TICE suggested that MAIT cells could potentially respond to the presence of BCG TICE *in vivo,* and in a partially MR1-dependent manner.

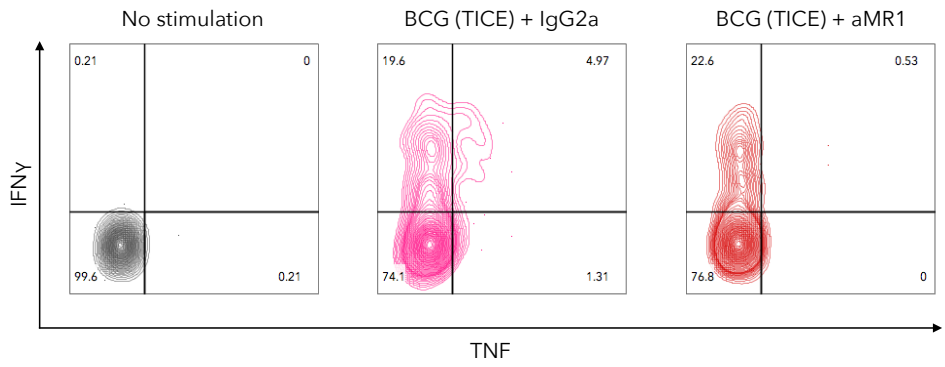

Figure 4-10 MAIT cells respond to BCG (TICE) in a partially MR1-dependent manner *in vitro*

PBMCs were isolated from a healthy donor and exposed to BCG (TICE) MOI 0.1 *in vitro* with either anti-MR1 blocking antibody (aMR1) (n = 5) or IgG2a isotype control. Cells were analysed by flow cytometry and MAIT cells were assessed for intracellular expression of cytokines IFNγ and TNF.

4.3.2 Circulating MAIT cells are low in frequency in individuals with bladder cancer and only undergo small changes in frequency during BCG treatment

We first wanted to determine whether circulating MAIT cells underwent changes during BCG therapy in individuals with bladder cancer. At the pre-BCG baseline analysis, we observed that overall the frequency of MAIT cells in those with bladder cancer was low compared to healthy controls. As we were aware that those with bladder cancer were older than our healthy controls, and that MAIT cells have been shown to decrease with age (Walker *et al.*, 2014, Novak *et al.*, 2014), we plotted the frequency of MAIT cells against age in both healthy donors and those with bladder cancer and saw a significant negative correlation (**Figure 4-11A**). This finding suggests that the low frequency observed in individuals with bladder cancer is likely due to the age of these individuals rather than their cancer disease status.

To determine whether changes in frequency in MAIT cells was occurring, indicating a migration from circulation to the site of inflammation induced by BCG treatment for bladder

cancer, we monitored the frequency of MAIT cells at several timepoints during treatment. The changes we observed in frequency compared to baseline were minor (less than 2-fold, comparable to fluctuations seen in healthy donors), with the exception of several individuals **(Figure 4-11B**). These results suggest that the frequency of MAIT cells either does not change in response to BCG treatment for bladder cancer or, as each of the blood sample timepoints were taken just prior to the next instillation of BCG, any changes that occurred in response were transient.

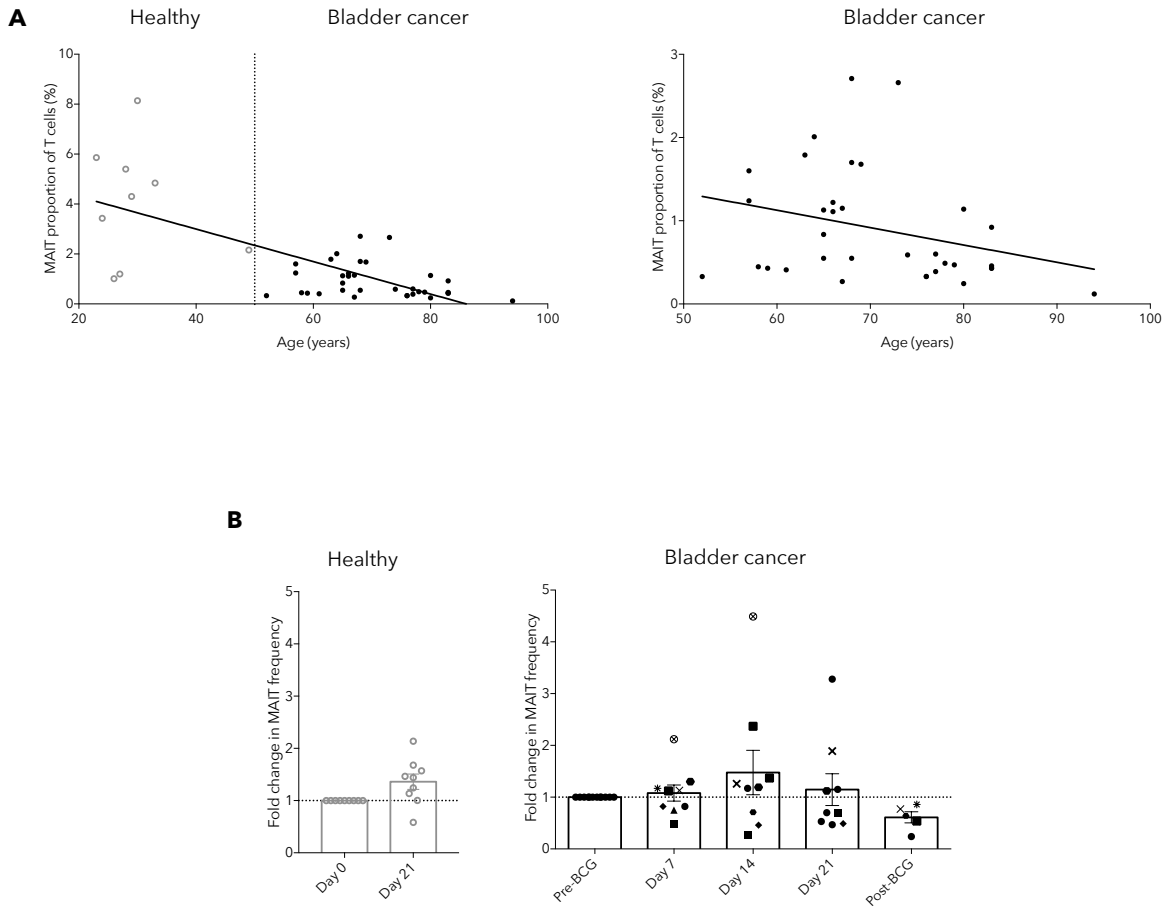

Figure 4-11 Circulating MAIT cells have a low frequency in individuals with bladder cancer and only undergo minor changes in frequency during BCG treatment

PBMCs were isolated at various time points from 12 individuals with bladder cancer undergoing BCG treatment and analysed by flow cytometry. PBMCs were isolated from nine healthy individuals as controls. (A) Graph on the left shows the frequency of MAIT cells as a percentage of the $CD3^+$ T cells plotted against age. Grey open circles represent healthy donors; black solid circles represent individuals with bladder cancer (Pre-BCG). A linear regression is shown in solid black line (r = -0.58, $P < 0.0001$ Spearman's rank). Graph on the right shows frequency of MAIT cells plotted against age only in individuals with bladder cancer (Pre-BCG). A linear regression is shown in solid black line (r = -0.30, P = 0.08 Spearman's rank). (B) Graph on left shows fold change of MAIT cells from baseline frequency in healthy donors taken 21 days apart. Graph on the right shows fold change of MAIT cells from baseline frequency during BCG treatment in individuals with bladder cancer. Each symbol represents a participant. Bar indicates mean and error bars represent SEM.

4.3.3 MAIT cells are present in the bladder mucosa following BCG treatment for bladder cancer and have an activated phenotype

MAIT cells are known to localise in the mucosal tissues and have been indirectly implicated in the bladder through presence in the urine of individuals suffering urinary tract infection (UTI) (Cui *et al.*, 2015). However, there is not yet direct evidence for their presence in bladder mucosa. To determine whether MAIT cells are resident or can infiltrate the bladder mucosa, we examined bladder mucosa biopsies taken after BCG therapy by flow cytometry to determine MAIT cell frequency and phenotype in the bladder following treatment.

The frequency of MAIT cells in the blood (1.1±0.56%) was similar to the frequency in the bladder (0.74±0.14%) (**Figure 4-12A**). However, the MAIT cells in the bladder biopsy had a much more activated phenotype compared to circulating MAIT cells from the same donor. Expression of the activation marker CD38 was observed on 12.3±4.35% of bladder MAIT cells compared to 2.3±0.34% of circulating MAIT cells (**Figure 4-12B**). More striking was the expression of the activation marker CD69, observed on 68±16.9% of bladder MAIT cells, compared to 18.2±7.8% of circulating MAIT cells (**Figure 4-12C**).

These findings provide evidence not only that MAIT cells are present in the bladder mucosa, but have an activated/tissue resident phenotype and could potentially be contributing to the local bladder immune response to BCG treatment.

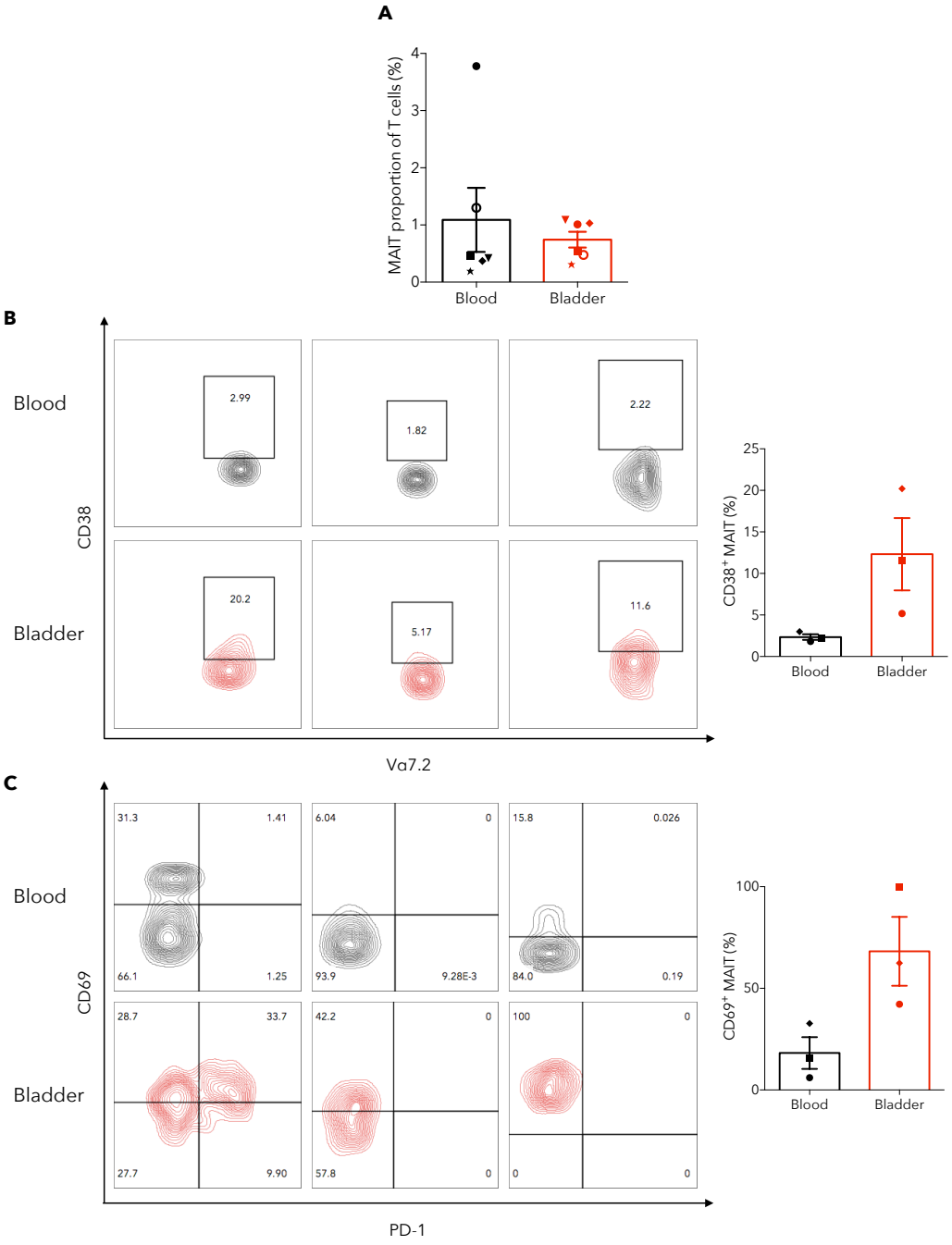

Figure 4-12 Similar frequency but altered phenotype of MAIT cells in bladder mucosa compared to blood following BCG treatment for bladder cancer

PBMCs and processed bladder mucosa biopsies from individuals following BCG treatment for bladder cancer were analysed by flow cytometry. (A) Graph shows frequency of MAIT cells in blood and bladder as proportion of $CD3^+$ T cells (n = 6). (B) Contour plots and summary graph show the activation of MAIT cells in the blood and bladder by expression of CD38 (n = 3). (C) Contour plots (CD69 vs PD-1) and summary graph (CD69) shows the activation of MAIT cells in the blood and bladder (n = 3). For contour plots, each column represents an individual. For graphs, each symbol represents an individual. Bar indicates mean and error bars represent SEM.

4.3.4 Enhanced cytokine response to *ex vivo* BCG infection by circulating MAIT cells following BCG treatment for bladder cancer

Although we were not able to see differences in the frequency of circulating MAIT cells during BCG treatment for bladder cancer, we wanted to determine whether we could detect functional differences in the circulating MAIT cells that occur in response to BCG treatment.

To address this, we used frozen PBMCs taken from before (Pre-BCG), during (week 6) and after (week 12) BCG treatment and challenged them *ex vivo* with various stimuli. We again examined the frequency of MAIT cells in these samples and confirmed that overall there were no large changes observed (**Figure 4-13A**). We first assessed whether there was a difference in cytokine response when stimulating MAIT cells with the TCR-independent PMA/ionomycin stimulation. We did not observe any difference in MAIT cell's IL-17, IFNγ or TNF production across the timepoints (**Figure 4-13B**). This suggests that the ability of MAIT cells to produce cytokine regardless of stimulus has not changed in these individuals.

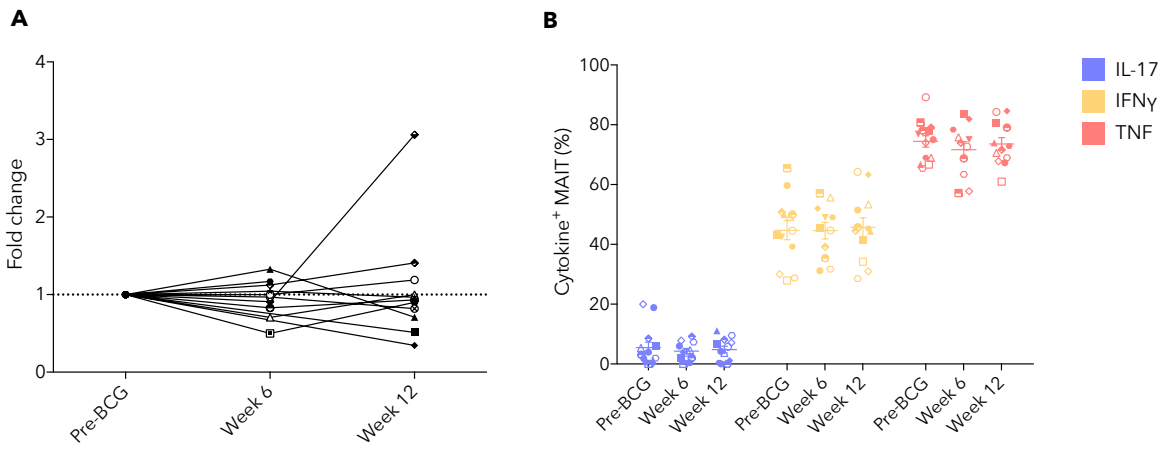

Figure 4-13 The frequency and non-specific cytokine response of circulating MAIT cells does not alter in response to BCG therapy for bladder cancer

PBMCs were isolated at various time points from 13 individuals undergoing BCG treatment for bladder cancer. Samples were stimulated with phorbol 12-myristate 13-acetate (PMA) and ionomycin, intracellular stained and analysed by flow cytometry. Unstimulated PBMCs were used as controls and to assess the frequency of MAIT cells in the $CD3^+$ T cell compartment. (A) Graph shows frequency of circulating MAIT cells expressed as fold change from baseline. (B) The production of IL-17, IFNγ and TNF in response to PMA/ionomycin stimulation. Each symbol represents an individual, the line is at the mean and error bars represent SEM.

We next examined whether the bacteria-specific response of MAIT cells was altered in response to BCG treatment for bladder cancer. We used BCG (TICE) and a control bacteria *E. coli* in the *ex vivo* stimulation. As BCG is slow growing and does not require addition of antibiotics as part of the *ex vivo* infection, we used *E. coli* fixed in PFA to make a more comparable control. We found no difference in activation measured by CD69 expression or production of IL-17 or IFNγ. However, when assessing the more MR1-restricted cytokine TNF, we saw that in five individuals there was a more than 2-fold increase in TNF production from baseline in response to BCG but not *E. coli*. following BCG treatment. This result suggests that the bacteria-specific response of MAIT cells could be altered by BCG during bladder cancer treatment in certain individuals.

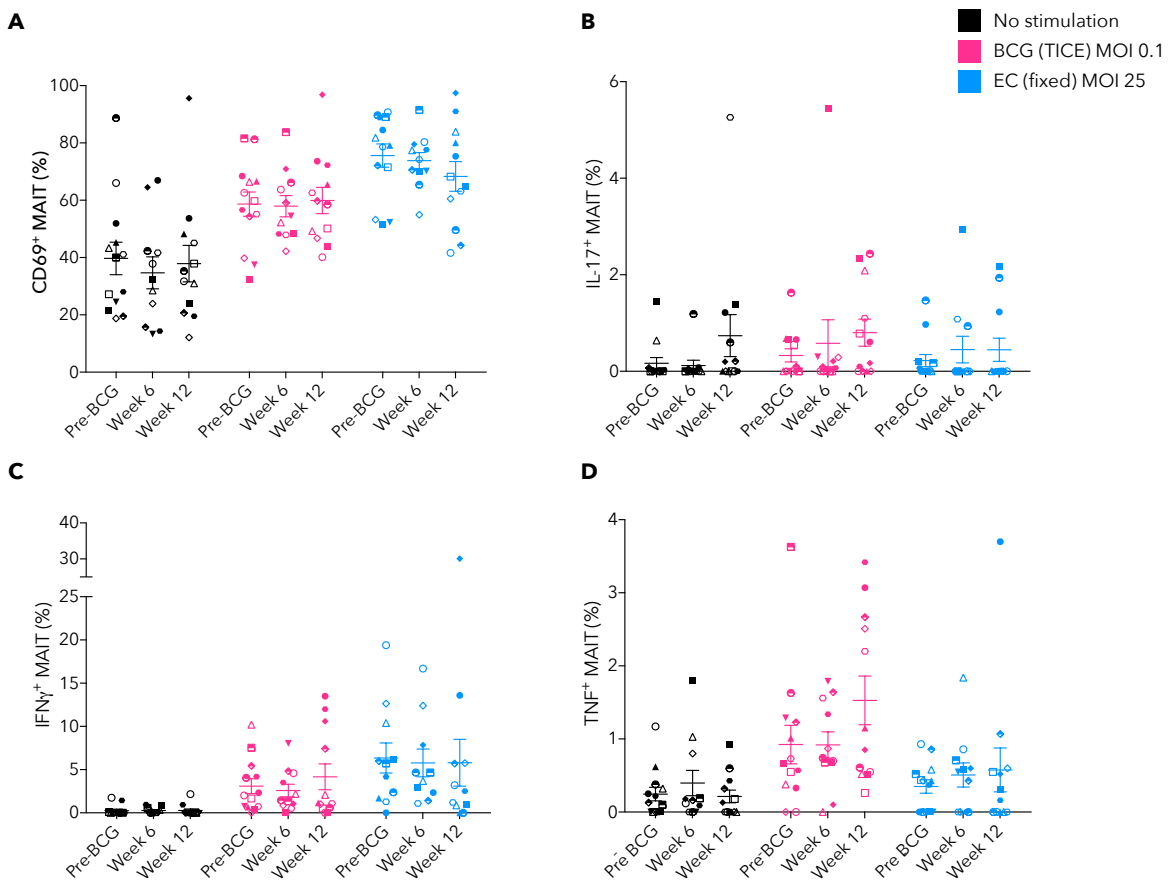

Figure 4-14 The BCG-specific cytokine response of circulating MAIT cells does alter in response to BCG therapy for bladder cancer in some individuals

PBMCs were isolated at various time points from 13 individuals undergoing BCG treatment for bladder cancer. Samples were stimulated with BCG (TICE) MOI 0.1 or PFA-fixed *E. coli* (DH5α) MOI 25, intracellular stained and analysed by flow cytometry. (A) Graph showing the activation of MAIT cells by surface expression of CD69. Graphs showing the production of (B) IL-17, (C) IFNγ and (D) TNF in response to no stimulation, BCG and *E. coli*. Each symbol represents an individual, the line is at the mean and error bars represent SEM.

4.4 Discussion

Although the MAIT cell ligand is derived from bacteria, there is great interest in understanding the role of MAIT cells in sterile inflammatory diseases as they can also respond in a TCR-independent manner and produce effector functions through cytokine-mediated activation (van Wilgenburg *et al.*, 2016, Sattler *et al.*, 2015, Ussher *et al.*, 2014). Most of the research has focussed on characterising MAIT cells in autoimmune disorders such as multiple sclerosis (Annibali *et al.*, 2011, Miyazaki *et al.*, 2011) and inflammatory bowel disease (Serriari *et al.*, 2014). Very little research has assessed the role of MAIT cells in cancer, and the several studies that have, focussed on MAIT cells in colorectal cancer.

We validated the findings of these previous studies that reported MAIT cell infiltration into colorectal tumours (Ling *et al.*, 2016, Won *et al.*, 2016, Zabijak *et al.*, 2015). We also extended these findings to demonstrate MAIT cells can infiltrate lung, melanoma and breast tumours, as shown by immunohistochemistry, and ovarian and renal tumours, as shown by flow cytometry. This provides evidence that the MAIT cell's potential role in cancer is not limited to mucosal-derived tumours.

We examined the MAIT cells present in ovarian tumours and found that, in both tumour and ascites, MAIT cells upregulated the expression of the activation marker CD38 compared to the circulating MAIT cells in these individuals. This suggests that in the sterile inflammatory environment of cancer, MAIT cells become activated and could potentially contribute to the pathogenesis of cancer. Alternatively, it could also indicate that the MAIT cells in the cancers are of tissue origin, as it has been reported that tissue-resident MAIT cells generally have higher expression of activation markers (Tang *et al.*, 2013).

We wanted to determine whether the source of MAIT cells in tumours was from the circulation or tissue-resident MAIT cells, as there are opposing findings from studies as to whether MAIT cells migrate from circulation into tumours. The first study to analyse circulating MAIT cell frequency in cancer found no difference when compared to healthy controls, suggesting MAIT cells do not migrate (Le Bourhis *et al.*, 2010). However, two papers that assessed MAIT cell frequency in colorectal cancer reported a decreased frequency of circulating MAIT cells in the blood compared with aged-matched controls (Ling *et al.*, 2016, Won *et al.*, 2016). Thus, we took a more direct approach, and assessed the TRAJ usage of MAIT cells in cancer as a previous study of healthy tissues suggested that TRAJ12 was more commonly used by tissue-resident MAIT cells and could be considered a functional subset of MAIT cells (Lepore *et al.*, 2014). We found that MAIT cells within tumours used more of the TRAJ12, as well as the previously considered rare TRAJ20, TCRα chain regions compared to the TRAJ33 that is predominant in the blood. Our results suggest that the TRAJ20 MAIT cell subset is also more commonly found in tissues and that the MAIT cells we observed infiltrating tumours are likely derived from the local tissue-resident MAIT cell subsets rather than infiltrating from the circulation.

We observed in an ovarian cancer patient that a large proportion of circulating T cells that survived chemotherapy were MAIT cells. This result is consistent with observations by a previous study, which suggested that MAIT cells are able to survive chemotherapy as they are non-cycling long-lived cells that express the multi-drug resistance transporter ABCB1 (Dusseaux *et al.*, 2011). It is thought that this may be a mechanism employed by MAIT cells to survive the xenobiotics that can be secreted by gut microbiota. These results show that MAIT cells may play an important role in protective immunity following chemotherapy as they are fast-recovering and predominant.

We had the opportunity to study the role of MAIT cells in response to BCG treatment for bladder cancer. We observed that the frequency of MAIT cells in individuals with bladder cancer prior to treatment was low compared to healthy individuals. This low frequency is not necessarily due to the cancer, as we observed that the frequency of MAIT cells negatively correlated with the age, an observation that has been reported previously (Novak *et al.*, 2014, Walker *et al.*, 2014).

During BCG treatment for bladder cancer we did not observe any large changes in the frequency of circulating MAIT cells. As we are creating a localised infection within the bladder through addition of BCG, it was hypothesised that we would observe a decrease in MAIT cells frequency as they move from the blood to the inflamed tissue. This migration of MAIT cells was observed and discussed in Section 3.2.1 in response to *Salmonella* infection and has been observed in several other infection models (Salerno-Goncalves *et al.*, 2017, Le Bourhis *et al.*, 2010, Chen *et al.*, 2017). It is possible that due to the timing of the blood samples being taken seven days after the instillation of BCG (just prior to the next instillation) that any changes in frequency could have been transient and not captured within our window of observation.

The presence of MAIT cells in the bladder with an activated phenotype following BCG treatment provided evidence that MAIT cells could be responding to the presence of BCG. This response may not only be due to the presence of their ligand from BCG, but further potentiated in a cytokine-driven manner as previous studies have detected the cytokines known to activate MAIT cells, IL-12 and IL-18 (Ussher *et al.*, 2014), in the urine of individuals undergoing BCG immunotherapy (Eto *et al.*, 2005, O'Donnell *et al.*, 1999).

The enhanced TNF production by circulating MAIT cells to BCG following treatment in some individuals suggested that the circulating MAIT cell population may have altered

following treatment. Such changes could be TCR repertoire, as discussed in Chapter 3, but due to limited access to samples the TCR repertoire in these individuals could not be investigated. However, as the changes in MAIT cell response to BCG were observed predominantly in the TNF-producing population, this provides indirect evidence that TCR repertoire reshaping could be occurring.

Together, our results suggest that MAIT cells may play a role in the pathogenesis of cancer, not only in mucosal tumours, but in a wide variety of different tumour settings. TCRα TRAJ usage suggests the source of these cells is likely to be the tissue-derived MAIT cells responding to local inflammatory signals. And finally, that MAIT cells are present and activated in the bladder following BCG treatment for bladder cancer, suggesting a potential role for MAIT cells in mediating this successful immunotherapy.

Chapter 5 – The influence of the TCR on MAIT cell responses

The analysis of MAIT cells in both *Salmonella* infection and cancer revealed distinct usage of semi-invariant TCRs. We wanted to investigate the importance of MAIT TCRα usage, as identified in our study of cancer tissues in Section 4.2, as well as the potential functional implication of the expansion of select TCRβ clonotypes in response to *S.* Paratyphi A infection from Section 3.3.

5.1 Production of APC lines to establish a MAIT cell TCR-MR1 *in vitro* assay

5.1.1 Differential expression of MR1 by different overexpressing cell lines

We produced APC lines overexpressing MR1 in order to study MAIT cell activation in an MR1- and TCR-dependent *in vitro* system. THP1, C1R and K562 cell lines were chosen as they all have different cell origins and different antigen presenting capabilities. We transduced each cell line with a GFP lentiviral vector, containing the MR1 gene under an SFFV promotor, and cell sorted each line based on high expression of GFP.

We next wanted to characterise both overexpressing and wild type (WT) cell lines and their expression of MR1. We measured the gene expression level of MR1 by quantitative PCR (qPCR) and found that in WT THP1 and C1R cell lines there were measureable MR1 transcripts present, whereas K562 did not have detectable levels (**Figure 5-1A**). In the over-expressing lines, THP1.MR1 had the highest expression, followed by C1R.MR1 then K562.MR1. This same pattern of expression was observed on the protein surface level analysed by flow cytometry (**Figure 5-1B**) and total protein level analysed by confocal

microscopy, which also showed that MR1 was mostly intracellular and contained within vesicles as indicated by the punctate staining pattern (**Figure 5-1C**).

These results suggest that the three MR1 overexpressing cell lines differ in their expression of MR1, mirroring the pattern of expression observed in the WT cell lines (K562 < C1R < THP1).

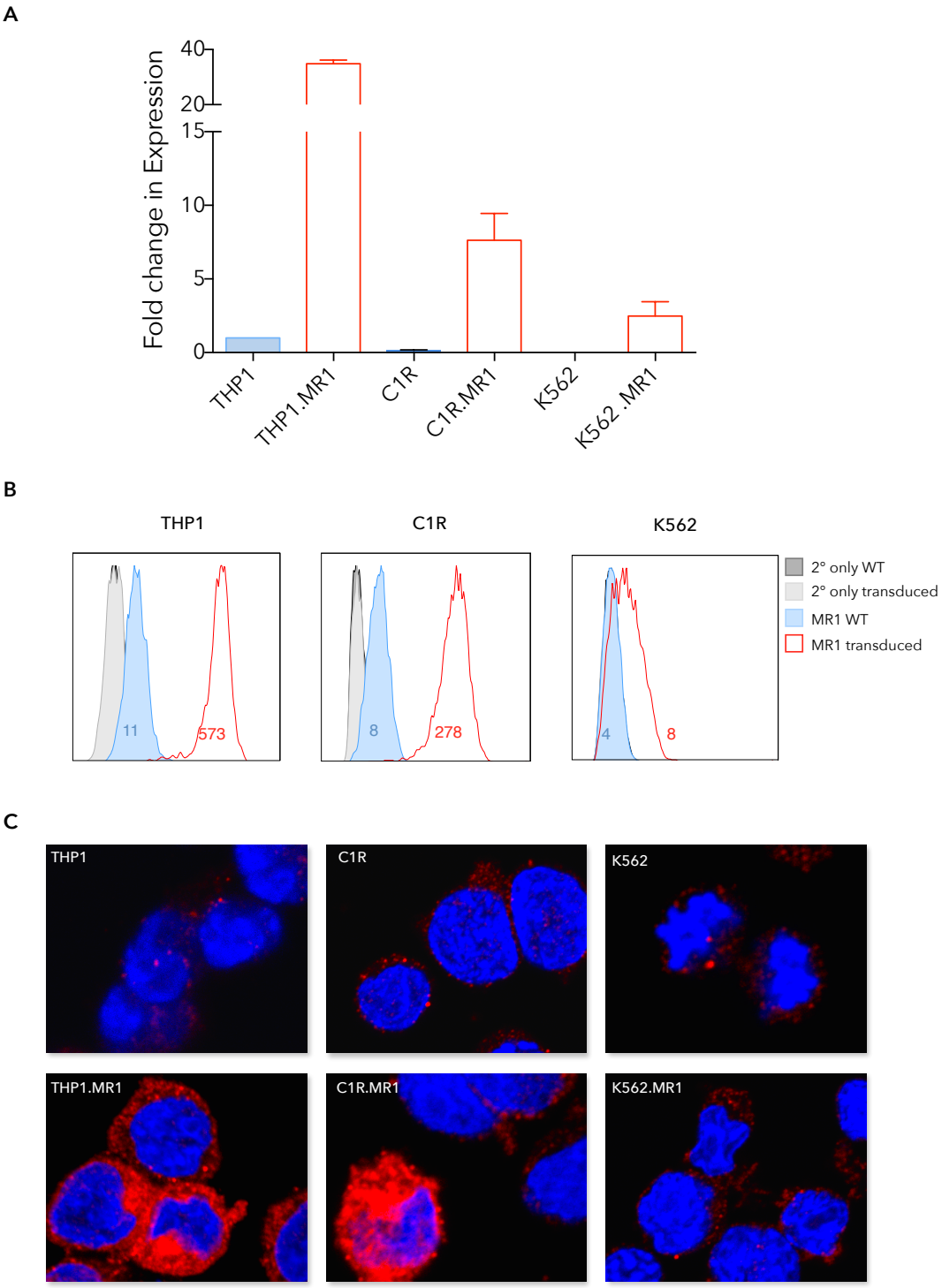

Figure 5-1 MR1 expression in wild-type and transduced cell lines

THP1, C1R and K562 cell lines were transduced with a lentiviral vector containing the human MR1 gene under an SFFV promoter. (A) Quantitative PCR (qPCR) was performed using TaqMan probes to MR1 and expression normalised to GAPDH. Expression is shown as fold change relative to THP1. Bar shows mean and error bar represents SEM between technical duplicates. (B) Flow cytometry of surface MR1. Number indicates the median value for fluorescence intensity divided by the baseline (2° only). (C) Confocal microscopy of cells stained with MR1 (red). Blue represents DAPI (nuclear) staining.

5.1.2 Level of MR1 expression by APC line correlates with IFNγ production by MAIT cells

To assess whether the different levels of MR1 expression affected the ability of these cell lines to activate MAIT cells, we analysed both WT and MR1-overexpressing cell lines ability to activate MAIT cells after infection with *E. coli* or BCG (TICE). Using an IFNγ ELISpot assay, we found that THP1.MR1 could activate MAIT cells more than WT THP1 and that this was largely an MR1-restricted response (**Figure 5-2A**). This was even more pronounced in the case of C1R.MR1 compared with WT CIR, as the WT cell line alone did not activate MAIT cells in this assay (**Figure 5-2B**). The K562.MR1 did not activate MAIT cells, similar to the WT K562, indicating that this cell line is not an appropriate APC line for studying MR1-dependent MAIT cell activation.

From these results, we concluded that the level of MR1 expression in APC lines correlated to the level of MR1-restricted activation of MAIT cells they could induce. As we observed the greatest level of MR1-restricted responses from the C1R cell lines (particularly to *E. coli*), we chose this as the cell line to be used in further MAIT cell *in vitro* activation assays.

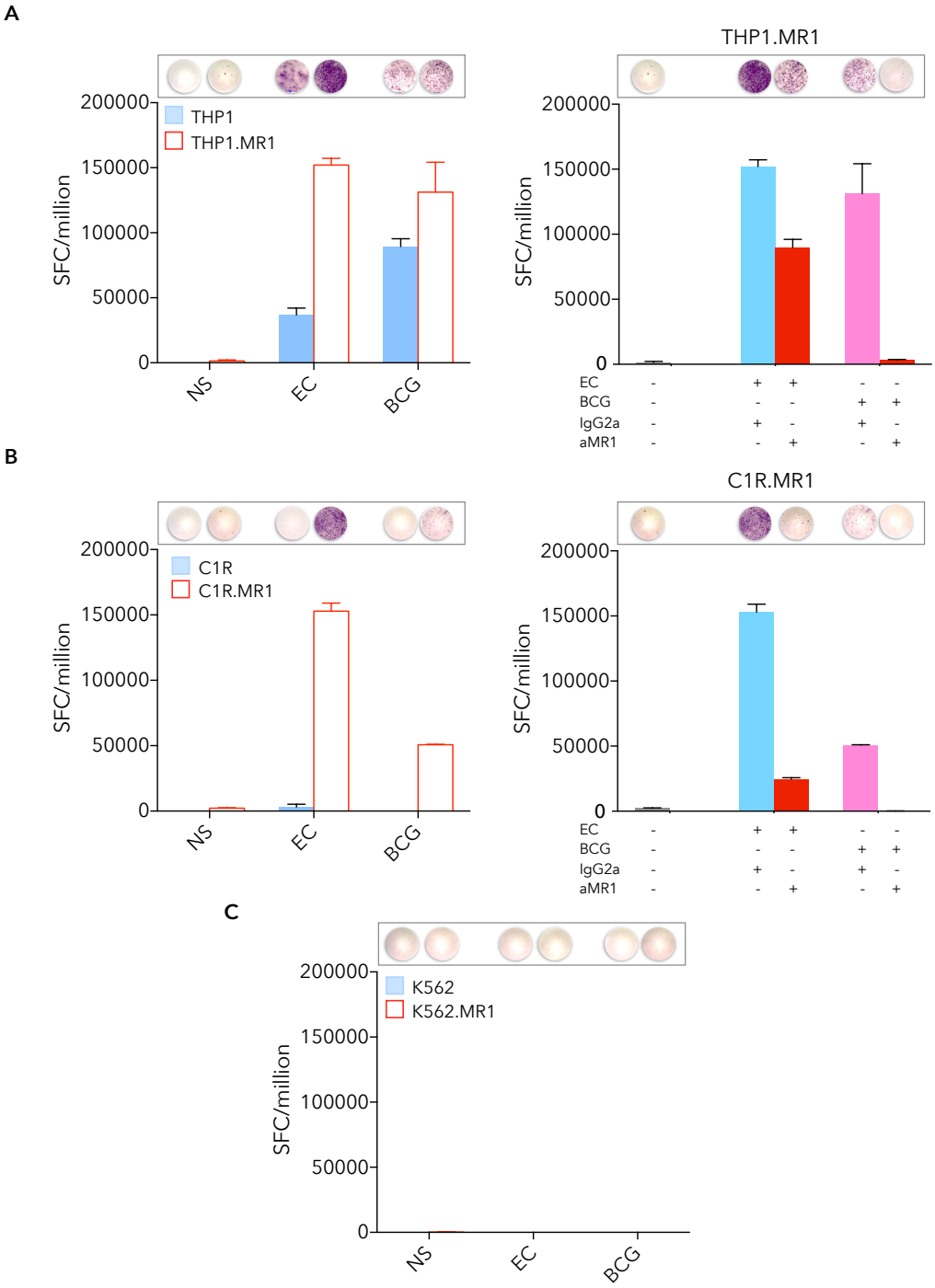

Figure 5-2 MR1-transduced cell lines can induce greater IFNγ production by MAIT cells and this correlates to their level of MR1 expression

MAIT cells were co-cultured with MR1-transduced and WT cell lines with no stimulation, live *E. coli* (DH5α) MOI 5 or BCG (TICE) MOI 0.1 and IFNγ production measured by ELISpot. Results shown for WT and MR1-overexpressing lines (A) THP1, (B) C1R and (C) K562. Circle images on the top x-axis show representative ELISpot well. Each purple dot represents an IFNγ spot forming cell (SFC). Bar shows mean and error bar represents SEM between technical duplicates. NS, no stimulation; EC, *E. coli*.

5.2 Functional analysis of the TCRα chains identified in cancer samples using Jurkat.MAIT lines

5.2.1 Comparable expression of TCR on Jurkat lines expressing MAIT TCRα chain of interest

We produced three TRAV1-2 Jurkat.MAIT lines expressing the most common TRAJ33, and the more tissue-resident TRAJ12 and TRAJ20 (CDR3α regions designed from the MAIT cell CDR3α identified in ovarian cancer blood and tissue in Section 4.2.3). All TCRα chains were inserted into lentiviral vector containing the same common TRAV20-1 to exclude the effect of TCRβ chain on activation. Both TCRα and TCRβ were under an SFFV promoter to ensure they were expressed at the same levels. JRT3 Jurkat cells, which have the TCRβ gene knocked out, were transduced with the MAIT TCRs. Details for each line are outlined in **Table 5-1.**

Table 5-1 TCR details of Jurkat.MAIT lines with differing TRAJ usage

NAME	TRAV	TRAJ	CDR3α	FREQUENCY IN BLOOD	FREQUENCY IN TUMOUR
TRAJ20/TRBV20	1-2	20	CAVRDGD**Y**KLSF	0.3%	50.1%
TRAJ12/TRBV20	1-2	12	CAVMDSS**Y**KLIF	0.1%	4.5%
TRAJ33/TRBV20	1-2	33	CAVMDSN**Y**QLIW	34.1%	8.5%

Bold **Y** indicates tyrosine residue at position 95 necessary for MR1-restriction; frequency refers to percentage of detected productive TRAV1-2 sequences from MiSeq results of the first ovarian blood and tumour samples from Section 4.2.3.

To be able to compare levels of activation across the cell lines, and attribute this to the TRAJ region usage, it was important to establish that all Jurkat.MAIT lines expressed the MAIT cell TCR at comparable levels at the surface, as this could impact the level of activation displayed by each cell line. Following transduction of the vector containing the TCRα and TCRβ sequences, the cell lines were analysed by flow cytometry for expression of both CD3 (which composes part of the TCR complex) and the TCR Vα7.2 region. The results showed

that in all cell lines, expression of both CD3 and TCR Vα7.2 was high and the level of expression of both markers were correlated (**Figure 5-3**). Furthermore, the same levels of expression were observed across all Jurkat.MAIT lines, enabling their activation levels to be compared, as this will correlate directly to TCR avidity and not level of expression.

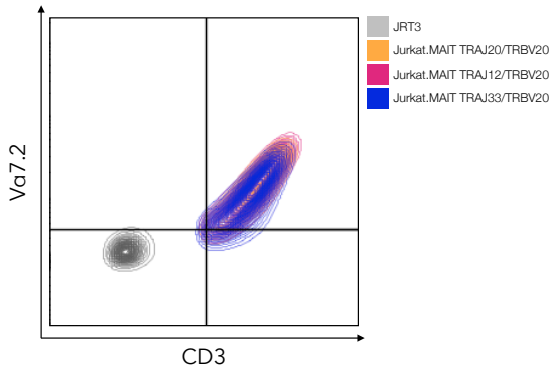

Figure 5-3 Comparable and correct expression of TCR across Jurkat.MAIT lines expressing different TRAJ regions

JRT3 cells were transduced with a vector containing TRAV1-2 with TRAJ33, TRAJ12 or TRAJ20 and containing the same TCRβ chain TRAV20-1 across the three lines. The expression of the correct TCR was confirmed by flow cytometry using antibodies against CD3 and Vα7.2. Overlaid contour plots showing expression of CD3 against Vα7.2 in the three Jurkat.MAIT lines compared to the untransduced JRT3 control.

5.2.2 The TRAJ usage influences the Jurkat.MAIT activation in response to *E. coli*

We first wanted to examine how the TRAJ usage influenced the Jurkat.MAIT response to *E. coli* culture supernatant, which is known to contain MAIT cell stimulating ligands. We observed a partially dose-dependent (**Figure 5-4A**) response by two of the cell lines TRAJ33/TRBV20 and TRAJ12/TRBV20. The activation level appears to be saturated at the higher 10 µL and 5 µL concentrations, but by 2 µL we were able to observe a clear titration of the activation. The activation observed in the TRAJ33/TRBV20 and TRAJ12/TRBV20 cell lines was also MR1-restricted, as it could be blocked with an anti-MR1 blocking antibody (**Figure 5-4B**). The activation of the TRAJ12/TRBV20 line was lower overall compared to TRAJ33/TRBV20. The TRAJ20/TRBV20 line showed no response to

stimulation with *E. coli* supernatant at any of the concentrations used. This was surprising, as we already established that all three cell lines could produce productive TCR at the surface and the TRAJ20 sequence that was transduced is a known MAIT cell TRAJ sequence.

These results suggest that TRAJ usage can greatly influence MAIT cell responsiveness to *E. coli* supernatant containing the MAIT cell ligand. The TRAJ33 region, most commonly found in the blood, showed the greater level of activation followed by the more tissue-resident TRAJ12 and TRAJ20.

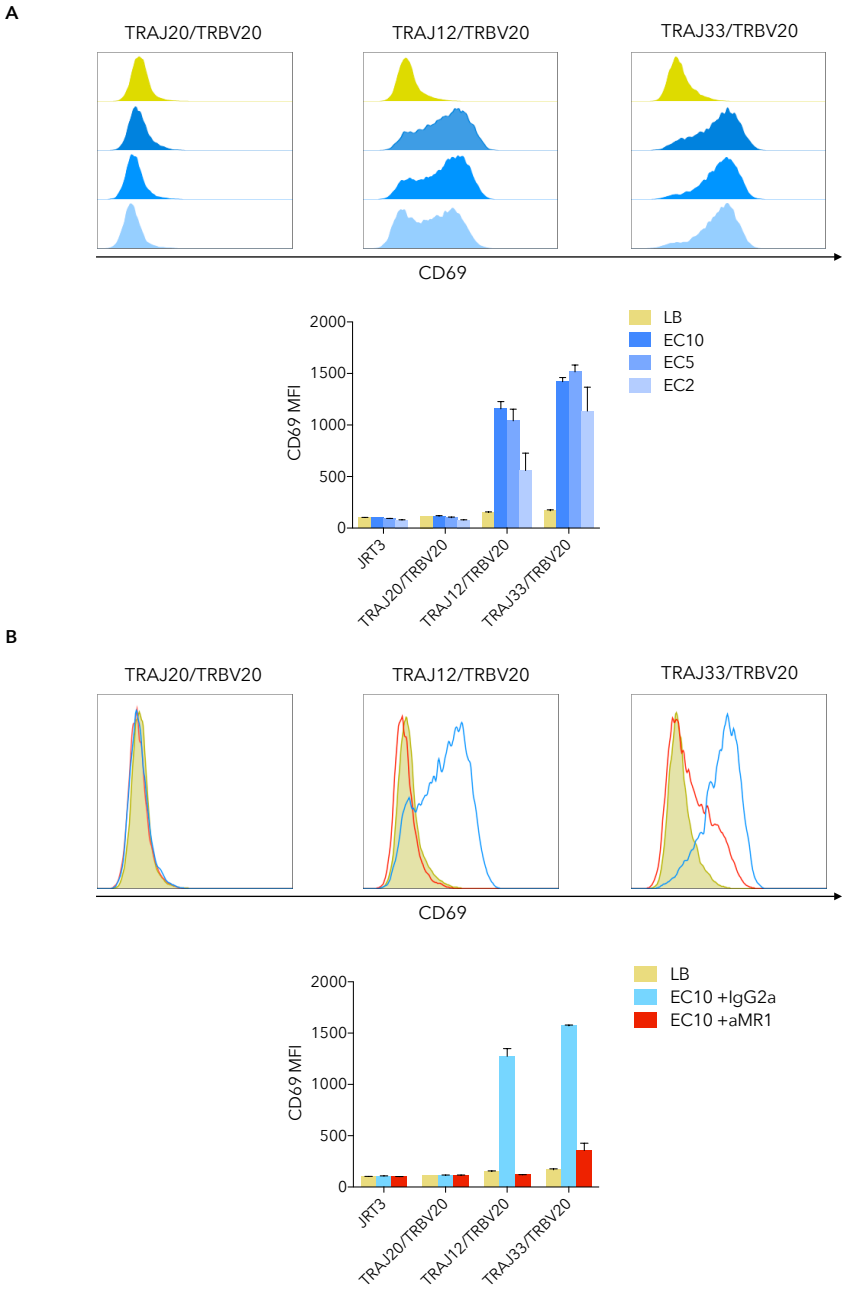

Figure 5-4 TRAJ usage by Jurkat.MAIT cells influences their activation in response to *E. coli* supernatant

JRT3 cells were transduced with a vector containing TRAV1-2 with TRAJ33, TRAJ12 or TRAJ20 and containing the same TCRβ chain TRBV20-1 across the three lines. (A) Using C1R.MR1 cells as APCs, the activation of Jurkat.MAIT cell lines was measured by flow cytometry using the MFI of CD69 in response to *in vitro E. coli* (EC) supernatant when co-cultured for 18–20 hours. Number indicating volume (µL) of supernatant added. (B) Activation of Jurkat.MAIT cell lines to *E. coli* supernatant after addition of 10 µg/mL of anti-MR1 blocking antibody (aMR1) or IgG2a isotype control. For graphs, bars show mean with error bars representing SEM between technical duplicates. MFI, mean fluorescence intensity; LB, L-broth.

5.2.3 The TRAJ usage influence on Jurkat.MAIT activation is slightly altered by TCRβ chain pairing

As the TRAJ20/TRBV20 cell line showed no activation in response to stimulation, we wanted to investigate whether pairing with another TCRβ chain would enable this TCR TRAJ region to recognise antigen and activate the cell. To address this, we produced Jurkat.MAIT cell lines expressing the same TRAJ regions as previously outlined, but paired with a TRBV6-1 TCRβ chain.

We observed that, when paired with a different TCRβ chain, the activation of the lines followed a similar pattern of activation as described in 5.2.2., however, we also observed a small dose-dependent (**Figure 5-5A**) and MR1-restricted (**Figure 5-5B**) response in the TRAJ20/TRBV6 line. This result suggests that the TRAJ20 is a functional MAIT cell TRAJ region, but only when paired with certain TCRβ chains. The response we observed in the TRAJ33 and TRAJ12 was similarly high as when paired with the TRBV20, but the TRAJ33 was no longer a consistent difference in activation levels seen between the two TRAJ regions.

These results indicate that the TCRβ chain pairing can influence the level of activation seen by different TRAJ regions, but only by a small increase or decrease, as the overall pattern of activation (TRAJ20 < TRAJ12/33) remains consistent.

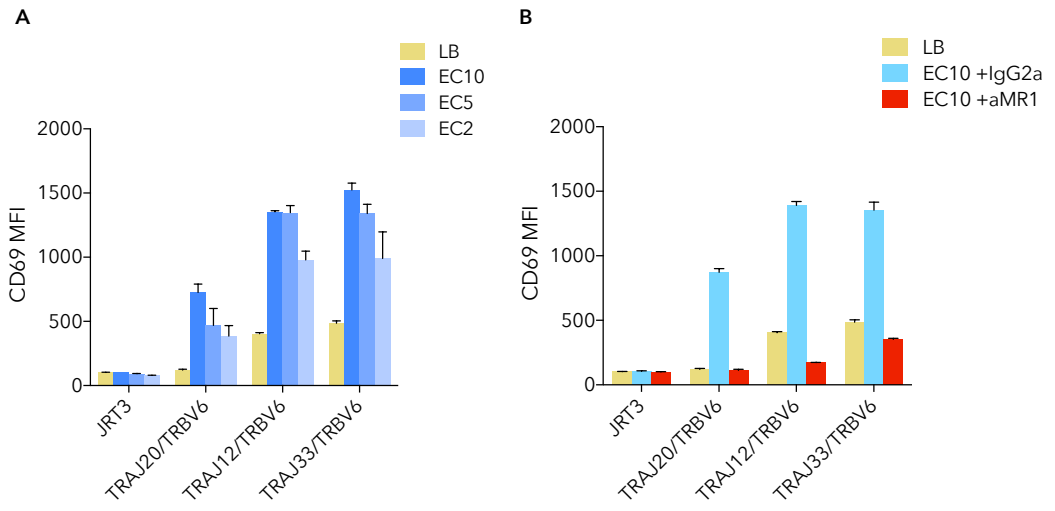

Figure 5-5 TRAJ usage influence on Jurkat.MAIT activation in response to *E. coli* supernatant is slightly altered by TCRβ usage

JRT3 cells were transduced with a vector containing TRAV1-2 with TRAJ33, TRAJ12 or TRAJ20 and containing the same TCRβ chain TRBV6-1 across the three lines. (A) Using C1R.MR1 cells as APCs, the activation of Jurkat.MAIT cell lines was measured by flow cytometry using the MFI of CD69 in response to *in vitro E. coli* (EC) supernatant when co-cultured for 18–20 hours. Number indicating volume (µL) of supernatant added. (B) Activation of Jurkat.MAIT cell lines to *E. coli* supernatant after addition of 10 µg/mL of anti-MR1 blocking antibody (aMR1) or IgG2a isotype control. Bars show mean with error bars representing SEM between technical duplicates. MFI, mean fluorescence intensity; LB, L-broth.

5.2.4 The TRAJ usage influence on the Jurkat.MAIT activation is similar across various bacterial stimuli

We next wanted to examine whether different strains of bacteria would yield different levels of activation in the three TRAJ/TRBV20 cell lines. We activated MAIT cells with either *E. coli, S.* Paratyphi A or *S.* Typhi supernatant. We observed that regardless of bacterial stimuli, the activation pattern of the cell lines (TRAJ20 < TRAJ12 < TRAJ33) remained the same. *S.* Paratyphi and *S.* Typhi showed even greater (approximately 2-fold) difference in activation between TRAJ12 and TRAJ33 compared to the much smaller difference in activation observed in response to *E. coli.* This may be due to *E. coli* being a stronger stimulator and causing a saturation of the activation response of these cell lines.

These results show that, regardless of bacteria species, the MAIT cell TCR response remains the consistent. This may be due to the TCRs responding to the same antigen present in all the bacterial supernatants.

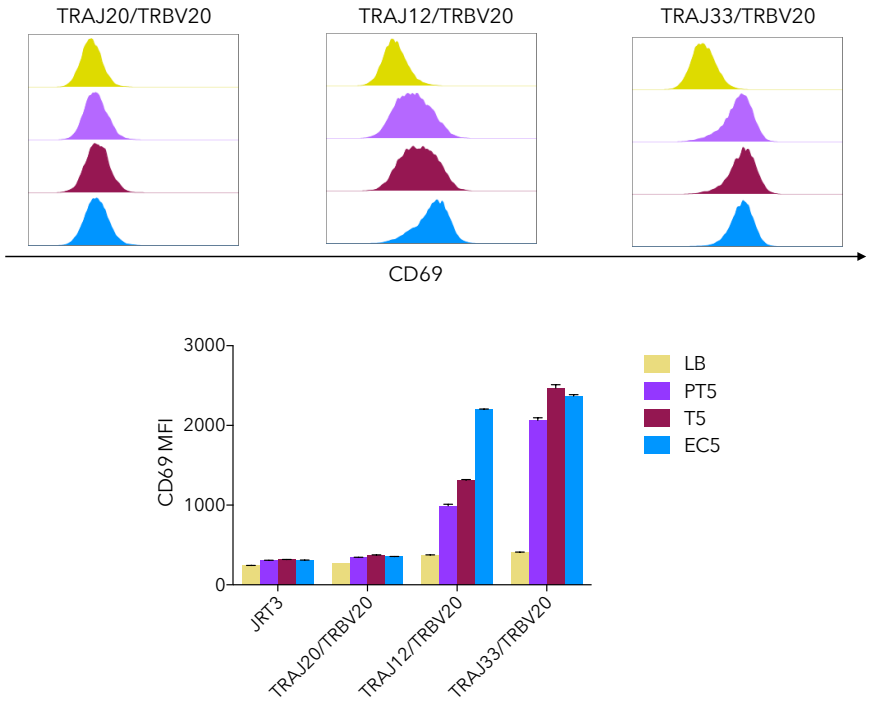

Figure 5-6 TRAJ usage influence on Jurkat.MAIT activation is consistent across different bacterial supernatant stimuli

JRT3 cells were transduced with a vector containing TRAV1-2 with TRAJ33, TRAJ12 or TRAJ20 and containing the same TCRβ chain TRBV20-1 across the three lines. Using C1R.MR1 cells as APCs, the activation of Jurkat.MAIT cell lines was measured by flow cytometry using the MFI of CD69 in response to *in vitro E. coli* (EC), *S.* Paratyphi A (PT) or *S.* Typhi (T) supernatant when co-cultured for 18–20 hours. Number indicating volume (µL) of supernatant added. Bars show mean with error bars representing SEM between technical duplicates. MFI, mean fluorescence intensity; LB, L-broth.

5.2.5 The TRAJ usage influence on the Jurkat.MAIT activation to bacteria reflects the response observed against the riboflavin metabolite ligand RL-6,7-DiMe

To determine whether the pattern of activation observed across the three TRAJ/TRBV20 cell lines is due to their responsiveness to the riboflavin metabolites, we stimulated the Jurkat.MAIT lines with the weaker riboflavin ligand RL-6,7-DiMe. We observed a dose-

dependent (**Figure 5-7A**) and MR1-restricted (**Figure 5-7B**) response to RL-6,7-DiMe from the TRAJ33/TRBV20 cell line. A very small response was observed in the TRAJ12/TRBV20 line at the highest concentration of RL-6,7-DiMe, whereas no response was observed in the TRAJ20/TRBV20 cell line.

This pattern of activation (TRAJ20 < TRAJ12 < TRAJ33) reflects what was observed in the Jurkat.MAIT lines response to various bacterial stimuli and confirms that the difference in response due to TRAJ usage is driven by the TCR specificity to MAIT cell riboflavin ligands.

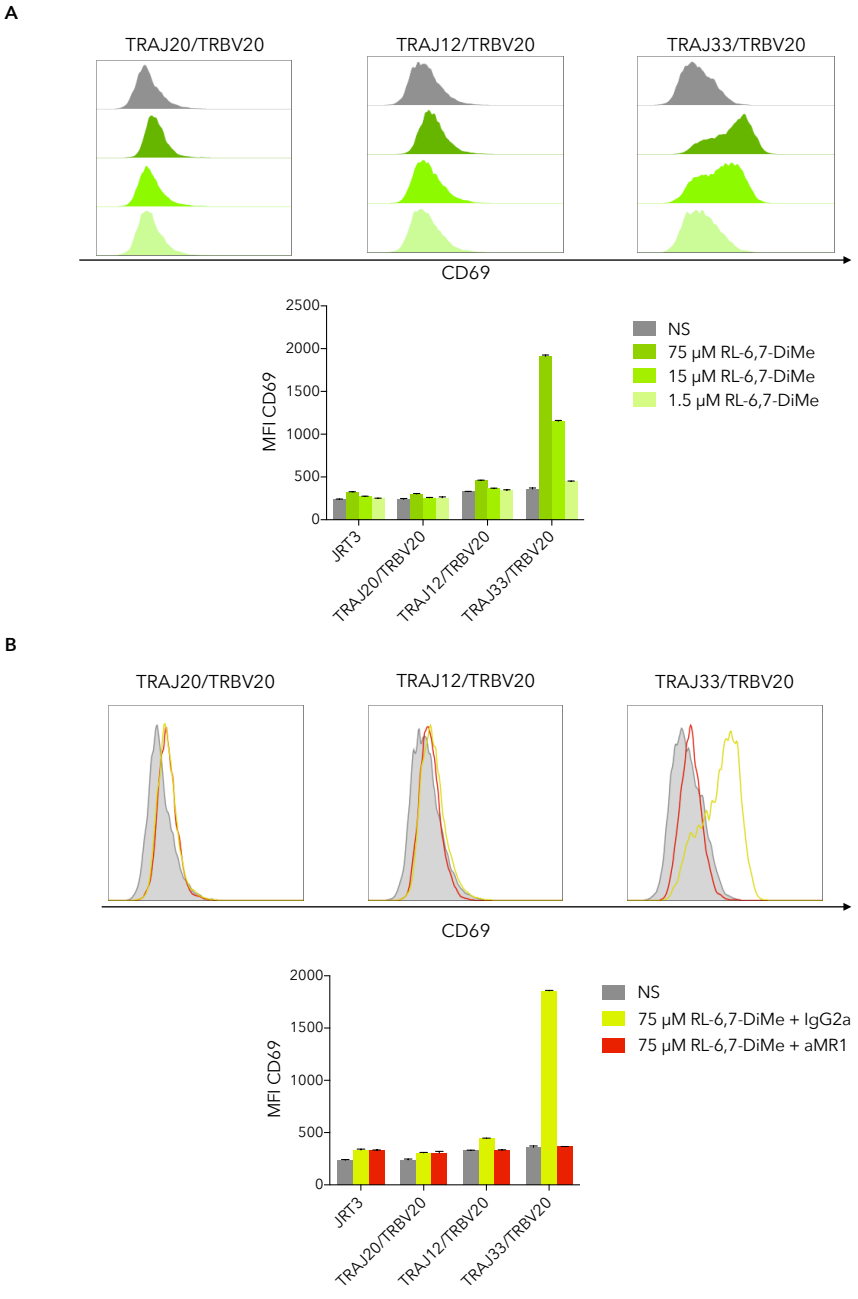

Figure 5-7 TRAJ usage influence on Jurkat.MAIT activation reflects response to riboflavin metabolite RL-6,7-DiMe

JRT3 cells were transduced with a vector containing TRAV1-2 with TRAJ33, TRAJ12 or TRAJ20 and containing the same TCRβ chain TRBV20 across the three lines. (A) Using C1R.MR1 cells as APCs, the activation of Jurkat.MAIT cell lines was measured by flow cytometry using the MFI of CD69 in response to 6,7-dimethyl-8-(1-D-ribityl)lumazine (RL-6,7-DiMe) when co-cultured for 18–20 hours. (B) Activation of Jurkat.MAIT cell lines to RL-6,7-DiMe after addition of 10 µg/mL of anti-MR1 blocking antibody (aMR1) or IgG2a isotype control was added. Bars show mean with error bars representing SEM between technical duplicates. MFI, mean fluorescence intensity; NS, no stimulation.

5.3 Functional analysis of the TCRβ clonotypes expanded following *S*. Paratyphi A infection on Jurkat.MAIT activation

5.3.1 Confirmation of TRAV1-2 expression and comparable levels of TCR expression on Jurkat cell lines expressing select MAIT TCRβ clonotypes

We produced three TRAV1-2–TRAJ33 Jurkat.MAIT cell lines expressing different TCRβ chains based on expanded and contracted clonotypes identified from donor 1 and donor 3 that were challenged with *S*. Paratyphi A and diagnosed with enteric fever. Sequences based on results generated in Section 3.3. Details for each line are outlined in **Table 5-2.**

Table 5-2 TCR details of Jurkat.MAIT lines with differing TCRβ usage

NAME	TRBV	TRBJ	CDR3β	FREQUENCY PRE-INFECTION	FREQUENCY POST-INFECTION
Donor 3 expanded	6-4	2-1	CASSDGTSDEQFF	0.01%	1.3%
Donor 3 contracted	20-1	2-7	CSARQRDYEQYF	1.8%	0.01%
Donor 1 expanded	6-1	2-3	CASSETSGSPDTQYF	1.21%	21.1%
Donor 1 contracted	20-1	2-7	CSASPRGRDLPEQYF	3.4%	0.02%

Frequency refers to the percentage of total of detected productive TCRβ sequences from MiSeq results for diagnosed individuals D3 or D1 as identified in Section 3.3.

To be able to compare levels of activation across the cell lines and attribute this to the TCRβ clonotype, it was important to establish that all lines expressed the MAIT cell TCR at comparable levels at the surface as this could influence the level of activation displayed by each cell line. It was also important to establish that the inserted TCRβ chain was pairing with the MAIT cell Vα7.2 TCR and not the endogenous JRT3 TCRα chain. Following transduction of the vector containing the TCRα and TCRβ sequences under SFFV promoter, the cell lines were analysed by flow cytometry for expression of both CD3 and the TCR Vα7.2 region. The results showed that in all cell lines, expression of both CD3 and TCR Vα7.2 was high and the level of expression of both markers were correlated, as shown in the example contour plot for donor 1 (**Figure 5-8A**). This confirmed that the TCRβ chain of

interest was pairing with the correct MAIT cell TCR Vα7.2. Furthermore, the same levels of expression were observed across the paired expanded/contracted cell lines for donor 1 and donor 3 (**Figure 5-8B**), enabling their activation levels to be compared between both paired clonotypes as it will correlate directly to TCR avidity and not level of TCR expression.

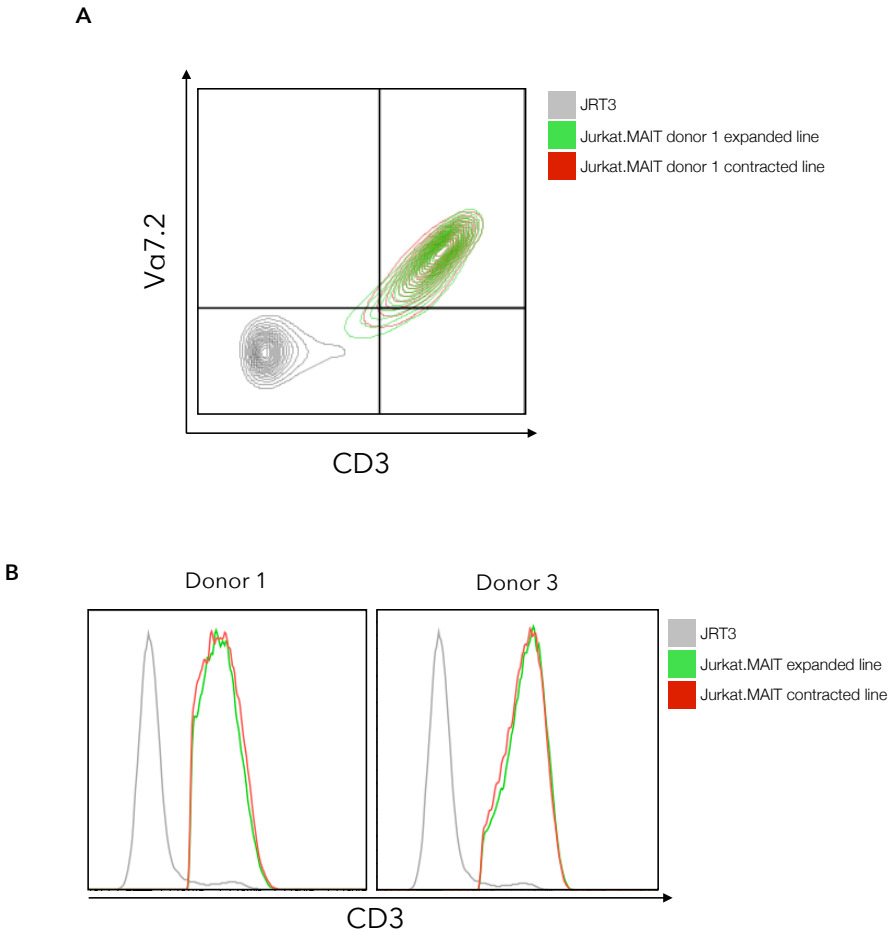

Figure 5-8 Correct and comparable expression of TCR across Jurkat.MAIT line expanded/contracted TCRβ clonotype pairs

JRT3 cells were transduced with a vector containing TRAV1-2–TRAJ33 and different TCRβ based on expanded and contracted clonotypes identified from the *S.* Paratyphi A infected individuals donor 1 and donor 3. The expression of the correct TCR was confirmed by flow cytometry using antibodies against CD3 and Vα7.2. (A) Overlaid contour plots showing expression of CD3 against Vα7.2 for the donor 1 cell lines. (B) Histogram overlay showing expression of CD3 for both donor 1 and donor 3 paired Jurkat.MAIT cell line clonotypes.

5.3.2 Jurkat.MAIT lines expressing expanded TCRβ clonotypes show greater activation in response to *S*. Paratyphi A

To determine whether the MAIT cell TCRβ clonotypes that expanded in individuals following *in vivo S*. Paratyphi A infection had a higher functional avidity to *S*. Paratyphi A, we activated Jurkat.MAIT cells expressing expanded or contracted clonotypes identified in diagnosed individuals D1 and D3 with *S*. Paratyphi A supernatant. We observed a greater dose-dependent activation by the expanded clonotypes in both individuals compared with their contracted counterpart (**Figure 5-9A**). We also confirmed that the activation observed in these Jurkat.MAIT lines was MR1-dependent as the response could be completely blocked using an anti-MR1 blocking antibody (**Figure 5-9B**). Therefore, the activation, and differences in activation, we were observing was a product of the differential TCRβ usage.

These results suggest that the MAIT cell clonotypes that expanded *in vivo* following *S*. Paratyphi A infection had a greater functional avidity to *S*. Paratyphi A supernatant compared with clonotypes that contracted in the same individual. What is not clear is whether this is a pathogen-specific increase in functional avidity, similar to what is observed in adaptive immune T cells, that would enable the formation of immunological memory against specific bacteria.

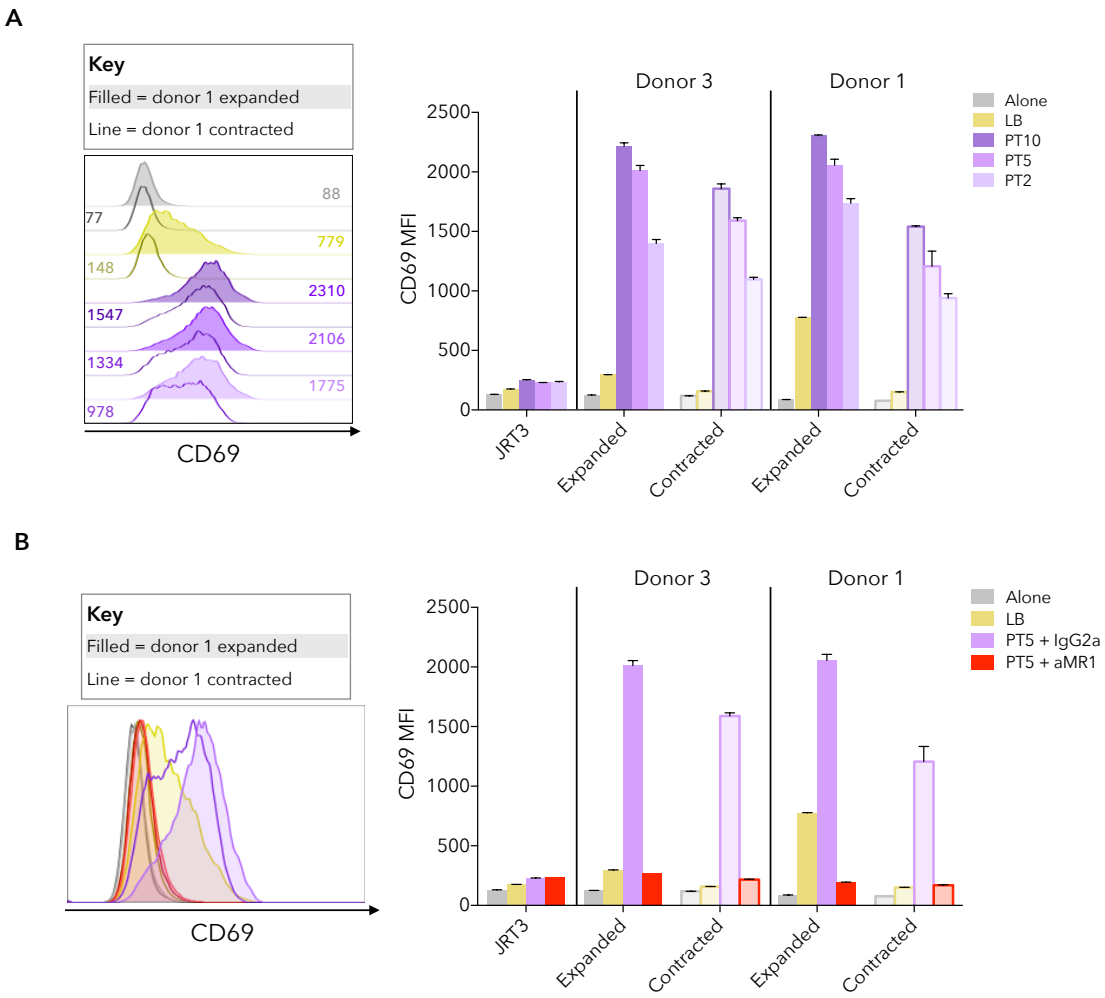

Figure 5-9 Greater activation in response to *in vitro* *S.* Paratyphi A supernatant by Jurkat.MAIT expressing clonotypes that expanded following *in vivo* *S.* Paratyphi A infection

JRT3 cells were transduced with a vector containing TRAV1-2–TRAJ33 and different TCRβ chains based on expanded and contracted clonotypes identified from the *S.* Paratyphi A infected donors 1 and 3. (A) Using C1R.MR1 cells as APCs, the activation of Jurkat.MAIT cell lines was measured by flow cytometry using the MFI of CD69 in response to *S.* Paratyphi A supernatant when co-cultured for 18–20 hours. (B) Activation of Jurkat.MAIT cell lines to *S.* Paratyphi A after addition of 10 µg/mL of anti-MR1 blocking antibody (aMR1) or IgG2a isotype control. Number indicates volume of supernatant added. Graph bars show mean with error bars representing SEM between technical duplicates. MFI, mean fluorescence intensity; LB, L-broth.

5.3.3 Jurkat.MAIT lines expressing expanded TCRβ clonotypes show greater activation in response to *E. coli*

To address whether the increased activation observed in Jurkat.MAIT expanded clonotype lines is specific to *S.* Paratyphi A, we activated the lines with *E. coli* supernatant. We observed that, similar to activation with *S.* Paratyphi A, the expanded clonotype lines showed greater dose-dependent activation in response to *E. coli* compared to the contracted clonotype from the same individual (**Figure 5-10A**). This activation to *E. coli* could be completely blocked using anti-MR1 blocking antibody (**Figure 5-10B**).

These results demonstrate that the MAIT cell clonotypes that expanded following *in vivo S.* Paratyphi A infection had enhanced functional avidity not only to *S.* Paratyphi A but also to *E. coli*, suggesting that the changes in TCR repertoire observed in these individuals is not pathogen-specific, and is more of an innate-like immune response.

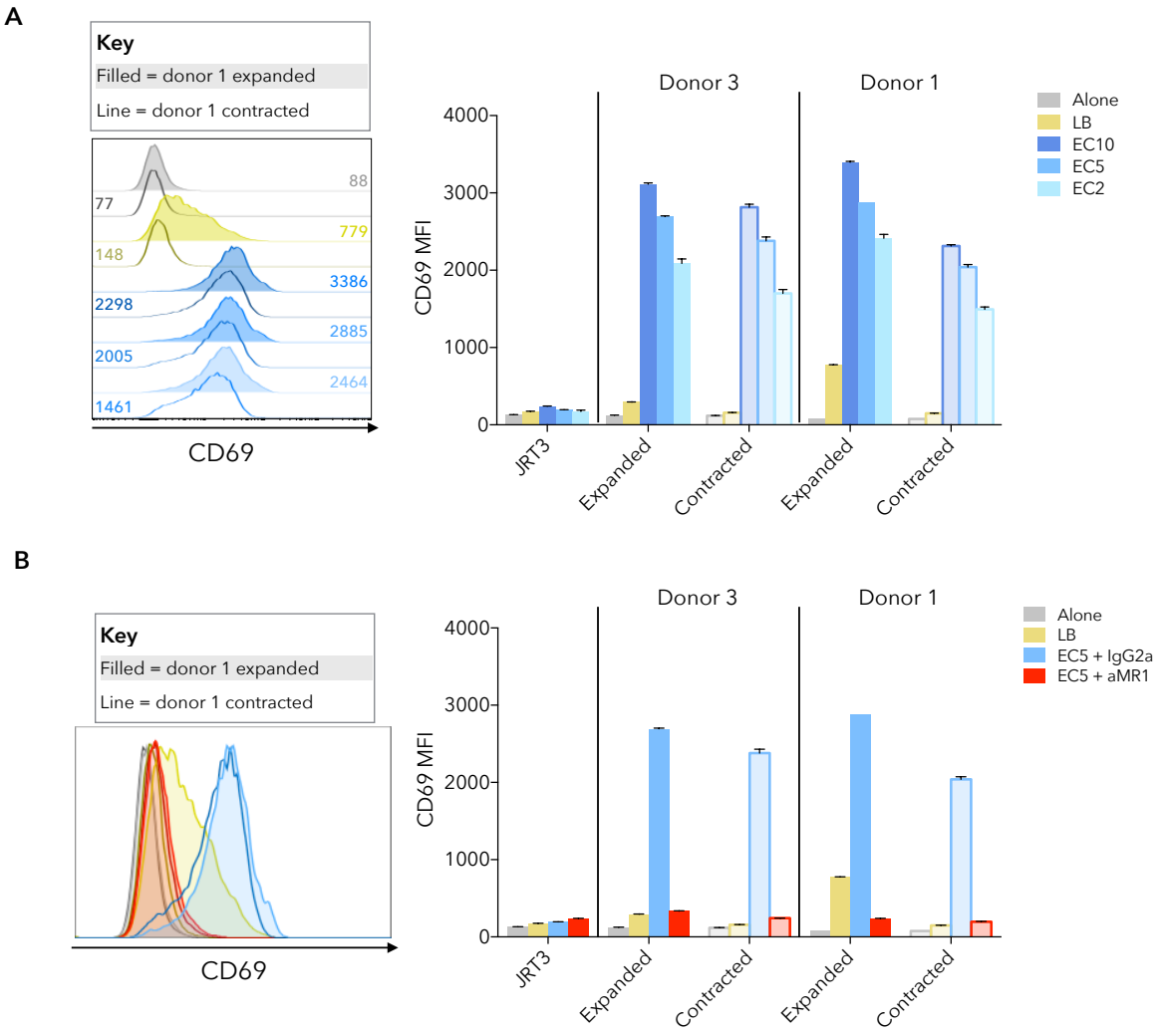

Figure 5-10 Greater activation in response to *E. coli* supernatant by Jurkat.MAIT expressing clonotypes that expanded following *in vivo* *S.* Paratyphi A infection

JRT3 cells were transduced with a vector containing TRAV1-2–TRAJ33 and different TCRβ based on expanded and contracted clonotypes identified from the *S.* Paratyphi A infected donors 1 and 3. (A) Using C1R.MR1 cells as APCs, the activation of Jurkat.MAIT cell lines was measured by flow cytometry using the MFI of CD69 in response to *E. coli* (EC) (DH5α) supernatant when co-cultured for 18–20 hours. (B) Activation of Jurkat.MAIT cell lines to EC after addition of 10 µg/mL of anti-MR1 blocking antibody (aMR1) or IgG2a isotype control. Number indicates volume of supernatant added. Graph bars show mean with error bars representing SEM between technical duplicates. MFI, mean fluorescence intensity; LB, L-broth.

5.3.4 Jurkat.MAIT lines expressing expanded TCRβ clonotypes show greater activation in response to live bacterial infections

To examine whether the expanded Jurkat.MAIT clonotype lines maintain their functional advantage over the contracted counterparts in response to live bacteria, we tested their response to APCs infected with either live *E.* coli or live *S.* Paratyphi A. We observed that the expanded lines do still maintain a higher level of activation compared to the contracted clonotype from the same individual both for *E. coli* (**Figure 5-11A**) and *S.* Paratyphi A (**Figure 5-11B**), although this difference was more pronounced in donor 1 compared with donor 3.

It was also observed that the response to *S.* Paratyphi A was much lower than *E. coli* at the same MOI, compared with the bacteria supernatant experiments, in which *E. coli* and *S.* Paratyphi A both produce high levels of activation. This is likely due to *S.* Paratyphi A being an invasive intracellular pathogen, and during live infection it may escape detection to a greater extent, compared with the extracellular bacteria *E. coli*.

Together, these results indicate that the expanded Jurkat.MAIT clonotypes also have enhanced activation to live bacterial infection compared to their contracted counterparts. It suggests that their expansion was driven by their functional avidity to the same family of ligands.

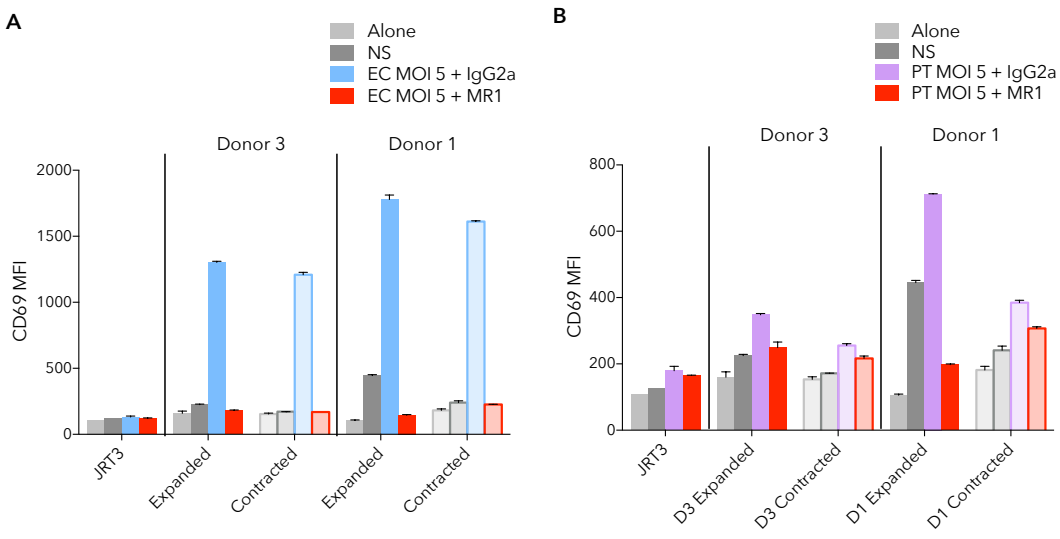

Figure 5-11 Greater activation in response to *in vitro* live infection by Jurkat.MAIT expressing clonotypes that expanded following *in vivo* *S.* Paratyphi A infection

JRT3 cells were transduced with a vector containing TRAV1-2–TRAJ33 and different TCRβ based on expanded and contracted clonotypes identified from the *S.* Paratyphi A infected donors 1 and 3. (A) Using C1R.MR1 cells as APCs, the activation of Jurkat.MAIT cell lines was measured by flow cytometry using the MFI of CD69 in response to (A) *E. coli* (EC) (DH5α) or (B) *S.* Paratyphi A MOI 5 live infection when co-cultured for 18–20 hours. Where indicated, 10 µg/mL of anti-MR1 blocking antibody (aMR1) or IgG2a isotype control was added. Graph bars show mean with error bars representing SEM between technical duplicates. MFI, mean fluorescence intensity; NS, no stimulation.

5.3.5 Jurkat.MAIT lines expressing expanded TCRβ clonotypes show greater activation in response to the strong MAIT cell precursor ligand 5-A-RU

To test whether the changes observed in the TCR repertoire following *S.* Paratyphi A infection were driven by the riboflavin metabolites known to stimulate MAIT cells, and be expressed by *S.* Paratyphi A, we stimulated Jurkat.MAIT cell clonotype lines with the strong precursor ligand 5-amino-6-(D-ribitylamino)uracil (5-A-RU) along with methylglyoxal, which together form the strong and unstable MAIT cell ligand 5-(2-oxopropylideneamino)-6-D-ribitylaminouracil (5-OP-RU) (Corbett *et al.*, 2014).

We observed a greater dose-dependent level of activation compared to the contracted clonotype from the same individual in response to the strong MAIT cell precursor ligand 5-A-RU (**Figure 5-12A**), although this difference was much more pronounced in donor 1 compared with donor. This activation could be blocked using an anti-MR1 blocking antibody (**Figure 5-12B**).

These results demonstrate that the pattern of activation is similar towards the MAIT cell riboflavin-derived ligand as it was to the bacterial stimuli, suggesting that it is the TCR specificity to this ligand that may drive the Jurkat.MAIT response seen towards the bacteria. What is not known, is whether this pattern of activation would be the case for weaker stimulating riboflavin metabolites.

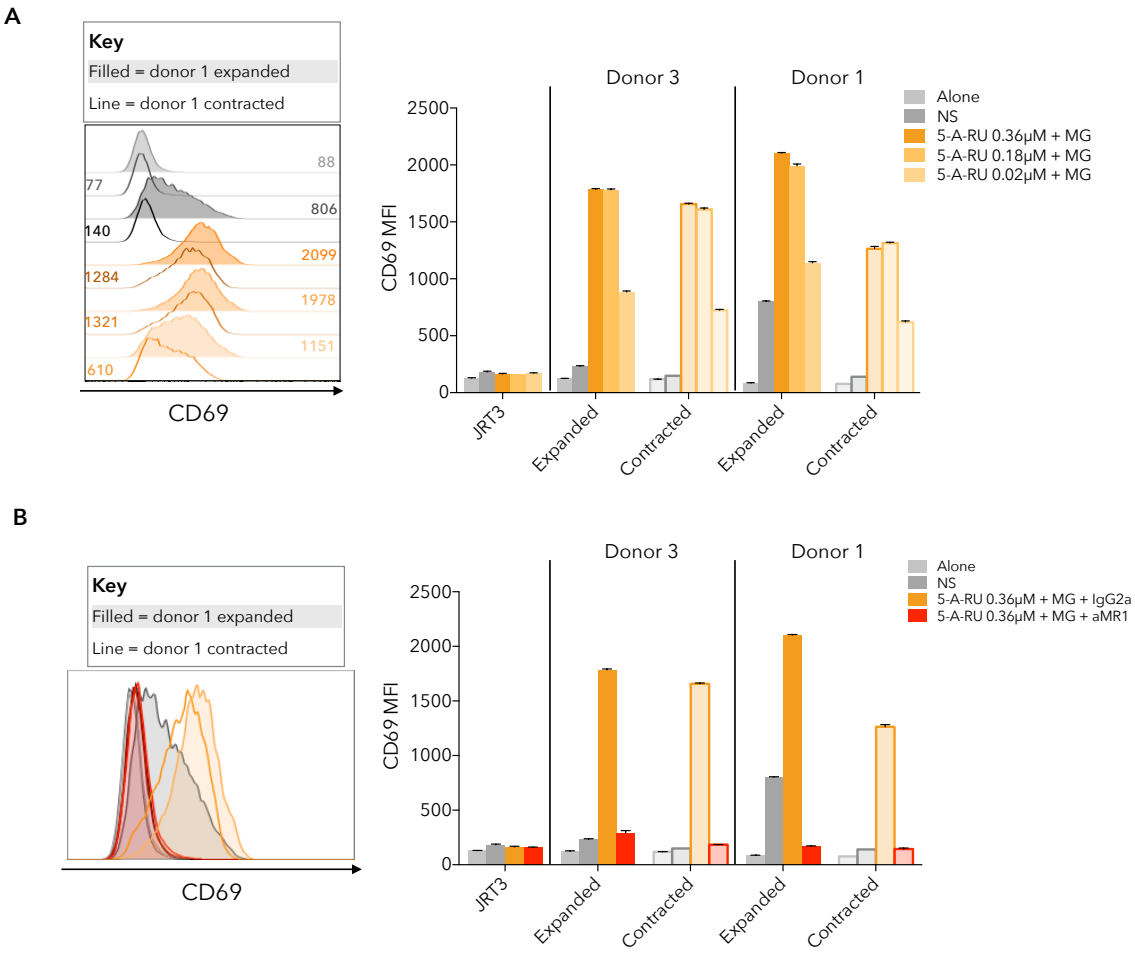

Figure 5-12 Greater activation in response to the strong MAIT cell ligand precursor 5-A-RU by Jurkat.MAIT expressing clonotypes that expanded following *in vivo S.* Paratyphi A infection

JRT3 cells were transduced with a vector containing TRAV1-2–TRAJ33 and different TCRβ based on expanded and contracted clonotypes identified from the *S.* Paratyphi A infected donors 1 and 3. (A) Using C1R.MR1 cells as APCs, the activation of Jurkat.MAIT cell lines was measured by flow cytometry using the MFI of CD69 in response to 5-amino-6-(D-ribitylamino)uracil (5-A-RU) and methylglyoxal (MG) when co-cultured for 18–20 hours. (B) Activation of Jurkat.MAIT cell lines to 5-A-RU and MG after addition of 10 μg/mL of anti-MR1 blocking antibody (aMR1) or IgG2a isotype control. Graph bars show mean with error bars representing SEM between technical duplicates. MFI, mean fluorescence intensity; NS, no stimulation.

5.3.6 Jurkat.MAIT lines expressing expanded TCRβ clonotypes show greater activation in response to the weak MAIT cell ligand RL-6,7-DiMe

To determine whether the expanded clonotype Jurkat.MAIT lines also had a greater response to other ligands within the riboflavin metabolite family, we activated the lines with the weaker MAIT cell ligand RL-6,7-DiMe. We observed that the overall level of activation was lower to this weaker ligand, as expected, but the expanded clonotype Jurkat.MAIT lines had overall a greater dose-dependent activation compared to the contracted clonotype from the same individual (**Figure 5-13A**). The activation of these lines could be blocked with an anti-MR1 blocking antibody (**Figure 5-13B**).

We also observed that the donor 1 contracted line, which had the lowest level of activation across the four lines in reponse to the stong precursor ligand 5-A-RU, had a higher activation to the weaker ligand compared to both lines from individual D3. This demonstrates that the MAIT cell TCR specificity towards the stronger ligand does not directly correlate to its specificity towards the weaker ligand.

These results suggest that the MAIT cell TCR specificity to the ligands is not entirely preserved across the family of riboflavin-derived ligands. However, as the expanded clonotype lines still had greater activation compared to the contracted clonotype from the same individual, both strong and weak MAIT cell ligands could both be factors that drove the expansion of MAIT cell clonotypes with higher TCR avidity during *in vivo S*. Paratyphi A infection.

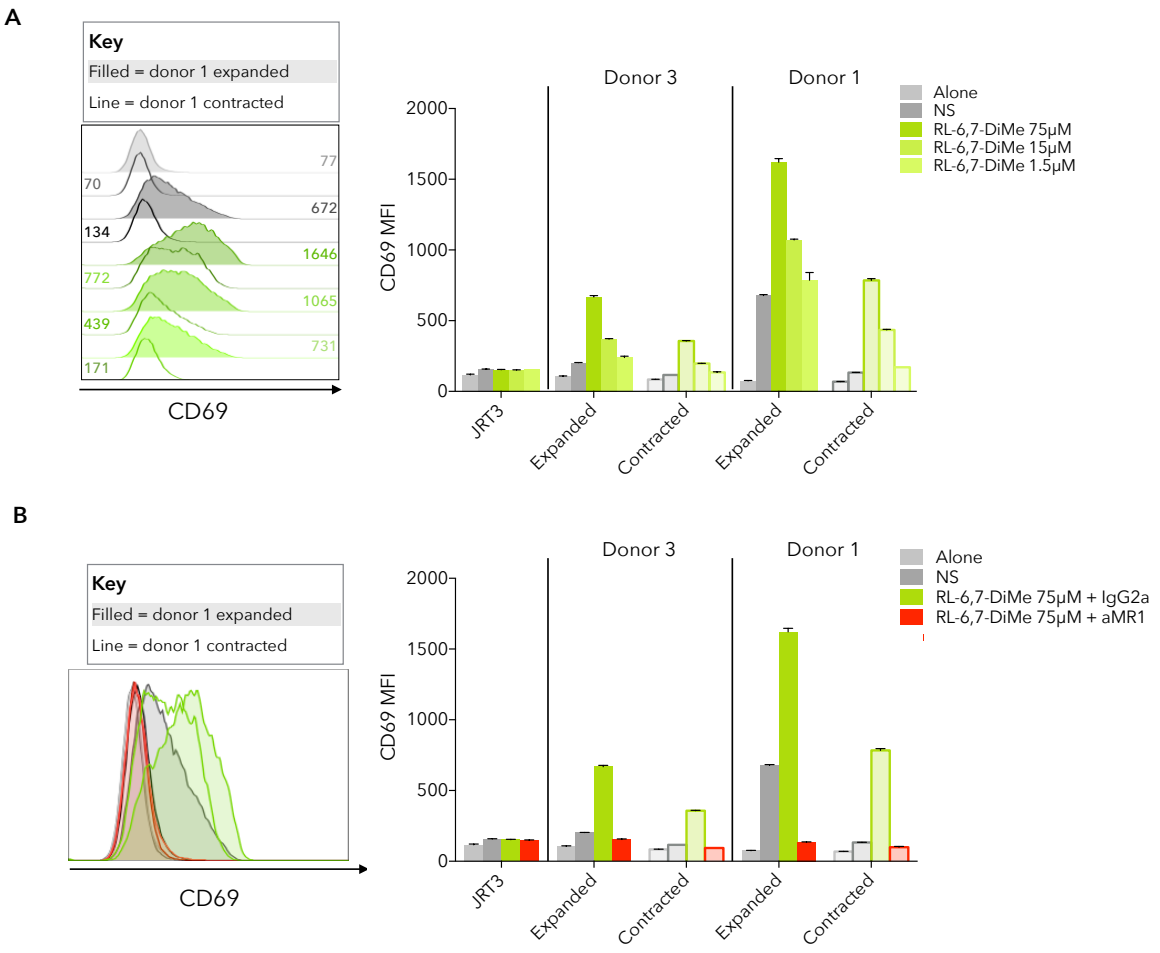

Figure 5-13 Greater activation in response to the weak MAIT cell ligand RL-6,7-DiMe by Jurkat.MAIT expressing clonotypes that expanded following *in vivo S.* Paratyphi A infection

JRT3 cells were transduced with a vector containing TRAV1-2–TRAJ33 and different TCRβ based on expanded and contracted clonotypes identified from the *S.* Paratyphi A infected donors 1 and 3. (A) Using C1R.MR1 cells as APCs, the activation of Jurkat.MAIT cell lines was measured by flow cytometry using the MFI of CD69 in response to RL-6,7-DiMe when co-cultured for 18–20 hours. (B) Activation of Jurkat.MAIT cell lines to 5 RL-6,7-DiMe after addition of 10 µg/mL of anti-MR1 blocking antibody (aMR1) or IgG2a isotype control. Graph bars show mean with error bars representing SEM between technical duplicates. MFI, mean fluorescence intensity; NS, no stimulation.

5.3.7 Jurkat.MAIT line expressing an expanded TCRβ clonotype from D1 displays baseline activation

An observation we made during the co-culture infection assays was that the donor 1 expanded cell line had a five-fold increase in activation in the presence of the C1R.MR1 without any additional stimulus, compared with when cultured alone. To investigate whether this was a specific response, we added an anti-MR1 blocking antibody to a co-culture with no stimulation. The addition of this blocking antibody reduced the baseline level of activation back to the level observed when this cell line was cultured alone (**Figure 5-14A**).

This result demonstrates that antigen presentation was occurring without the addition of stimuli, and is likely a result of presentation of metabolites present in the media, particularly FBS. To confirm this, we co-cultured the C1R-MR1 cells with the Jurkat.MAIT lines in medium containing dialysed FBS (which has the small molecules removed) and saw a complete reduction in the expression of CD69 by the donor 1 line, confirming that it was responding to components (likely vitamin metabolites) present in FBS (**Figure 5-14B**). This result demonstrates the highly sensitive nature of the donor 1 clonotype to the presence of ligand in low abundance.

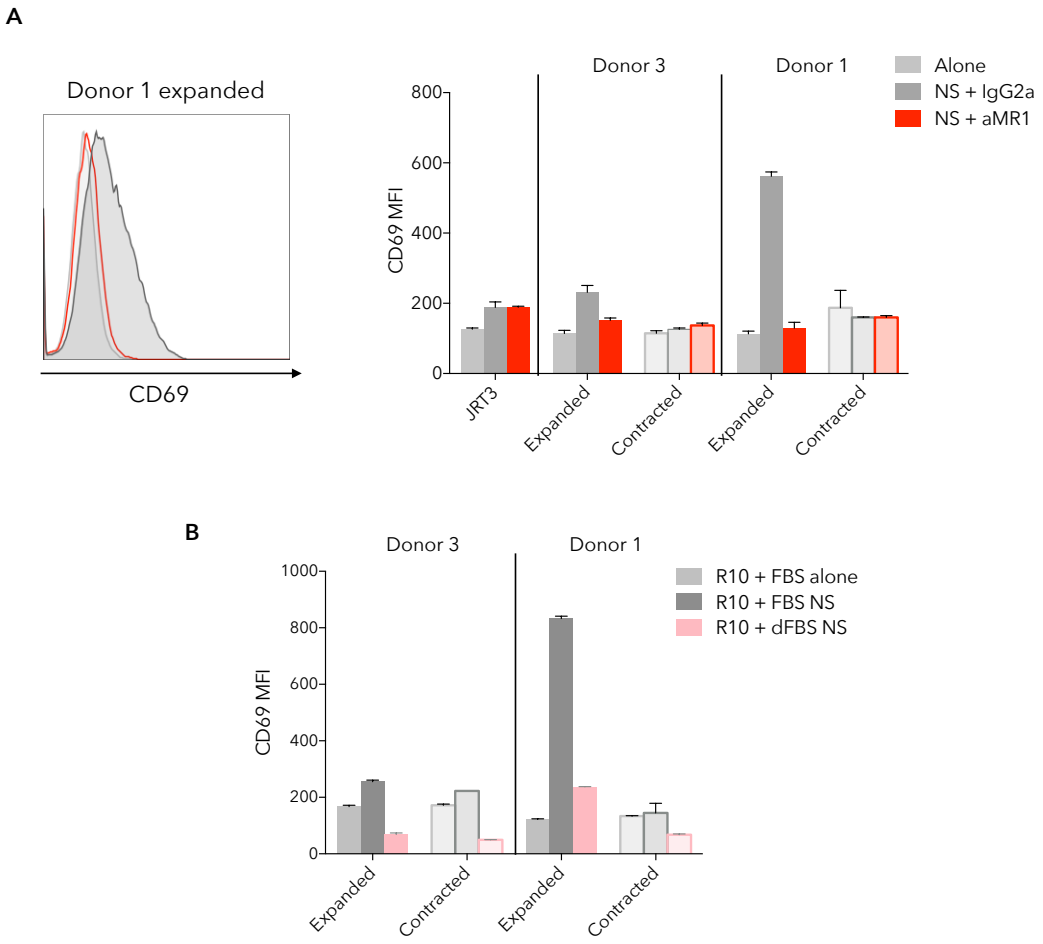

Figure 5-14 Baseline activation by a Jurkat.MAIT line expressing a clonotype that expanded following *in vivo S.* Paratyphi A infection

JRT3 cells were transduced with a vector containing TRAV1-2–TRAJ33 and different TCRβ based on expanded and contracted clonotypes identified from the *S.* Paratyphi A infected individuals D1 and D3. (A) Using C1R.MR1 cells as APCs, the activation of Jurkat.MAIT cell lines was measured by flow cytometry using the MFI of CD69 when co-cultured for 18–20 hours with no stimulation. 10 μg/mL of anti-MR1 blocking antibody (aMR1) or IgG2a isotype control was added where indicated. (B) Activation of Jurkat.MAIT cell lines when cultured in media with FBS compared to dialysed FBS (dFBS). Graph bars show mean with error bars representing SEM between technical duplicates. MFI, mean fluorescence intensity; NS, no stimulation; R10, complete RPMI-1640 media.

5.4 Discussion

The study of MAIT cell's TCR, in terms of its structure and interaction with MR1 and ligands, has been extensive (Keller *et al.*, 2017, Gherardin *et al.*, 2016, Corbett *et al.*, 2014, Eckle *et al.*, 2014, Reantragoon *et al.*, 2013, Kjer-Nielsen *et al.*, 2012) and the findings of which have shown that the MAIT cell population is heterogeneous in TCR usage and, therefore, may be composed of different functional subsets. We wanted to explore this concept further by investigating the functional avidity of the TCR sequences identified in our two diseases models, cancer and *Salmonella* infection.

Our results revealed that that the TRAJ usage greatly influenced the functional avidity of Jurkat.MAIT cell lines. The TRAJ20 region, which is the least characterised of the three MAIT cell TRAJ regions, had the lowest activation in response to both bacteria and ligand stimuli. This was followed by TRAJ12 and, overall, TRAJ33 had the greatest functional avidity. Our findings support the observations made in a previous study that assessed MAIT cell TCR heterogeneity and reported that TRAV1-2–TRAJ33 transduced SKW-3 cells displayed greater activation compared to TRAJ12 or TRAJ20 (Reantragoon *et al.*, 2013).

As discussed previously in Section 4.4, TRAJ20 and TRAJ12 were more predominant in the tissue and TRAJ33 was more predominant in the blood of individuals with cancer. A pattern of distribution supported by what has been observed for TRAJ12 and TRAJ33 distribution in healthy tissue (Lepore *et al.*, 2014). Therefore, based on our *in vitro* TCR activation results, the functional avidity of MAIT cells TCR to riboflavin metabolites may be overall lower in the tissue than that of circulating MAIT cells. This may, in part, explain why MAIT cells located at mucosal sites, in which commensal flora that contain the riboflavin biosynthetic pathway (and can produce MAIT cell ligands) are present, do not induce an inflammatory response towards commensal bacteria. These tissue-resident MAIT cells using

TRAJ20 and TRAJ12 might be more cytokine-driven in their response to both sterile and non-sterile inflammation, compared with TRAJ33 MAIT cells in the blood that only move to tissue sites after the onset of an infection (Chen *et al.*, 2017).

The role of the TCRβ chains influence of MAIT cell responses has been previously suggested, based on structural evidence, as a 'fine-tuner' of the MAIT cells functional avidity to stimuli (Eckle *et al.*, 2014). We also observed this fine-tuning effect of the Jurkat.MAIT response in Section 5.2.3. Therefore, we wanted to determine whether there was any functional significance in the circulating MAIT cell TCRβ clonotypes that we observed expanding and contracting in response to *in vivo S.* Paratyphi A infection as discussed in Section 3.4.

We demonstrated that the expanded MAIT cell clonotypes had a stronger functional avidity when stimulated with *S.* Paratyphi A supernatant compared to the contracted clonotype from the same individual. The increased functional avidity could, in part, explain the selective clonal expansion we observed in *S.* Paratyphi A diagnosed individuals. The concept of MAIT cell selectivity based on TCR sequence has been suggested previously, by a study assessing MAIT cell TCR repertoire after *in vitro* infection (Gold *et al.*, 2014). This study also suggested MAIT cell TCR usage may enable ligand/pathogen discrimination as they observed different TCRβ clonotypes responding to different pathogens.

To determine whether the MAIT cell clonotypes identified in *S.* Paratyphi A diagnosed individuals were pathogen-specific, we tested their functional avidity to a different bacterial species, *E. coli*. We found that the expanded clonotypes also had a higher functional avidity towards *E. coli,* similar to what was observed in their response to *S.* Paratyphi A. This suggests that these clonotypes are not displaying pathogen discrimination and, therefore,

would not be contributing to the formation of memory-like responses similar to conventional T cells.

We observed an increased functional avidity of expanded MAIT cell clonotypes to both the strong and weak riboflavin ligands compared with contracted clonotypes from the same diagnosed individual. The increased functional avidity towards riboflavin metabolites is what is likely responsible for the activation observed towards the bacterial stimulation and is likely the responsible for driving the selective clonal expansion we observed in *S.* Paratyphi A diagnosed individuals.

We did observe that the difference between the MAIT cell clonotypes was greater when looking at the weaker stimulators (*S.* Paratyphi A and RL-6,7-DiMe) compared to the stronger ones (*E. coli* and 5-OP-RU). A similar observation has been made in a study assessing TCRβ-mediated alterations in TCR affinity in mouse iNKT cells. They showed that cells expressing iNKT TCRs with different TCRβ chains could all respond strongly to the most potent antigen (α-GalCer) but only select high affinity TCRs paired with particular TCRβ chains could respond to the pool of weaker ligands (Mallevaey *et al.*, 2009). This functional avidity as a product of TCRβ usage mirrors what we have observed for MAIT cell's response to stimulus.

The baseline reactivity we observed in the Jurkat.MAIT donor 1 clonotype further strengthens the concept of functional avidity as a product of TCRβ usage. As this was our strongest responding cell line to all stimuli that also displayed an MR1-restricted baseline level of activation towards components present in cell culture FBS.

It is likely that the increase in TCR functional avidity for riboflavin metabolites is not exclusively the driving factor for preferential expansion of certain MAIT clonotypes. Recent advances in methodology that can couple TCR sequence with transcriptional profiling of

single cells (Eltahla *et al.*, 2016) could help elucidate other factors that contribute to MAIT cell clonal expansion in response to infection and also identify whether distinct functional subsets of MAIT cells exist.

Together, our results provide an insight into the important role the MAIT cell TCR has in both in terms of their TCRα and TCRβ usage. The TCRα usage is much stricter, with the major difference seen in their TRAJ usage in different tissues conferring what appears to be an overall functionally weaker TCR repertoire in the tissues and stronger in circulation. We confirmed that the oligoclonal TCRβ usage is a "fine-tuner" of the TCR affinity and response, and could contribute to the changes seen in the TCRβ repertoire in circulation following a systemic bacterial infection.

Summary and Conclusions

Since the discovery of MAIT cells, and their bacteria-derived vitamin metabolite antigens, the unconventional T cell research field has focussed on characterising the phenotype and function of this subset of T cells. There has been great progress in the fundamental understanding of MAIT cells and their TCR-MR1 interaction, but understanding the role they play in disease is still unclear. This project aimed to further our understanding of the role MAIT cells play in both sterile and non-sterile inflammation using two different models, a human infection model of *S*. Paratyphi A and cancer.

We showed the timing and dynamic response of MAIT cells during *S*. Paratyphi A, both in diagnosed and undiagnosed individuals. We demonstrated that MAIT cells undergo a clonal response to infection in individuals diagnosed with *S*. Paratyphi A, with expansion/contraction of certain clonotypes in response to infection. The concept of MAIT cell clonal responses had only been previously hypothesised based on the observed heterogeneity of the MAIT cell TCR repertoire (Gold *et al.*, 2014, Eckle *et al.*, 2014).

We next investigated the role MAIT cells play in responding to a disease in the absence of antigen. A sterile disease in which the role of MAIT cells had not been extensively explored was in cancer. We established that MAIT cells not only infiltrate cancers at mucosal sites, such as colon and lung, where MAIT cells would be abundant in healthy tissue, but also established they could infiltrate various organs including breast, ovarian and the non-necrotic tissue of renal cancers. We also provided strong evidence that the MAIT cells infiltrating tumours are sourced primarily from local tissue areas, based on their TCRα TRAJ usage. The high abundance of MAIT cells in peripheral sites rather than lymphoid tissues shows that they are poised to respond rapidly to inflammation, and we show that this includes response to many different tumour types.

We hypothesised that if bacteria containing the MAIT cell ligand were introduced into a sterile inflammation setting such as cancer, then the MAIT cells could potentiate the effect this has on the immune response. We showed that in a bacteria-based bladder cancer immunotherapy, of intravesicular instilment of BCG, MAIT cells were present and activated in the bladder mucosa following treatment. We also observed changes to the antigen-specific cytokine response of MAIT cells following treatment, which provided indirect evidence that MAIT cells could be contributing to amplification of the immune response in the bladder and contributing to the efficacy of this immunotherapy.

Our findings on the role of MAIT cell response to inflammation, both in infection and cancer, brought in to focus the MAIT cell TCR repertoire and its importance for MAIT cells in terms of their location, clonotype frequency and activation. The MAIT cell TCR was previously considered similar to a PRR, as they use their TCR to recognise the same inflammatory signal (vitamin metabolites) for mounting a fast and broad immune response. However, we provide evidence that the MAIT cell TCR usage also has some adaptive properties. Our results showing the contrast of distinct TCRα TRAJ usage in cancer tissues compared to blood, and that the TRAJ12/20, found more predominantly in the tissue, had a lower TCR functional avidity towards both bacterial and ligand stimulation, provides compelling evidence that there are subsets of MAIT cells with different responsiveness to antigen-driven activation that also have different tissue-homing properties.

Our results regarding the MAIT cell TCRβ clonotypes that expanded within the host in response to *S.* Paratyphi A infection, showing a greater functional avidity to both bacteria and ligand, demonstrates a possible explanation for the heterogeneous TCRβ repertoire of MAIT cells. That is, that certain TCRβ clonotypes have a functional advantage in responding to antigen-driven stimulation and that exposure to antigen could drive repertoire changes.

Therefore, a host's circulating MAIT cell TCR repertoire may consistently be undergoing reshaping, and reflect the lifetime exposure to bacteria and their vitamin metabolite antigens. Furthermore, our results also showed that the MAIT cell TCRβ clonotypes do not appear to discriminate between pathogens. This suggests that the repertoire reshaping does not mirror conventional T cells and result in memory formation, but rather shape the circulating MAIT cell repertoire, possibly to retain MAIT cells with an overall higher functional avidity towards vitamin antigens. To directly address this, future studies would need to assess the MAIT cell repertoire either after a multiple infection challenge or examine the correlation between age and MAIT cell TCR repertoire diversity, which would be expected to decrease with age, as it has been previously reported that the total T cell repertoire diversity in the host decreases with age (Britanova *et al.*, 2014).

In conclusion, we have provided an insight into the nature of MAIT cells response to both non-sterile inflammation, in the human *S.* Paratyphi A infection model, and sterile inflammation, in the context of cancer and cancer immunotherapy. We have also highlighted the importance of the MAIT cell TCR, showing that innate-like subset of T cells also have adaptive qualities due to their TCR heterogeneity and selective clonal expansion in response to stimuli. Although MAIT cells are considered as functionally diverse cells, they may still consist of distinct tissue-resident and circulating subsets that differ functionally in their response to sterile and non-sterile inflammation.

Appendix

Appendix I - Map for pHR-SIN-IRES-GFP expression vector

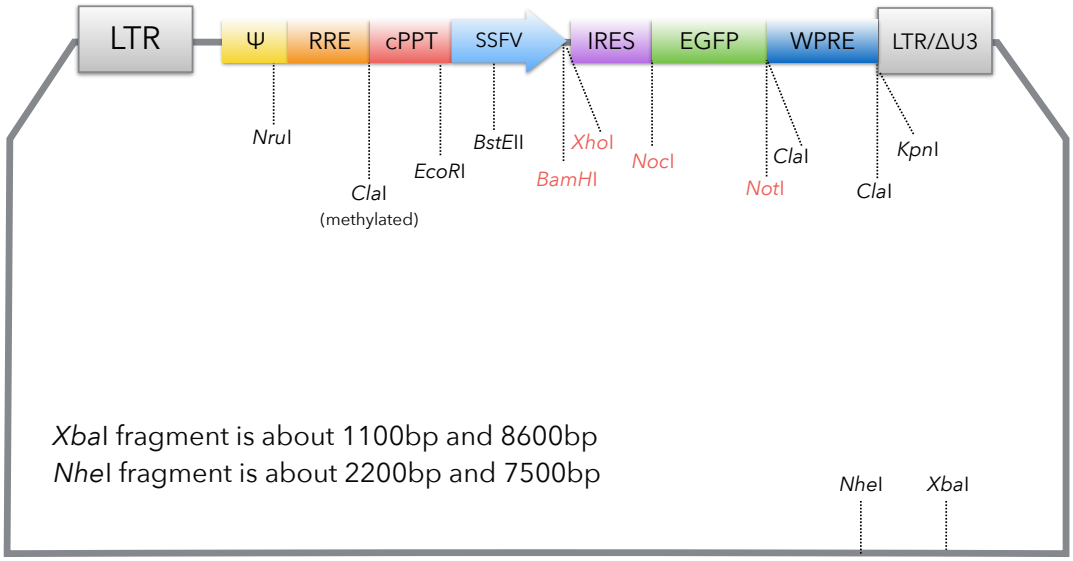

LTR	Long terminal repeat
Ψ	Packaging signal sequence
RRE	Rev-responsive element
cPPT	Central polypurine tract
SFFV	Spleen focus-forming virus promoter
IRES	Internal ribosome entry site
EGFP	Enhanced green fluorescent protein
WPRE	Woodchuck provirus response element
LTR/ΔU3	Transcriptional activator of HIV

References

Annibali, V., Ristori, G., Angelini, D. F., Serafini, B., Mechelli, R., Cannoni, S., Romano, S., Paolillo, A., Abderrahim, H., Diamantini, A., Borsellino, G., Aloisi, F., Battistini, L. & Salvetti, M. 2011. CD161(high)CD8+T cells bear pathogenetic potential in multiple sclerosis. *Brain,* 134**,** 542-54.

Billerbeck, E., Kang, Y. H., Walker, L., Lockstone, H., Grafmueller, S., Fleming, V., Flint, J., Willberg, C. B., Bengsch, B., Seigel, B., Ramamurthy, N., Zitzmann, N., Barnes, E. J., Thevanayagam, J., Bhagwanani, A., Leslie, A., Oo, Y. H., Kollnberger, S., Bowness, P., Drognitz, O., Adams, D. H., Blum, H. E., Thimme, R. & Klenerman, P. 2010. Analysis of CD161 expression on human CD8+ T cells defines a distinct functional subset with tissue-homing properties. *Proceedings of the National Academy of Sciences of the United States of America,* 107**,** 3006-11.

Bolotin, D. A., Shugay, M., Mamedov, I. Z., Putintseva, E. V., Turchaninova, M. A., Zvyagin, I. V., Britanova, O. V. & Chudakov, D. M. 2013. MiTCR: software for T-cell receptor sequencing data analysis. *Nature Methods,* 10**,** 813-4.

Brenchley, J. M., Price, D. A., Schacker, T. W., Asher, T. E., Silvestri, G., Rao, S., Kazzaz, Z., Bornstein, E., Lambotte, O., Altmann, D., Blazar, B. R., Rodriguez, B., Teixeira-Johnson, L., Landay, A., Martin, J. N., Hecht, F. M., Picker, L. J., Lederman, M. M., Deeks, S. G. & Douek, D. C. 2006. Microbial translocation is a cause of systemic immune activation in chronic HIV infection. *Nature Medicine,* 12**,** 1365-71.

Brinker, D. A., Amin, M. B., de Peralta-Venturina, M., Reuter, V., Chan, D. Y. & Epstein, J. I. 2000. Extensively necrotic cystic renal cell carcinoma: a clinicopathologic study with comparison to other cystic and necrotic renal cancers. *The American Journal of Surgical Pathology,* 24**,** 988-95.

Britanova, O. V., Putintseva, E. V., Shugay, M., Merzlyak, E. M., Turchaninova, M. A., Staroverov, D. B., Bolotin, D. A., Lukyanov, S., Bogdanova, E. A., Mamedov, I. Z., Lebedev, Y. B. & Chudakov, D. M. 2014. Age-related decrease in TCR repertoire diversity measured with deep and normalized sequence profiling. *Journal of Immunology,* 192**,** 2689-98.

Calabi, F., Jarvis, J. M., Martin, L. & Milstein, C. 1989. Two classes of CD1 genes. *European Journal of Immunology,* 19**,** 285-92.

Chen, Z., Wang, H., D'Souza, C., Sun, S., Kostenko, L., Eckle, S. B., Meehan, B. S., Jackson, D. C., Strugnell, R. A., Cao, H., Wang, N., Fairlie, D. P., Liu, L., Godfrey, D. I., Rossjohn, J., McCluskey, J. & Corbett, A. J. 2017. Mucosal-associated invariant T-cell activation and accumulation after in vivo infection depends on microbial riboflavin synthesis and co-stimulatory signals. *Mucosal Immunology,* 10**,** 58-68.

Chiba, A., Tamura, N., Yoshikiyo, K., Murayama, G., Kitagaichi, M., Yamaji, K., Takasaki, Y. & Miyake, S. 2017. Activation status of mucosal-associated invariant T cells reflects disease activity and pathology of systemic lupus erythematosus. *Arthritis Research & Therapy,* 19**,** 58.

Cho, Y. N., Kee, S. J., Kim, T. J., Jin, H. M., Kim, M. J., Jung, H. J., Park, K. J., Lee, S. J., Lee, S. S., Kwon, Y. S., Kee, H. J., Kim, N. & Park, Y. W. 2014. Mucosal-associated invariant T cell deficiency in systemic lupus erythematosus. *Journal of Immunology,* 193**,** 3891-901.

Chua, W. J., Truscott, S. M., Eickhoff, C. S., Blazevic, A., Hoft, D. F. & Hansen, T. H. 2012. Polyclonal mucosa-associated invariant T cells have unique innate functions in bacterial infection. *Infection and Immunity,* 80**,** 3256-67.

Cooper, M. D. & Alder, M. N. 2006. The evolution of adaptive immune systems. *Cell,* 124**,** 815-22.

Corbett, A. J., Eckle, S. B., Birkinshaw, R. W., Liu, L., Patel, O., Mahony, J., Chen, Z., Reantragoon, R., Meehan, B., Cao, H., Williamson, N. A., Strugnell, R. A., Van Sinderen, D., Mak, J. Y., Fairlie, D. P., Kjer-Nielsen, L., Rossjohn, J. & McCluskey, J. 2014. T-cell activation by transitory neo-antigens derived from distinct microbial pathways. *Nature,* 509**,** 361-5.

Cosgrove, C., Ussher, J. E., Rauch, A., Gartner, K., Kurioka, A., Huhn, M. H., Adelmann, K., Kang, Y. H., Fergusson, J. R., Simmonds, P., Goulder, P., Hansen, T. H., Fox, J., Gunthard, H. F., Khanna, N., Powrie, F., Steel, A., Gazzard, B., Phillips, R. E.,

Frater, J., Uhlig, H. & Klenerman, P. 2013. Early and nonreversible decrease of CD161++ /MAIT cells in HIV infection. *Blood,* 121**,** 951-61.

Croxford, J. L., Miyake, S., Huang, Y. Y., Shimamura, M. & Yamamura, T. 2006. Invariant V(alpha)19i T cells regulate autoimmune inflammation. *Nature Immunology,* 7**,** 987-94.

Cui, Y., Franciszkiewicz, K., Mburu, Y. K., Mondot, S., Le Bourhis, L., Premel, V., Martin, E., Kachaner, A., Duban, L., Ingersoll, M. A., Rabot, S., Jaubert, J., De Villartay, J. P., Soudais, C. & Lantz, O. 2015. Mucosal-associated invariant T cell-rich congenic mouse strain allows functional evaluation. *The Journal of Clinical Investigation,* 125**,** 4171-85.

Dunne, M. R., Elliott, L., Hussey, S., Mahmud, N., Kelly, J., Doherty, D. G. & Feighery, C. F. 2013. Persistent changes in circulating and intestinal gammadelta T cell subsets, invariant natural killer T cells and mucosal-associated invariant T cells in children and adults with coeliac disease. *PLoS One,* 8**,** e76008.

Dusseaux, M., Martin, E., Serriari, N., Peguillet, I., Premel, V., Louis, D., Milder, M., Le Bourhis, L., Soudais, C., Treiner, E. & Lantz, O. 2011. Human MAIT cells are xenobiotic-resistant, tissue-targeted, CD161hi IL-17-secreting T cells. *Blood,* 117**,** 1250-9.

Dzopalic, T., Rajkovic, I., Dragicevic, A. & Colic, M. 2012. The response of human dendritic cells to co-ligation of pattern-recognition receptors. *Immunologic Research,* 52**,** 20-33.

Eckle, S. B., Birkinshaw, R. W., Kostenko, L., Corbett, A. J., McWilliam, H. E., Reantragoon, R., Chen, Z., Gherardin, N. A., Beddoe, T., Liu, L., Patel, O., Meehan, B., Fairlie, D. P., Villadangos, J. A., Godfrey, D. I., Kjer-Nielsen, L., McCluskey, J. & Rossjohn, J. 2014. A molecular basis underpinning the T cell receptor heterogeneity of mucosal-associated invariant T cells. *The Journal of Experimental Medicine,* 211**,** 1585-600.

Eltahla, A. A., Rizzetto, S., Pirozyan, M. R., Betz-Stablein, B. D., Venturi, V., Kedzierska, K., Lloyd, A. R., Bull, R. A. & Luciani, F. 2016. Linking the T cell receptor to the

single cell transcriptome in antigen-specific human T cells. *Immunology and Cell Biology,* 94**,** 604-11.

Estes, J. D., Harris, L. D., Klatt, N. R., Tabb, B., Pittaluga, S., Paiardini, M., Barclay, G. R., Smedley, J., Pung, R., Oliveira, K. M., Hirsch, V. M., Silvestri, G., Douek, D. C., Miller, C. J., Haase, A. T., Lifson, J. & Brenchley, J. M. 2010. Damaged intestinal epithelial integrity linked to microbial translocation in pathogenic simian immunodeficiency virus infections. *PLoS Pathogens,* 6**,** e1001052.

Eto, M., Koga, H., Noma, H., Yamaguchi, A., Yoshikai, Y. & Naito, S. 2005. Importance of urinary interleukin-18 in intravesical immunotherapy with bacillus calmette-guerin for superficial bladder tumors. *Urologia Internationalis,* 75**,** 114-8.

Fernandez, C. S., Amarasena, T., Kelleher, A. D., Rossjohn, J., McCluskey, J., Godfrey, D. I. & Kent, S. J. 2014. MAIT cells are depleted early but retain functional cytokine expression in HIV infection. *Immunology and Cell Biology,* 93**,** 177-88.

Finck, R., Simonds, E. F., Jager, A., Krishnaswamy, S., Sachs, K., Fantl, W., Pe'er, D., Nolan, G. P. & Bendall, S. C. 2013. Normalization of mass cytometry data with bead standards. *Cytometry. Part A : the Journal of the International Society for Analytical Cytology,* 83**,** 483-94.

Georgel, P., Radosavljevic, M., Macquin, C. & Bahram, S. 2011. The non-conventional MHC class I MR1 molecule controls infection by *Klebsiella pneumoniae* in mice. *Molecular Immunology,* 48**,** 769-75.

Gherardin, N. A., Keller, A. N., Woolley, R. E., Le Nours, J., Ritchie, D. S., Neeson, P. J., Birkinshaw, R. W., Eckle, S. B., Waddington, J. N., Liu, L., Fairlie, D. P., Uldrich, A. P., Pellicci, D. G., McCluskey, J., Godfrey, D. I. & Rossjohn, J. 2016. Diversity of T Cells Restricted by the MHC Class I-Related Molecule MR1 Facilitates Differential Antigen Recognition. *Immunity,* 44**,** 32-45.

Giuntoli, R. L., 2nd, Webb, T. J., Zoso, A., Rogers, O., Diaz-Montes, T. P., Bristow, R. E. & Oelke, M. 2009. Ovarian cancer-associated ascites demonstrates altered immune environment: implications for antitumor immunity. *Anticancer Research,* 29**,** 2875-84.

Godfrey, D. I., Uldrich, A. P., McCluskey, J., Rossjohn, J. & Moody, D. B. 2015. The burgeoning family of unconventional T cells. *Nature Immunology,* 16**,** 1114-23.

Gold, M. C., Cerri, S., Smyk-Pearson, S., Cansler, M. E., Vogt, T. M., Delepine, J., Winata, E., Swarbrick, G. M., Chua, W. J., Yu, Y. Y., Lantz, O., Cook, M. S., Null, M. D., Jacoby, D. B., Harriff, M. J., Lewinsohn, D. A., Hansen, T. H. & Lewinsohn, D. M. 2010. Human mucosal associated invariant T cells detect bacterially infected cells. *PLoS Biology,* 8**,** e1000407.

Gold, M. C., McLaren, J. E., Reistetter, J. A., Smyk-Pearson, S., Ladell, K., Swarbrick, G. M., Yu, Y. Y., Hansen, T. H., Lund, O., Nielsen, M., Gerritsen, B., Kesmir, C., Miles, J. J., Lewinsohn, D. A., Price, D. A. & Lewinsohn, D. M. 2014. MR1-restricted MAIT cells display ligand discrimination and pathogen selectivity through distinct T cell receptor usage. *The Journal of Experimental Medicine,* 211**,** 1601-10.

Gozalbo-Lopez, B., Gomez del Moral, M., Campos-Martin, Y., Setien, F., Martin, P., Bellas, C., Regueiro, J. R. & Martinez-Naves, E. 2009. The MHC-related protein 1 (MR1) is expressed by a subpopulation of CD38+, IgA+ cells in the human intestinal mucosa. *Histology and Histopathology,* 24**,** 1439-49.

Greathead, L., Metcalf, R., Gazzard, B., Gotch, F., Steel, A. & Kelleher, P. 2014. CD8+/CD161++ mucosal-associated invariant T-cell levels in the colon are restored on long-term antiretroviral therapy and correlate with CD8+ T-cell immune activation. *AIDS,* 28**,** 1690-2.

Greene, J. M., Dash, P., Roy, S., McMurtrey, C., Awad, W., Reed, J. S., Hammond, K. B., Abdulhaqq, S., Wu, H. L., Burwitz, B. J., Roth, B. F., Morrow, D. W., Ford, J. C., Xu, G., Bae, J. Y., Crank, H., Legasse, A. W., Dang, T. H., Greenaway, H. Y., Kurniawan, M., Gold, M. C., Harriff, M. J., Lewinsohn, D. A., Park, B. S., Axthelm, M. K., Stanton, J. J., Hansen, S. G., Picker, L. J., Venturi, V., Hildebrand, W., Thomas, P. G., Lewinsohn, D. M., Adams, E. J. & Sacha, J. B. 2016. MR1-restricted mucosal-associated invariant T (MAIT) cells respond to mycobacterial vaccination and infection in nonhuman primates. *Mucosal Immunology,* 10**,** 802-13.

Grimaldi, D., Le Bourhis, L., Sauneuf, B., Dechartres, A., Rousseau, C., Ouaaz, F., Milder, M., Louis, D., Chiche, J. D., Mira, J. P., Lantz, O. & Pene, F. 2014. Specific MAIT

cell behaviour among innate-like T lymphocytes in critically ill patients with severe infections. *Intensive Care Medicine,* 40**,** 192-201.

Harriff, M. J., Cansler, M. E., Toren, K. G., Canfield, E. T., Kwak, S., Gold, M. C. & Lewinsohn, D. M. 2014. Human lung epithelial cells contain *Mycobacterium tuberculosis* in a late endosomal vacuole and are efficiently recognized by CD8+ T cells. *PLoS One,* 9**,** e97515.

Harriff, M. J., Karamooz, E., Burr, A., Grant, W. F., Canfield, E. T., Sorensen, M. L., Moita, L. F. & Lewinsohn, D. M. 2016. Endosomal MR1 Trafficking Plays a Key Role in Presentation of Mycobacterium tuberculosis Ligands to MAIT Cells. *PLoS Pathogens,* 12**,** e1005524.

Hashimoto, K., Hirai, M. & Kurosawa, Y. 1995. A gene outside the human MHC related to classical HLA class I genes. *Science,* 269**,** 693-5.

Howson, L. J., Salio, M. & Cerundolo, V. 2015. MR1-Restricted Mucosal-Associated Invariant T Cells and Their Activation during Infectious Diseases. *Frontiers in Immunology,* 6**,** 303.

Hrvatin, S., Deng, F., O'Donnell, C. W., Gifford, D. K. & Melton, D. A. 2014. MARIS: method for analyzing RNA following intracellular sorting. *PLoS One,* 9**,** e89459.

Huang, S., Gilfillan, S., Cella, M., Miley, M. J., Lantz, O., Lybarger, L., Fremont, D. H. & Hansen, T. H. 2005. Evidence for MR1 antigen presentation to mucosal-associated invariant T cells. *The Journal of Biological Chemistry,* 280**,** 21183-93.

Huang, S., Martin, E., Kim, S., Yu, L., Soudais, C., Fremont, D. H., Lantz, O. & Hansen, T. H. 2009. MR1 antigen presentation to mucosal-associated invariant T cells was highly conserved in evolution. *Proceedings of the National Academy of Sciences of the United States of America,* 106**,** 8290-5.

Illes, Z., Shimamura, M., Newcombe, J., Oka, N. & Yamamura, T. 2004. Accumulation of Valpha7.2-Jalpha33 invariant T cells in human autoimmune inflammatory lesions in the nervous system. *International Immunology,* 16**,** 223-30.

Iwasaki, A. & Medzhitov, R. 2015. Control of adaptive immunity by the innate immune system. *Nature Immunology,* 16**,** 343-53.

Jiang, J., Wang, X., An, H., Yang, B., Cao, Z., Liu, Y., Su, J., Zhai, F., Wang, R., Zhang, G. & Cheng, X. 2014. MAIT Cell Function is Modulated by PD-1 Signaling in Patients with Active Tuberculosis. *American Journal of Respiratory and Critical Care Medicine,* 190**,** 329-39.

Keller, A. N., Eckle, S. B., Xu, W., Liu, L., Hughes, V. A., Mak, J. Y., Meehan, B. S., Pediongco, T., Birkinshaw, R. W., Chen, Z., Wang, H., D'Souza, C., Kjer-Nielsen, L., Gherardin, N. A., Godfrey, D. I., Kostenko, L., Corbett, A. J., Purcell, A. W., Fairlie, D. P., McCluskey, J. & Rossjohn, J. 2017. Drugs and drug-like molecules can modulate the function of mucosal-associated invariant T cells. *Nature Immunology,* 18**,** 402-11.

Kjer-Nielsen, L., Patel, O., Corbett, A. J., Le Nours, J., Meehan, B., Liu, L. G., Bhati, M., Chen, Z. J., Kostenko, L., Reantragoon, R., Williamson, N. A., Purcell, A. W., Dudek, N. L., McConville, M. J., O'Hair, R. A. J., Khairallah, G. N., Godfrey, D. I., Fairlie, D. P., Rossjohn, J. & McCluskey, J. 2012. MR1 presents microbial vitamin B metabolites to MAIT cells. *Nature,* 491**,** 717-23.

Koay, H.-F., Gherardin, N. A., Enders, A., Loh, L., Mackay, L. K., Almeida, C. F., Russ, B. E., Nold-Petry, C. A., Nold, M. F., Bedoui, S., Chen, Z., Corbett, A. J., Eckle, S. B. G., Meehan, B., d'Udekem, Y., Konstantinov, I. E., Lappas, M., Liu, L., Goodnow, C. C., Fairlie, D. P., Rossjohn, J., Chong, M. M., Kedzierska, K., Berzins, S. P., Belz, G. T., McCluskey, J., Uldrich, A. P., Godfrey, D. I. & Pellicci, D. G. 2016. A three-stage intrathymic development pathway for the mucosal-associated invariant T cell lineage. *Nature Immunology,* 17**,** 1300-11.

Kurioka, A., Ussher, J. E., Cosgrove, C., Clough, C., Fergusson, J. R., Smith, K., Kang, Y. H., Walker, L. J., Hansen, T. H., Willberg, C. B. & Klenerman, P. 2014. MAIT cells are licensed through granzyme exchange to kill bacterially sensitized targets. *Mucosal Immunology*.

Le Bourhis, L., Dusseaux, M., Bohineust, A., Bessoles, S., Martin, E., Premel, V., Core, M., Sleurs, D., Serriari, N.-E., Treiner, E., Hivroz, C., Sansonetti, P., Gougeon, M.-L.,

Soudais, C. & Lantz, O. 2013. MAIT cells detect and efficiently lyse bacterially-infected epithelial cells. *PLoS Pathogens,* 9**,** e1003681.

Le Bourhis, L., Martin, E., Peguillet, I., Guihot, A., Froux, N., Core, M., Levy, E., Dusseaux, M., Meyssonnier, V., Premel, V., Ngo, C., Riteau, B., Duban, L., Robert, D., Rottman, M., Soudais, C. & Lantz, O. 2010. Antimicrobial activity of mucosal-associated invariant T cells. *Nature Immunology,* 11**,** 701-8.

Lee, O. J., Cho, Y. N., Kee, S. J., Kim, M. J., Jin, H. M., Lee, S. J., Park, K. J., Kim, T. J., Lee, S. S., Kwon, Y. S., Kim, N., Shin, M. G., Shin, J. H., Suh, S. P., Ryang, D. W. & Park, Y. W. 2014. Circulating mucosal-associated invariant T cell levels and their cytokine levels in healthy adults. *Experimental Gerontology,* 49**,** 47-54.

Leeansyah, E., Ganesh, A., Quigley, M. F., Sonnerborg, A., Andersson, J., Hunt, P. W., Somsouk, M., Deeks, S. G., Martin, J. N., Moll, M., Shacklett, B. L. & Sandberg, J. K. 2013. Activation, exhaustion, and persistent decline of the antimicrobial MR1-restricted MAIT-cell population in chronic HIV-1 infection. *Blood,* 121**,** 1124-35.

Leeansyah, E., Loh, L., Nixon, D. F. & Sandberg, J. K. 2014. Acquisition of innate-like microbial reactivity in mucosal tissues during human fetal MAIT-cell development. *Nature Communications,* 5**,** 3143.

Lepore, M., Kalinichenko, A., Calogero, S., Kumar, P., Paleja, B., Schmaler, M., Narang, V., Zolezzi, F., Poidinger, M., Mori, L. & De Libero, G. 2017. Functionally diverse human T cells recognize non-microbial antigens presented by MR1. *Elife,* 6.

Lepore, M., Kalinichenko, A., Colone, A., Paleja, B., Singhal, A., Tschumi, A., Lee, B., Poidinger, M., Zolezzi, F., Quagliata, L., Sander, P., Newell, E., Bertoletti, A., Terracciano, L., De Libero, G. & Mori, L. 2014. Parallel T-cell cloning and deep sequencing of human MAIT cells reveal stable oligoclonal TCRbeta repertoire. *Nature Communications,* 5**,** 3866.

Leung, D. T., Bhuiyan, T. R., Nishat, N. S., Hoq, M. R., Aktar, A., Rahman, M. A., Uddin, T., Khan, A. I., Chowdhury, F., Charles, R. C., Harris, J. B., Calderwood, S. B., Qadri, F. & Ryan, E. T. 2014. Circulating mucosal associated invariant T cells are

activated in Vibrio cholerae O1 infection and associated with lipopolysaccharide antibody responses. *PLoS Neglected Tropical Diseases,* 8**,** e3076.

Li, J., Reantragoon, R., Kostenko, L., Corbett, A. J., Varigos, G. & Carbone, F. R. 2016. The frequency of mucosal-associated invariant T cells is selectively increased in dermatitis herpetiformis. *The Australasian Journal of Dermatology*.

Ling, L., Lin, Y., Zheng, W., Hong, S., Tang, X., Zhao, P., Li, M., Ni, J., Li, C., Wang, L. & Jiang, Y. 2016. Circulating and tumor-infiltrating mucosal associated invariant T (MAIT) cells in colorectal cancer patients. *Scientific Reports,* 6**,** 20358.

Mallevaey, T., Scott-Browne, J. P., Matsuda, J. L., Young, M. H., Pellicci, D. G., Patel, O., Thakur, M., Kjer-Nielsen, L., Richardson, S. K., Cerundolo, V., Howell, A. R., McCluskey, J., Godfrey, D. I., Rossjohn, J., Marrack, P. & Gapin, L. 2009. T cell receptor CDR2 beta and CDR3 beta loops collaborate functionally to shape the iNKT cell repertoire. *Immunity,* 31**,** 60-71.

Mamedov, I. Z., Britanova, O. V., Zvyagin, I. V., Turchaninova, M. A., Bolotin, D. A., Putintseva, E. V., Lebedev, Y. B. & Chudakov, D. M. 2013. Preparing unbiased T-cell receptor and antibody cDNA libraries for the deep next generation sequencing profiling. *Frontiers in Immunology,* 4**,** 456.

Martin, E., Treiner, E., Duban, L., Guerri, L., Laude, H., Toly, C., Premel, V., Devys, A., Moura, I. C., Tilloy, F., Cherif, S., Vera, G., Latour, S., Soudais, C. & Lantz, O. 2009. Stepwise development of MAIT cells in mouse and human. *PLoS Biology,* 7**,** e54.

McWilliam, H. E., Eckle, S. B., Theodossis, A., Liu, L., Chen, Z., Wubben, J. M., Fairlie, D. P., Strugnell, R. A., Mintern, J. D., McCluskey, J., Rossjohn, J. & Villadangos, J. A. 2016. The intracellular pathway for the presentation of vitamin B-related antigens by the antigen-presenting molecule MR1. *Nature Immunology,* 17**,** 531-7.

Meermeier, E. W., Laugel, B. F., Sewell, A. K., Corbett, A. J., Rossjohn, J., McCluskey, J., Harriff, M. J., Franks, T., Gold, M. C. & Lewinsohn, D. M. 2016. Human TRAV1-2-negative MR1-restricted T cells detect S. pyogenes and alternatives to MAIT riboflavin-based antigens. *Nature Communications,* 7**,** 12506.

Meierovics, A., Yankelevich, W. J. C. & Cowley, S. C. 2013. MAIT cells are critical for optimal mucosal immune responses during in vivo pulmonary bacterial infection. *Proceedings of the National Academy of Sciences of the United States of America,* 110**,** E3119-E28.

Mellman, I., Coukos, G. & Dranoff, G. 2011. Cancer immunotherapy comes of age. *Nature,* 480**,** 480-9.

Miyazaki, Y., Miyake, S., Chiba, A., Lantz, O. & Yamamura, T. 2011. Mucosal-associated invariant T cells regulate Th1 response in multiple sclerosis. *International Immunology,* 23**,** 529-35.

Nazarov, V. I., Pogorelyy, M. V., Komech, E. A., Zvyagin, I. V., Bolotin, D. A., Shugay, M., Chudakov, D. M., Lebedev, Y. B. & Mamedov, I. Z. 2015. tcR: an R package for T cell receptor repertoire advanced data analysis. *BMC Bioinformatics,* 16**,** 175.

Nograles, K. E., Zaba, L. C., Guttman-Yassky, E., Fuentes-Duculan, J., Suarez-Farinas, M., Cardinale, I., Khatcherian, A., Gonzalez, J., Pierson, K. C., White, T. R., Pensabene, C., Coats, I., Novitskaya, I., Lowes, M. A. & Krueger, J. G. 2008. Th17 cytokines interleukin (IL)-17 and IL-22 modulate distinct inflammatory and keratinocyte-response pathways. *The British Journal of Dermatology,* 159**,** 1092-102.

Novak, J., Dobrovolny, J., Novakova, L. & Kozak, T. 2014. The decrease in number and change in phenotype of mucosal-associated invariant T cells in the elderly and differences in males and females of reproductive age. *Scandinavian Journal of Immunology*.

O'Donnell, M. A., Luo, Y., Chen, X., Szilvasi, A., Hunter, S. E. & Clinton, S. K. 1999. Role of IL-12 in the induction and potentiation of IFN-gamma in response to bacillus Calmette-Guerin. *Journal of Immunology,* 163**,** 4246-52.

Peterfalvi, A., Gomori, E., Magyarlaki, T., Pal, J., Banati, M., Javorhazy, A., Szekeres-Bartho, J., Szereday, L. & Illes, Z. 2008. Invariant Valpha7.2-Jalpha33 TCR is expressed in human kidney and brain tumors indicating infiltration by mucosal-associated invariant T (MAIT) cells. *International Immunology,* 20**,** 1517-25.

Pinkoski, M. J., Hobman, M., Heibein, J. A., Tomaselli, K., Li, F., Seth, P., Froelich, C. J. & Bleackley, R. C. 1998. Entry and trafficking of granzyme B in target cells during granzyme B-perforin-mediated apoptosis. *Blood,* 92**,** 1044-54.

Porcelli, S., Yockey, C. E., Brenner, M. B. & Balk, S. P. 1993. Analysis of T cell antigen receptor (TCR) expression by human peripheral blood CD4-8- alpha/beta T cells demonstrates preferential use of several V beta genes and an invariant TCR alpha chain. *The Journal of Experimental Medicine,* 178**,** 1-16.

Reantragoon, R., Corbett, A., Sakala, I., Gherardin, N., Furness, J., Chen, Z., Eckle, S., Uldrich. AP, Birkinshaw, R., Patel, O., Kostenko, L., Meehan, B., Kedzierska, K., Liu, L., Fairlie, D., Hansen, T., Godfrey, D., Rossjohn, J., McCluskey, J. & L., K.-N. 2013. Antigen-loaded MR1 tetramers define T cell receptor heterogeneity in mucosal-associated invariant T cells. *The Journal of Experimental Medicine,* 210**,** 2305-20.

Riegert, P., Wanner, V. & Bahram, S. 1998. Genomics, isoforms, expression, and phylogeny of the MHC class I-related MR1 gene. *Journal of Immunology,* 161**,** 4066-77.

Salerno-Goncalves, R., Luo, D., Fresnay, S., Magder, L., Darton, T. C., Jones, C., Waddington, C. S., Blohmke, C. J., Angus, B., Levine, M. M., Pollard, A. J. & Sztein, M. B. 2017. Challenge of Humans with Wild-type Salmonella enterica Serovar Typhi Elicits Changes in the Activation and Homing Characteristics of Mucosal-Associated Invariant T Cells. *Frontiers in Immunology,* 8**,** 398.

Salerno-Goncalves, R., Rezwan, T. & Sztein, M. B. 2014. B cells modulate mucosal associated invariant T cell immune responses. *Frontiers in Immunology,* 4**,** 511.

Sattler, A., Dang-Heine, C., Reinke, P. & Babel, N. 2015. IL-15 dependent induction of IL-18 secretion as a feedback mechanism controlling human MAIT-cell effector functions. *European Journal of Immunology,* 45**,** 2286-98.

Savage, A. K., Constantinides, M. G., Han, J., Picard, D., Martin, E., Li, B., Lantz, O. & Bendelac, A. 2008. The transcription factor PLZF directs the effector program of the NKT cell lineage. *Immunity,* 29**,** 391-403.

Seach, N., Guerri, L., Le Bourhis, L., Mburu, Y., Cui, Y., Bessoles, S., Soudais, C. & Lantz, O. 2013. Double positive thymocytes select mucosal-associated invariant T cells. *Journal of Immunology,* 191**,** 6002-9.

Serriari, N. E., Eoche, M., Lamotte, L., Fumery, M., Marcelo, P., Chatelain, D., Barre, A., Nguyen-Khac, E., Lantz, O., Dupas, J. L. & Treiner, E. 2014. Innate mucosal-associated invariant T (MAIT) cells are activated in inflammatory bowel diseases. *Clinical and Experimental Immunology,* 176**,** 266-74.

Sharma, P. K., Wong, E. B., Napier, R. J., Bishai, W. R., Ndung'u, T., Kasprowicz, V. O., Lewinsohn, D. A., Lewinsohn, D. M. & Gold, M. C. 2015. High expression of CD26 accurately identifies human bacteria-reactive MR1-restricted MAIT cells. *Immunology*.

Shugay, M., Bagaev, D. V., Turchaninova, M. A., Bolotin, D. A., Britanova, O. V., Putintseva, E. V., Pogorelyy, M. V., Nazarov, V. I., Zvyagin, I. V., Kirgizova, V. I., Kirgizov, K. I., Skorobogatova, E. V. & Chudakov, D. M. 2015. VDJtools: Unifying Post-analysis of T Cell Receptor Repertoires. *PLoS Computational Biology,* 11**,** e1004503.

Smith, D. J., Hill, G. R., Bell, S. C. & Reid, D. W. 2014. Reduced mucosal associated invariant T-cells are associated with increased disease severity and *Pseudomonas aeruginosa* infection in cystic fibrosis. *PLoS One,* 9**,** e109891.

Tang, X. Z., Jo, J., Tan, A. T., Sandalova, E., Chia, A., Tan, K. C., Lee, K. H., Gehring, A. J., De Libero, G. & Bertoletti, A. 2013. IL-7 licenses activation of human liver intrasinusoidal mucosal-associated invariant T cells. *Journal of Immunology,* 190**,** 3142-52.

Teunissen, M. B., Yeremenko, N. G., Baeten, D. L., Chielie, S., Spuls, P. I., de Rie, M. A., Lantz, O. & Res, P. C. 2014. The IL-17A-producing CD8(+) T-cell population in psoriatic lesional skin comprises mucosa-associated invariant T cells and conventional T cells. *The Journal of Investigative Dermatology,* 134**,** 2898-907.

Tilloy, F., Treiner, E., Park, S. H., Garcia, C., Lemonnier, F., de la Salle, H., Bendelac, A., Bonneville, M. & Lantz, O. 1999. An invariant T cell receptor alpha chain defines a

novel TAP-independent major histocompatibility complex class Ib-restricted alpha/beta T cell subpopulation in mammals. *The Journal of Experimental Medicine,* 189**,** 1907-21.

Treiner, E., Duban, L., Bahram, S., Radosavljevic, M., Wanner, V., Tilloy, F., Affaticati, P., Gilfillan, S. & Lantz, O. 2003. Selection of evolutionarily conserved mucosal-associated invariant T cells by MR1. *Nature,* 423**,** 164-9.

Treiner, E., Duban, L., Moura, I. C., Hansen, T., Gilfillan, S. & Lantz, O. 2005. Mucosal-associated invariant T (MAIT) cells: an evolutionarily conserved T cell subset. *Microbes and infection / Institut Pasteur,* 7**,** 552-9.

Ussher, J. E., Bilton, M., Attwod, E., Shadwell, J., Richardson, R., de Lara, C., Mettke, E., Kurioka, A., Hansen, T. H., Klenerman, P. & Willberg, C. B. 2014. CD161++ CD8+ T cells, including the MAIT cell subset, are specifically activated by IL-12+IL-18 in a TCR-independent manner. *European Journal of Immunology,* 44**,** 195-203.

van Wilgenburg, B., Scherwitzl, I., Hutchinson, E. C., Leng, T., Kurioka, A., Kulicke, C., de Lara, C., Cole, S., Vasanawathana, S., Limpitikul, W., Malasit, P., Young, D., Denney, L., Moore, M. D., Fabris, P., Giordani, M. T., Oo, Y. H., Laidlaw, S. M., Dustin, L. B., Ho, L. P., Thompson, F. M., Ramamurthy, N., Mongkolsapaya, J., Willberg, C. B., Screaton, G. R. & Klenerman, P. 2016. MAIT cells are activated during human viral infections. *Nature Communications,* 7**,** 11653.

Walker, L. J., Tharmalingam, H. & Klenerman, P. 2014. The rise and fall of MAIT cells with age. *Scandinavian Journal of Immunology,* 80**,** 462-3.

Won, E. J., Ju, J. K., Cho, Y. N., Jin, H. M., Park, K. J., Kim, T. J., Kwon, Y. S., Kee, H. J., Kim, J. C., Kee, S. J. & Park, Y. W. 2016. Clinical relevance of circulating mucosal-associated invariant T cell levels and their anti-cancer activity in patients with mucosal-associated cancer. *Oncotarget,* 7**,** 76274-90.

Wong, Michael T., Chen, J., Narayanan, S., Lin, W., Anicete, R., Kiaang, Henry Tan K., De Lafaille, Maria Alicia C., Poidinger, M. & Newell, Evan W. 2015. Mapping the Diversity of Follicular Helper T Cells in Human Blood and Tonsils Using High-Dimensional Mass Cytometry Analysis. *Cell Reports,* 11**,** 1822-33.

Zabijak, L., Attencourt, C., Guignant, C., Chatelain, D., Marcelo, P., Marolleau, J. P. & Treiner, E. 2015. Increased tumor infiltration by mucosal-associated invariant T cells correlates with poor survival in colorectal cancer patients. *Cancer immunology, immunotherapy*.